

IMPERIAL COLLEGE LONDON
National Heart & Lung Institute

The Determinants of Intra-Plaque Neovascularisation

A Study by Contrast-Enhanced Carotid Ultrasonography

Dr Benoy Nalin Shah BSc MBBS MRCP

Under the supervision of

Professor Roxy Senior

**Thesis submitted for the Degree of
Doctorate of Medicine**

2015

Abstract

Atherosclerosis is a chronic inflammatory disorder, initiated by arterial wall injury, mediated by well-recognised cardiovascular risk factors and culminating in formation of plaques, the patho-biological substrate that precedes events such as stroke and myocardial infarction.

Intraplaque neovascularisation (IPN) is one of several defence mechanisms in response to atherosclerosis. With development of an atherosclerotic plaque within the intima, the distance between the deeper intimal layers and the luminal surface increases, producing hypoxia within the arterial wall. This stimulates release of pro-angiogenic factors that induces neoangiogenesis in an attempt to normalise oxygen tension. However, these neo-vessels are fragile, immature and leaky and thought to be the primary cause of intraplaque haemorrhage, now appreciated to be a key risk factor for plaque rupture. Therefore, the presence of IPN is now widely recognised as a precursor of the “vulnerable plaque”.

Contrast-enhanced ultrasound (CEUS) is a non-invasive method of imaging carotid plaques and, as contrast bubbles travel wherever erythrocytes travel, they permit visualization of IPN. Prior research studies have demonstrated that CEUS can detect IPN with a high degree of accuracy (on comparison with histological plaque specimens) and have shown a relationship between extent of plaque neovessels and plaque echogenicity and between plaque neovascularization and prior cardiovascular events. However, CEUS is a relatively recently described imaging technique and there were a number of unanswered questions in this field, some of which formed the basis for study in this research Thesis. In this Thesis, research studies were conducted on human subjects using CEUS imaging to identify IPN and its determinants.

The incidence and determinants of IPN in healthy asymptomatic individuals was unknown and was studied in subjects from the London Life Sciences Population (LOLIPOP) study, a large study exploring mechanisms for differences in cardiovascular disease (CVD) between South Asian and European White individuals. The study found that approximately half of all plaques contain IPN. The only variable associated with IPN presence in an adjusted analysis was Asian ethnicity. This finding potentially has significant implications as it may help explain, in part, the greater CVD burden observed in Asian populations. A study comparing visualization of the carotid tree during B-mode and CEUS imaging was also conducted. Both IMT visualization and plaque detection were significantly improved by CEUS, implying that CEUS is superior to B-mode imaging for detection of sub-clinical atherosclerosis.

Radiotherapy (RT) damages arterial walls and promotes atherosclerosis. The carotid arteries frequently receive significant incidental doses of radiation during RT treatment of head and neck cancers. The effect of RT on plaque composition – specifically IPN – had not been studied and thus a collaborative cardio-oncological study was conducted to assess the effects of RT upon IPN in cancer survivors who had previously received RT. A significant association between RT and IPN was found which may provide insights into the mechanisms underlying the increased stroke risk amongst cancer survivors treated by RT.

Finally, a collaboration with biophysicists was formed to develop and validate a novel algorithm for quantitative analysis of IPN. Patients clinically scheduled to undergo carotid endarterectomy were recruited and underwent CEUS imaging prior to surgery. This study did not achieve its principal aims due to challenges with patient recruitment, challenges in image quality and with the quantification software also. Future directions of study in this promising field have been addressed in the thesis summary.

CONTENTS

Title Page	
Abstract	1
Contents	3
Declaration of Originality	7
Copyright Statement	8
List of Figures	9
List of Tables	13
List of Abbreviations	15
Publications / Presentations arising from this Thesis	16
Personal Contribution Statement	20
Acknowledgements	21
PART I – BACKGROUND, AIMS & OBJECTIVES	23
<u>Chapter 1 – Project Background</u>	
1.1 The Global Burden of Cardiovascular Disease	24
1.2 Risk Stratification – The Imperfection of Risk Scores	25
1.3 Sub-clinical Disease – Imaging Atherosclerosis by Ultrasonography	27
1.4 Carotid Ultrasonography & Risk Prediction	
1.4.1 The Discovery of Carotid Ultrasonography	28
1.4.2 Intima-Media Thickness in Health & Disease	29
1.4.3 Carotid Plaques – Superior to Intima-Media Thickness	31
1.4.4 Unmet Challenges of CVD Risk Stratification – Beyond Intima-Media Thickness & Plaque	33

Chapter 2 – The Patho-Biology of Atherosclerosis

2.1	Atherosclerosis as an Inflammatory Disorder	35
2.2	The Vulnerable Plaque	36
2.3	Intra-Plaque Neovascularization – A marker of plaque vulnerability?	40
2.4	Imaging the Vulnerable Plaque	
2.4.1	Ultrasound	42
2.4.2	Computed Tomography & Magnetic Resonance Imaging	48
2.4.3	Positron Emission Tomography	49
2.5	Intra-Plaque Neovascularization & Contrast-Enhanced Ultrasound – Current Status	49

Chapter 3 – The Unknowns of Plaque Neovascularization

3.1	Impact of Ethnicity on Intra-Plaque Neovascularization in Asymptomatic Individuals	
3.1.1	Cardiovascular Risk and Asian Ethnicity	50
3.1.2	Why are South Asians at higher cardiovascular risk?	51
3.1.3	Risk stratification: are risk models valid in South Asians?	52
3.1.4	The London Life Sciences Population (LOLIPOP) study	53
3.2	Intra-Plaque Neovascularization in Radiotherapy	
3.2.1	Radiotherapy and the Vascular System	56
3.2.2	Expected effects of radiotherapy upon angiogenesis	58
3.3	Quantitative vs. Qualitative Assessment of Plaque Neovascularization	
3.3.1	Quantification – The Holy Grail of Contrast Imaging	60
3.3.2	CEUS Quantification – The Technical Challenges	61
3.3.3	CEUS Quantification – Limitations to Current Approaches	61

Chapter 4 – Research Aims & Objectives

4.1	Aims and Objectives of this research thesis	65
-----	---	----

PART 2 – RESULTS OF RESEARCH STUDIES 67

Chapter 5 – Contrast-Enhanced Ultrasound for Arterial Segment Assessment

5.1	Abstract	68
5.2	Introduction	70
5.3	Methods	72
5.4	Results	76
5.5	Discussion	85

Chapter 6 – Intra-Plaque Neovascularization in Asymptomatic Individuals

6.1	Abstract	90
6.2	Introduction	92
6.3	Methods	93
6.4	Results	95
6.5	Discussion	98

Chapter 7 – Intra-Plaque Neovascularization & Radiotherapy

7.1	Abstract	101
7.2	Introduction	103
7.3	Methods	104
7.4	Results	110
7.5	Discussion	117

Chapter 8 – Development of Novel Quantification Methods for CEUS Analysis

8.1	Abstract	124
8.2	Introduction	126
8.3	Methods	128
8.4	Results	137
8.5	Discussion	141

Chapter 9 – CEUS Quantification versus Visual Accuracy for IPN Detection

9.1	Abstract	146
9.2	Introduction	148
9.3	Methods	149
9.4	Results	150
9.5	Discussion	156

PART 3 – SUMMARY

<u>Chapter 10 – Future Directions & Conclusions</u>	159
--	-----

<u>Chapter 11 – References</u>	162
---------------------------------------	-----

<u>Appendices</u>	185
--------------------------	-----

DECLARATION OF ORIGINALITY

I declare that the work contained within this Thesis represents my own except that mentioned from previously published studies, all of which have been acknowledged and appropriately referenced. The scientific studies reported within this Thesis represent original work which has been accepted and/or submitted for publication but none of the work had previously been published.

COPYRIGHT STATEMENT

The copyright of this thesis rests with the author and is made available under a Creative Commons Attribution Non-Commercial No Derivatives licence. Researchers are free to copy, distribute or transmit the thesis on the condition that they attribute it, that they do not use it for commercial purposes and that they do not alter, transform or build upon it. For any reuse or redistribution, researchers must make clear to others the licence terms of this work.

LIST OF FIGURES

- Figure 1.1 – First reported use of ultrasound to produce a B-mode image showing the typical appearances of a normal carotid arterial wall 28
- Figure 1.2 – B-mode image from a healthy human left common carotid artery (CCA) using a contemporary ultrasound system 29
- Figure 1.3 – B-mode still image showing a large plaque in the carotid bulb, with calcific (echobright) and ‘soft’ (echolucent) plaque seen above 32
- Figure 2.1 – Flow diagram illustrating the patho-aetiology of intraplaque neovascularisation and the point at which CEUS can detect IPN 39
- Figure 2.2 – Patho-biology of atherosclerotic plaque formation and subsequent neoangiogenesis 41
- Figure 2.3 – B-mode image showing echobright and echolucent regions of a near wall carotid plaque, corresponding to ‘hard’ and ‘soft’ regions of a plaque 43
- Figure 2.4 – Contrast enhanced ultrasound image of a human common carotid artery 45
- Figure 2.5 – Early human CEUS scan demonstrating a large near wall plaque with multiple neovessels seen within 47

<u>Figure 2.6</u> – B-mode and CEUS images showing a large echolucent plaque at the carotid bifurcation with clear IPN noted during CEUS imaging	47
<u>Figure 5.1</u> – Illustration of a common carotid artery with bifurcation into its internal and external branches	73
<u>Figure 5.2</u> – B-mode examples of clear IMT visualization in both near and far walls and an example of a clear far wall but poor near wall IMT visualization	77
<u>Figure 5.3</u> – Example of near wall and far wall visualization during CEUS imaging	77
<u>Figure 5.4</u> – Distribution of plaques within the carotid arterial tree during B-mode and CEUS imaging	80
<u>Figure 5.5</u> – Number of plaques detected in each segment of the carotid artery during B-mode and CEUS imaging	81
<u>Figure 5.6</u> – Suspicion of a large plaque in long and short axis images during B-mode imaging that were proven to be artefacts after CEUS imaging	84
<u>Figure 6.1</u> – CEUS still image showing a plaque in the carotid bulb, extending into the origin of the internal carotid artery with contrast bubbles within the plaque	96
<u>Figure 6.2</u> – B-mode and carotid CEUS images demonstrating plaques with and without intra-plaque neovascularization	97

<u>Figure 7.1</u> – Examples of B-mode, colour Doppler and CEUS imaging of the carotid arterial tree	<i>107</i>
<u>Figure 7.2</u> – Drawn representation of carotid tree, with plaque and IMT measurements according to Mannheim consensus	<i>107</i>
<u>Figure 7.3</u> – Graphs illustrating differences between RT and non-RT arteries	<i>116</i>
<u>Figure 7.4</u> – Long axis examples of plaques with grade 0 IPN, grade 1 IPN and grade 2 IPN. Contrast bubbles within plaques (P) are indicated by arrows	<i>117</i>
<u>Figure 8.1</u> – Regions of interest drawn on a CEUS image within the lumen, a plaque and the adventitia	<i>131</i>
<u>Figure 8.2</u> – Long-axis and short axis B-mode images from a right carotid artery showing a large flow-limiting plaque in the carotid bulb	<i>139</i>
<hr/>	
<u>Figure 8.3:</u> Long axis B-mode and CEUS images of a large plaque, illustrating significant shadowing artefact as a result of the echo-bright calcium in the near wall	<i>139</i>
<u>Figure 8.4:</u> An example of significant attenuation / shadowing artefact caused by a near wall plaque which obscured a far wall plaque	<i>140</i>
<u>Figure 8.5:</u> A large plaque seen on B-mode imaging is less clearly seen on CEUS imaging as the calcified regions of plaque were seemingly washed out	

by the contrast opacification in the lumen 143

Figure 8.6: Simultaneous side-by-side CEUS and B-mode imaging,
acquired using a radiology (rather than cardiology) ultrasound system 144

Figure 9.1: Scatter plots showing distribution of CVOT values and
% RAA by visual IPN grade, illustrating significant overlap between categories 152

Figure 9.2: Snapshot from the quantification algorithm in which a grade 0
plaque is correctly identified as having no IPN detected within the ROI 153

Figure 9.3: Snapshot from quantification algorithm in which a grade 0
plaque is incorrectly identified as containing IPN 154

Figure 9.4: Snapshot from quantification algorithm in which a grade 2
plaque is correctly identified as containing IPN 155

LIST OF TABLES

<u>Table 2.1</u> – Historical milestones in understanding of plaque biology	37
<u>Table 2.2</u> – Key studies in humans published to date regarding IPN as studied by CEUS	46
<u>Table 3.1</u> – Published studies (human and animal) reporting on accuracy of quantification software	62
<u>Table 5.1</u> – Baseline characteristics of the study patients	76
<u>Table 5.2</u> – IMT visualization during B-mode and CEUS imaging, in all segments and in the ICA only	78
<u>Table 5.3</u> – Mean near wall and far wall IMT visualization scores for the right and left carotid arteries during B-mode and CEUS imaging	79
<u>Table 5.4</u> – Categories of plaque detection between B-mode and CEUS imaging	82
<u>Table 6.1</u> – Baseline patient characteristics	95
<u>Table 7.1</u> – Baseline characteristics of the 49 enrolled patients	111
<u>Table 7.2</u> – Comparison of patients with bilateral versus unilateral plaques	113

<u>Table 7.3</u> – Per-patient and per-plaque data analyses of B-mode and CEUS imaging in RT-side and non-RT side arteries	114
<u>Table 7.4</u> – Relationship between presence or absence of IPN and patient variables in all patients and RT-side only plaques	115
<u>Table 8.1</u> – Attenuation coefficient of different tissues at a frequency of 1MHz	128
<u>Table 8.2</u> – Sample sizes with corresponding strengths of correlation	138
<u>Table 8.3</u> – Baseline patient characteristics	139
<u>Table 9.1</u> – Mean CVOT and % RAA values stratified by IPN Grade	152

LIST OF ABBREVIATIONS

BMI	Body Mass Index
BP	Blood Pressure
CCA	Common Carotid Artery
CEUS	Contrast Enhanced Ultrasound
CHD	Coronary Heart Disease
CVD	Cardiovascular Disease
CVE	Cerebrovascular Events
CT	Computed Tomography
ECA	External Carotid Artery
ECG	Electrocardiogram
HNC	Head & Neck Cancer
ICA	Internal Carotid Artery
IMT	Intima-Media Thickness
IPH	Intraplaque Haemorrhage
IPN	Intraplaque Neovascularisation
MI	Myocardial Infarction
MRI	Magnetic Resonance Imaging
PAD	Peripheral Arterial Disease
PET	Positron Emission Tomography
RT	Radiotherapy
UCA	Ultrasound Contrast Agent

PUBLICATIONS / PRESENTATIONS ARISING FROM THIS RESEARCH

[A] FIRST AUTHOR PAPERS (studies described in this Thesis)

1) **Shah BN**, Gujral DG, Chahal NS, Harrington KJ, Nutting CM & Senior R. Plaque neovascularization is increased in human carotid atherosclerosis related to prior neck radiotherapy. A contrast enhanced ultrasound study. **J Am Coll Cardiol Img** 2016; 9(6): 668-675

2) **Shah BN**, Chahal NS, Anantharam B, Kooner JS & Senior R. Higher Prevalence of Plaque Neovascularization – a Marker of Plaque Vulnerability – in South Asians versus Northern European Asymptomatic Subjects: Implications for a Possible Mechanism for Differential Ethnic Outcome. *Manuscript submitted; currently under peer review*

3) **Shah BN**, Chahal NS, Anantharam B, Kooner JS & Senior R. Contrast-enhanced ultrasound improves visualization of carotid artery intima-media thickness and improves detection of carotid plaques. *Manuscript submitted; currently under peer review*

[B] CO-AUTHOR PAPERS (arising from collaborative research related to this Thesis)

4) Gujral DM, Cheung WK, **Shah BN**, Chahal NS, Bhattacharyya S, Hooper J, Senior R, Tang MX, Harrington KJ, Nutting CM. Contrast enhancement of carotid adventitial vasa vasorum as a biomarker of radiation-induced atherosclerosis. **Radiotherapy & Oncology** 2016; 120(1): 63-68

5) Gujral DM, **Shah BN**, Bhattacharyya S, Senior R, Harrington KJ, Nutting CM. Contrast-enhanced ultrasound to assess plaque neovascularization in irradiated carotid arteries. **Int J Cardiol.** 2016; 202:3-4.

- 6) Gujral DG, **Shah BN**, Chahal NS, Bhattacharyya S, Senior R, Harrington KJ & Nutting CM. Do traditional risk stratification models for cerebrovascular events apply in irradiated head and neck cancer patients? **Quart J Med** 2016; 109(6):383-89
- 7) Gujral DG, **Shah BN**, Chahal NS, Bhattacharyya S, Hooper J, Senior R, Harrington KJ & Nutting CM. Carotid intima-medial thickness as a marker of radiation-induced carotid atherosclerosis. **Radiotherapy & Oncology** (2016); 118(2): 323-29
- 8) Gujral DM, **Shah BN**, Chahal NS, Bhattacharyya S, Senior R, Harrington KJ, Nutting CM. Arterial stiffness as a biomarker of radiation-induced carotid atherosclerosis. **Angiology** 2015; 67(3):266-71
- 9) Cheung WK, Gujral DG, **Shah BN**, Chahal NS, Bhattacharyya S, Cosgrove DO, Eckersely RJ, Harrington KJ, Senior R, Nutting CM & Tang M. Attenuation correction and normalisation for quantification of contrast enhancement in ultrasound images of carotid arteries. **Ult Med Biol** 2015; 41(7): 1876-1883
- 10) Gujral DG, **Shah BN**, Chahal NS, Clinical features of radiation-induced carotid atherosclerosis. **Clin Oncol** 2014; 26(2):94-102

[C] RESEARCH ABSTRACTS: FIRST-AUTHOR PRESENTATIONS

1) BCS Conference 2015 – Manchester, England

Shah BN, Chahal NS, Anantharam B, Kooner JS & Senior R.

Poster Presentation - Increased Carotid Plaque Neovascularization, a marker of plaque vulnerability, is independently associated with asymptomatic South Asians vs Europeans: A possible mechanism underlying higher Cardiovascular Events in South Asians vs Europeans.

2) ESC Congress 2014 – Barcelona, Spain

Shah BN, Gujral DG, Chahal NS, Harrington KJ, Nutting CM & Senior R.

Poster Presentation – Plaque Neovascularization is Increased in Human Carotid Atherosclerosis Related to Prior Neck Radiotherapy – A Contrast Enhanced Ultrasound Study.

3) BCS Conference 2014 – Manchester, England

Shah BN, Gujral DG, Chahal NS, Harrington KJ, Nutting CM & Senior R.

Carotid Intra-Plaque Neovascularization is Increased In Patients With Prior Ipsilateral Neck Irradiation – A Contrast Enhanced Ultrasound Study.

[D] RESEARCH ABSTRACTS: CO-AUTHOR PRESENTATIONS

1) 2014: 19th European Symposium of Contrast Ultrasound Imaging, Rotterdam

Cheung WK, Gujral DM, **Shah BN**, Chahal NS, Bhattacharyya S, Yildiz Y, Cosgrove D, Eckersley RJ, Harrington KJ, Senior R, Nutting CM, Tang MX.

Poster Presentation – Attenuation correction and image normalization improve quantification of ultrasound contrast enhancement in carotid artery adventitia in cancer patients after radiation therapy

2) 2013: European Cancer Congress (ECCO) Annual Meeting, Amsterdam, Netherlands

Gujral DM, **Shah BN**, Chahal N, Bhattacharyya S, Schick U, Senior R, Harrington K & Nutting CM

Poster Presentation – Speckle tracking to measure arterial strain as a marker of radiation-induced atherosclerosis.

3) 2013: American Society for Radiation Oncology (ASTRO) Annual Conference, Atlanta

Gujral DM, **Shah BN**, Chahal N, Bhattacharyya S, Schick U, Senior R, Harrington K & Nutting CM

Poster Presentation – Arterial stiffness and elasticity as markers of radiation-induced atherosclerosis.

4) 2013: European Society for Radiotherapy & Oncology (ESTRO) Annual Forum, Geneva

Gujral DM, **Shah BN**, Chahal N, Bhattacharyya S, Senior R, Harrington K & Nutting CM

Poster Presentation - Carotid intima-medial thickness as a marker of radiation-induced atherosclerosis

5) 2013: 18th European Symposium of Contrast Ultrasound Imaging, Rotterdam

Girard-Desprolet J, Mavropoulos N, Cheung W, **Shah BN**, Chahal NS, Cosgrove D, Senior R, Eckersley RJ & Tang M.

Poster Presentation – Towards quantification of plaque neovascularisation and vasa vasorum in carotid arteries – a preliminary study on attenuation correction and segmentation in CEUS images.

PERSONAL CONTRIBUTION TO THE THESIS

I was responsible for the analysis of all carotid images, B-mode and CEUS, from the LOLIPOP patients (I did not perform the scans for this part of the project personally). I tabulated these results in an XL spreadsheet and was responsible for all data analysis. I organised and analysed the results of the inter-observer and intra-observer variability exercises to assess the technique's reproducibility.

I was responsible for scanning all patients from the Royal Marsden hospital in the collaborative radiotherapy project. I also analysed all the datasets (blinded to the side of therapy) and performed intra- and inter-observer variability analyses.

I helped to conceive the study design for the quantification project, obtained ethical approval, wrote the relevant study documents (e.g. Patient Information Sheet, Study Protocol, and Consent Form) and was responsible for patient recruitment from the wards of Northwick Park Hospital. I performed the carotid scans and was responsible for collection of the excised plaques and transfer to the Pathology department for further analysis.

I have performed all data analyses and calculations myself and I was involved in the development of the hypotheses for all the studies presented in this Thesis. I was also responsible for undertaking all statistical analyses.

ACKNOWLEDGEMENTS

First and foremost, I am indebted to **Professor Roxy Senior**, my supervisor and mentor during my time as a Research Fellow in London. It is hard to put into words how much I have learnt whilst working with him, on all aspects of clinical cardiology, scientific research principles and, of course, echocardiography and carotid imaging. I am extremely grateful for his unwavering support and generous time he always provided me with to discuss the project.

I am grateful to **Dr Navtej Chahal**, a former Research Fellow of Professor Senior, who previously performed the LOLIPOP carotid scans, taught me interpretation of CEUS scans and always provided sound advice whenever approached. I would like to thank **Dr Dorothy Gujral**, Clinical Research Fellow at Royal Marsden Hospital, who recruited patients for our collaborative study on the radiotherapy patients and for her tireless work and incredible organization, all of which made our project run very smoothly.

I am grateful to the Cardiovascular Biomedical Research Unit at the Royal Brompton Hospital for the superb research facilities afforded to me, including the Echocardiography Suite in which many of the carotid research scans were undertaken. I am grateful to all the members of the Cardiac Research Department at Northwick Park, in particular **Mrs Ann Banfield, Ms Grace Young, Mr Christopher Kinsey, Mrs Minoo Shah and Mrs Mary Crisp**, for their support during my time in London.

I wish to thank the Biomedical physicists with whom we collaborated at Imperial College – I am grateful to **Dr Mengxing Tang** and his team, including **Mr Tony Cheung, Professor**

David Cosgrove and **Mr Rob Eckersley** for their support and expertise during our collaboration.

I would also like to thank **Professor Steve Feinstein** from Rush Medical Center in Chicago. He is the pioneer of contrast carotid imaging and I was very fortunate to have the opportunity to spend a half day with him in 2012 during the ACC annual scientific sessions. He spent a lot of time talking to me about the CEUS technique and reviewed scans that I had taken on a memory stick to ensure that the machine settings and interpretation were correct. I am grateful to him for his time, wisdom and exceptional enthusiasm that day.

Finally, I am exceptionally indebted to my long-suffering wife **Anamika**, who endured many lonely nights and weekends over the years whilst I worked on this project. Without her support and understanding, this Thesis would not have reached its conclusion.

PART I

BACKGROUND, AIMS & OBJECTIVES

CHAPTER 1 – PROJECT BACKGROUND

1.1 The Global Burden of Cardiovascular Disease

The phrase ‘cardiovascular disease’ (CVD) is an umbrella term that incorporates coronary heart disease (CHD), cerebrovascular events (CVE) such as stroke, peripheral arterial disease (PAD), congenital heart disease and rheumatic heart disease. In spite of a significant reduction in mortality from CVDs due to improved public health campaigns (e.g. to reduce smoking) and wider availability of proven pharmacological therapies (e.g. statins), CVDs remain the number one cause of death globally. CVDs have also over-taken infectious diseases as the most common cause of death in low and middle-income nations.¹

A report from the World Health Organization (WHO) found that an estimated 17.3 million people died from CVDs in 2008, representing 30% of all global deaths.¹ Of these deaths, an estimated 7.3 million were due to CHD and 6.2 million were due to CVEs.² It is projected that the number of people who die from CVDs – mainly heart disease and stroke – will increase to reach 23.3 million by 2030.^{1,3} CVDs are projected to remain the single leading cause of death over the next three decades.³

This significant health burden is large in Europe also. Each year, CVD causes over 4 million deaths in Europe, almost half of all deaths.⁴ The socio-economic costs associated with the burden of CVD is huge – overall CVD is estimated to cost the EU economy almost €196 billion a year. Of the total cost of CVD in the EU, around 54% is due to health care costs, 24% due to productivity losses and 22% due to the informal care of people with CVD.⁴

An unfortunate truth regarding CVD is that a significant proportion of such patients have no prior symptoms⁵ and may first present with a fatal myocardial infarction (MI) or stroke, or a clinically large event resulting in significant morbidity thereafter. Consequently, over the past quarter century, there have been huge research efforts to improve our understanding of the underlying disease mechanisms in “at risk” CVD patients, in the hope we may be able to predict those individuals at risk of a clinically significant CVD event. This work initially led to the development and use of risk stratification tools for physicians, such as the Framingham Risk Score (FRS) from America and, more recently, the QRISK score in the United Kingdom (UK).

1.2 Risk Stratification – The Imperfection of Risk Scores

The Framingham Study, conducted over three generations in the small East American town of Framingham, Massachusetts, is the largest research study ever conducted. It has spawned over 1000 publications and continues to study children and grand-children of the original Framingham cohort. The study was conceived in the early-mid 20th century in an attempt to better understand the reasons for premature deaths amongst Americans from heart disease. It was the Framingham study that identified smoking, diabetes mellitus, hypertension, hyperlipidaemia and family history of premature CHD as the five principal “risk factors” for CHD. This information was subsequently combined to create the FRS, first described in 1998.⁶ Since then, the score has been refined with the latest version produced in 2002.⁷

The FRS calculates the risk of CHD over a ten-year period in any given individual as a percentage and patients are then assigned to arbitrarily defined categories as low risk (<10% CHD risk at 10 years), intermediate risk (10-20%) and high risk (>20%). The FRS has limitations, however. Firstly, the score predicts CHD events but not all CVD events. Secondly,

the score was developed from an ethnically homogenous (i.e. white Caucasian) population in America and it is uncertain if the score's accuracy is maintained when used in other populations, for example Blacks or South Asians who have a higher CVD risk. Thirdly, the Framingham risk equations were developed during the peak incidence of CVD in America and thus may over-estimate risk in contemporary European populations where the incidence of CVD is lower. Fourthly, the Framingham algorithm does not include factors such as social deprivation, body mass index, family history of cardiovascular disease, and current treatment with anti-hypertensive medications.

As a result, alternative scoring systems have been developed and validated. In the United Kingdom, the QRISK score was first proposed in 2007 and incorporated a number of additional factors, including [body mass index](#), ethnicity, measures of deprivation, chronic kidney disease, rheumatoid arthritis and atrial fibrillation.⁸ This was subsequently validated by an independent group using an external data set⁹ and the score was updated to become QRISK2 in 2009.¹⁰ QRISK2 has also subsequently been validated against the UK population and shown to be a better risk predictor in the UK than FRS.^{11,12} Consequently, the QRISK2 score is recommended by the National Institute for Health and Clinical Excellence (NICE) whereas the Systematic Coronary Risk Evaluation (SCORE) system¹³ is endorsed by the European Society of Cardiology (ESC).

However, despite virtually ubiquitous use of these various risk calculators by primary care (family) doctors in the developed world, predominantly for identifying patients that should commence primary preventative medications, death from CVD remains the largest killer in each nation. Thus, superior methods are needed – beyond risk scoring systems – that can identify those individuals at risk of future CVD events.

1.3 Sub-Clinical Disease – Imaging Atherosclerosis

Non-invasive imaging techniques permit the detection of atherosclerosis within arteries before it has caused symptoms or clinical events (i.e. sub-clinical disease). Sub-clinical atherosclerosis has been heavily investigated in recent years, in the hope that detection at an early stage may allow initiation of therapies that may reduce future CVD risk. As the carotid arteries are superficial in the neck – and ultrasound is cheap, safe and free from ionizing radiation – carotid ultrasonography has been widely studied as a means of detecting sub-clinical atherosclerosis. A large number of studies have investigated carotid ultrasound parameters – namely intima media thickness (IMT) and presence/absence of plaque – to determine if these data can improve the accuracy of current risk stratification processes further.

Carotid ultrasonography allows direct visualization of the common carotid artery as well as its bifurcation into internal and external carotid arteries (ICA and ECA respectively). The proximal segments of the ICA and ECA can also be examined by ultrasound. 2-dimensional or B-mode ultrasound provides an image of the arterial walls and the lumen, whilst colour Doppler imaging detects blood flow and can highlight areas of stenosis (or even occlusion).

1.4 CAROTID ULTRASONOGRAPHY and RISK PREDICTION

1.4.1 Discovery of Carotid Ultrasonography

The normal arterial wall consists of three layers – the tunica intima, tunica media and tunica adventitia. In 1986, Italian researchers led by Paolo Pignoli¹⁴ reported for the first time the use of ultrasound to assess the structure of the wall of the human carotid artery, demonstrating that

it was possible to visualise the intima and media as separate entities from the brighter adventitia (see figure 1.1). They also analysed carotid and aortic samples from autopsy specimens and validated the thickness measurements against histology, demonstrating excellent agreement between the two methods. Following this landmark publication, a number of studies were initiated to investigate the utility of this new measure.

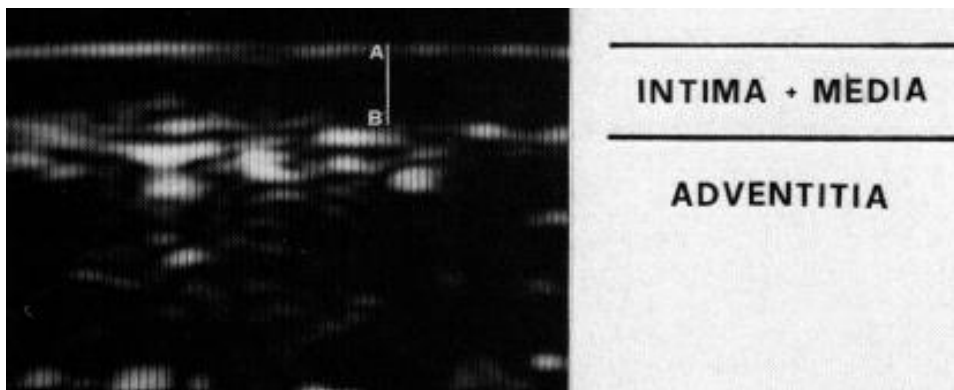


Figure 1.1: First reported use of ultrasound to produce a B-mode image the typical appearances of a normal carotid arterial wall. The A-B line represents the distance between the inner and the outer echogenic lines and corresponds to the B mode image of intimal + medial thickness (Reproduced from Pignoli et al¹⁴)

1.4.2 The Intima-Media Thickness (IMT) in Health and Disease

In health, the intima and media are virtually indistinguishable (figure 1.2). With advancing age, medial hypertrophy is frequently seen – the most common cause is systemic hypertension – resulting in an increased thickness of the intima-media complex. This is also accompanied by gradual intimal thickening, a process that commences in the third decade of life. IMT measurements have been made in a number of large epidemiological longitudinal studies, all of which have shown that increased baseline IMT measurement is independently associated with future CVD events. A recent meta-analysis of 8 such studies, incorporating 37,197

subjects, found that for an absolute increase in IMT of 0.1mm, the risk of MI increased by 10-15% and of cerebrovascular events by 13-18%.¹⁵ Previous investigators have shown that IMT is frequently abnormal even in patients with very low (<5%) FRS¹⁶ and also that IMT is more likely than coronary artery calcium (CAC) score to re-classify the FRS.¹⁷ IMT has also been shown to be superior to CAC score for prediction of cerebrovascular events in the Pittsburgh Field Study, though the Multi Ethnic Study of Atherosclerosis (MESA) study found the CAC score superior to IMT for prediction of future CVD events.¹⁸

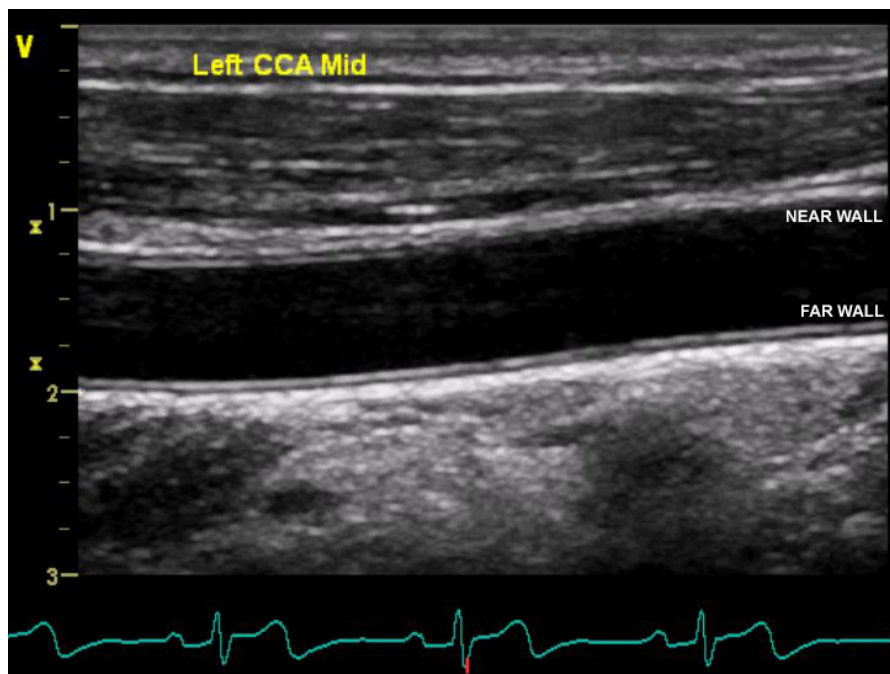


Figure 1.2: B-mode image from a healthy human left common carotid artery (CCA) using a contemporary ultrasound system. Note the typical ‘double tramline’ appearance of the intima-media complex with the echo-bright adventitia external to this.

However, use of carotid IMT remains predominantly a research tool and IMT assessment has several limitations. Firstly, there is a technical challenge, since the recent Framingham Offspring cohort study has shown that IMT in the internal carotid artery (ICA) only predicts events and re-classifies the FRS, not common carotid artery (CCA) IMT.¹⁹ However, the CCA

is usually very easy to visualise whereas the ICA, higher in the neck, is frequently challenging to image and ICA IMT is poorly seen in up to 33% patients. Secondly, no sufficiently large (and thus adequately powered) study to date has randomized patients to conventional care or intensive treatment (e.g. lifestyle changes, statin therapy) and shown that reduction in IMT on serial measurements leads to a reduction in CVD events. Finally, as discussed below, carotid plaque appears superior to IMT for risk prediction, most probably because increased IMT frequently is secondary to thickening of the media (e.g. due to hypertension) and thus is less reflective of generalised atherosclerosis than plaque formation.

Consequently, the United States Preventive Services Task Force (USPSTF) recently recommended against measuring anatomic markers of atherosclerosis, including IMT.^{20, 21} The USPSTF based its negative recommendation regarding IMT, in part, on the absence of specific data regarding the independent predictive value of IMT for patients at intermediate CHD risk and on concerns about this test's ability to reclassify such patients into lower or higher risk categories, therefore altering their clinical management. They also criticized the evidence base supporting IMT as a risk prediction tool since some studies associating IMT with CHD risk included patients with pre-existing CHD or risk equivalent conditions, were of relatively short duration, and had few CHD events.²¹ Thus, in conclusion, though IMT is considered a risk *marker* for CVD, it does not fulfil the criteria of an independent risk *factor* for CVD.

1.4.3 Carotid Plaques – Superior to IMT assessment

Atherosclerotic plaques are most commonly found in areas of low shear stress, particularly in areas of marked oscillation in the direction of wall shear stress.²² This is most frequently seen in the carotid bifurcation (bulb) and at the origin of the ICA (see figure 1.3). Such

haemodynamic changes are far less commonly seen in the main CCA, thus explaining the lower preponderance of plaques in the CCA.

Carotid plaques have been varyingly defined over the years. In some original studies, plaque presence was not measured but was judged subjectively (i.e. visually).²³ Other studies used plaque height (e.g. >1.0mm) as a cut-off.²⁴ Recognising this heterogeneity, a consensus was reached by multiple research groups (the *Mannheim consensus*), originally published in 2004²⁵ and subsequently updated in 2007.²⁶ This defined a carotid plaque as a:

- ❖ Focal structure > 0.5mm encroaching into the lumen
- ❖ Focal structure > 50% thickness of surrounding IMT
- ❖ Structure with thickness >1.5mm (from media-adventitia to intima-lumen borders)

A large body of evidence has accumulated supporting the predictive role of plaque disease in future CVD events. Unlike increased IMT, which may reflect age-related medial hypertrophy, plaque formation is more representative of systemic atherosclerosis. Early studies confirmed the association between plaque prevalence and age²⁷ and proposed plaque scoring systems for quantifying plaque burden.²⁴ Longitudinal population studies, such as the Tromso Study, demonstrated that carotid plaque is an independent predictor of both CVEs²⁸ and first MI.²⁹ The British Regional Heart Study also found that carotid plaque, not IMT, appeared to be the major determinant of symptoms status and presence or absence of known CVD.³⁰ The method by which plaques are assessed also has varied, with some finding total plaque area superior to the number of plaques³¹ whereas other researchers found the opposite to be true.²³

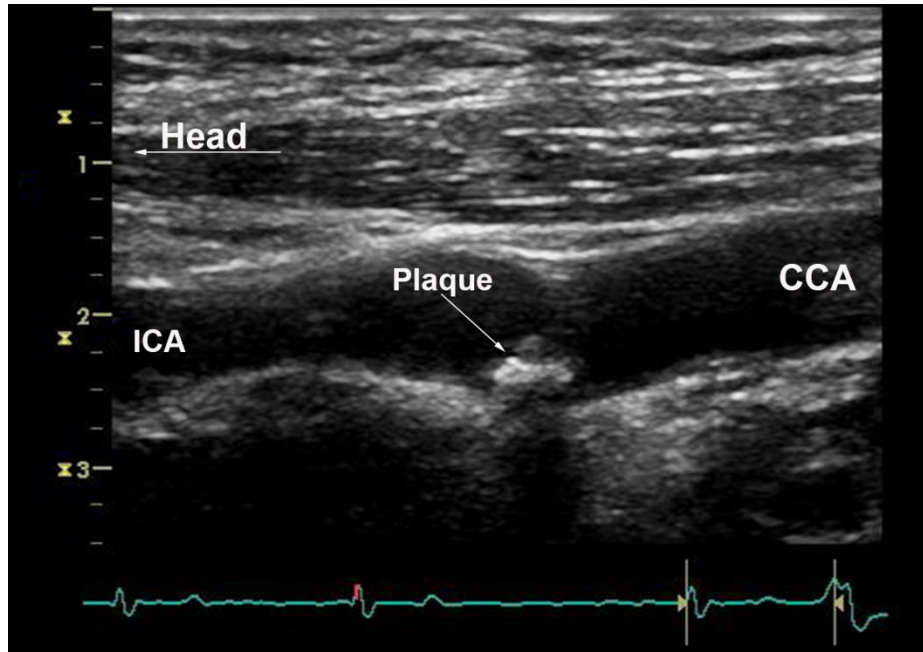


Figure 1.3: B-mode still image showing a large plaque in the carotid bulb, with a calcific (echobright) base and 'soft' (echolucent) plaque additionally seen above this.

A recent meta-analysis that evaluated 11 population-based studies (combined $n=54,336$) found that carotid plaque, in comparison with IMT, had a superior diagnostic accuracy for prediction of CAD events.³² Finally, the long-term results of the Atherosclerosis Risk In Communities (ARIC) study have recently been published, in which Nambi *et al*³³ studied 13,145 subjects who were free of prevalent CHD or stroke at the inception of the study. After a mean follow-up period of 15.1 years, participants had 1,812 CHD events. The authors evaluated the additional predictive value of IMT, plaque presence, or both findings to CHD risk prediction. They found that the area under the receiver operating characteristic curve (AUC) for traditional risk factor prediction of CHD events (0.742) was significantly increased by the addition of increased IMT (0.750) or carotid plaque presence (0.751), and that the combination of risk factors, IMT, and plaque yielded the highest AUC (0.755).³³

Although the 0.008 to 0.013 increments in AUC achieved using the carotid ultrasound data may seem small, they are on the same order of magnitude as the individual contributions of smoking status and systolic blood pressure to the Reynold's Risk Score for women, and greater than the contributions of lipids, family history, and high-sensitivity C-reactive protein.³⁴ Indeed, after age and sex are considered in almost any CHD predictive model, additional risk factors contribute little on an individual basis, but are very important when considered in aggregate.³⁵ Following this paper's publication, the ACC/AHA Guideline for Assessment of Cardiovascular Risk in Asymptomatic Adults gave the use of carotid ultrasound to provide risk assessment in asymptomatic adults a Class IIa recommendation (Level of Evidence: B).³⁶ Assessment of carotid IMT and assessment of plaque by carotid ultrasound is also given a Class IIa recommendation in the European Society of Cardiology guidelines on management of patients with stable angina³⁷ and chronic hypertension.³⁸

1.4.4 The Unmet Challenges of CVD Risk Stratification – Beyond IMT and plaque

In spite of numerous studies demonstrating that data obtained from carotid ultrasonography can improve risk prediction, carotid imaging is rarely employed in clinical practice and is not advocated in screening asymptomatic individuals in the UK. This is largely down to the fact that data collected so far are observational only, with no trials to date demonstrating that acting upon an ultrasound finding, irrespective of baseline risk (e.g. as calculated by FRS), can improve outcome.

More recently, fuelled by significant advances in technologies underpinning non-invasive carotid imaging techniques, there has been an additional realization that studying plaques in greater detail (i.e. beyond mere presence/absence and area) may further improve risk

stratification. This has led to a deeper study of the underlying pathological substrate responsible for CVD – atherosclerosis, which is discussed in the next Chapter.

CHAPTER 2 – THE PATHO-BIOLOGY OF ATHEROSCLEROSIS

2.1 Atherosclerosis as an inflammatory disorder

Atherosclerosis describes the hardening of arterial walls and narrowing of arteries due to abnormal plaque formation. The term is derived from the Greek words ‘athera’ (meaning ‘gruel’) and ‘sclerosis’ (meaning ‘hardening’). It is a chronic disease with acute vascular complications, including MI and stroke. The development of atherosclerosis generally starts in early life and progresses silently for decades through adulthood.

Atherosclerosis is an inflammatory disorder initiated by arterial wall injury and mediated by known cardiovascular risk factors such as hyperlipidaemia, hypertension, smoking, diabetes mellitus and advancing age.³⁹ This damage to the endothelium permits the sub-endothelial passage of lipoproteins which are oxidised and become cytotoxic, pro-inflammatory, chemotactic and pro-atherogenic.⁴⁰ Thus, at its earliest stages, atherosclerosis is akin to an acute inflammatory reaction. The inflammatory response is in fact a defence mechanism to attempt to restore arterial wall integrity, but results in further endothelial dysfunction and plaque formation.

As our knowledge of the basic science underlying atherosclerosis has improved, however, a new focus has evolved on aspects of plaque composition rather than stenosis severity as a key determinant of future CVD events. Research studies, largely post-mortem pathology studies, have suggested that certain features of plaque composition appear to be related to likelihood of plaque rupture and clinical CVD events. This has led to such plaques being labelled as unstable or “vulnerable plaques”, a paradigm now widely embraced in cardiology and the subject of enormous research efforts worldwide.

2.2 The Vulnerable Plaque

The composition of plaques has been studied for over 200 years. Table 1 lists the historical milestones in our understanding of atherosclerosis. It is now known that in the majority of acute CVD events, the arterial plaque ruptures, exposing the plaque contents to blood within the lumen, triggering an inflammatory response mediated by platelets and culminating in thrombosis. This inevitably led to the next question, namely “Which plaques tend to rupture?” A number of ‘high risk’ features have been described, including a thin fibrous cap and large lipid pool. However, it was during the quest to understand the mechanisms of plaque rupture that the significance of the vasa vasorum (VV) was recognised.

The vasa vasorum (Latin: ‘*arteries of the arteries*’) form a microvascular network on the outside of arteries and arterioles. In health, they are responsible for providing the tunica adventitia and outer aspects of the tunica media with oxygen (the tunica intima and inner aspect of the tunica media rely on diffusion of oxygen from blood within the lumen). As alluded to in Table 1, it was recognised decades ago that the VV appeared to proliferate significantly in areas of atherosclerotic plaque formation. The pathological reasons for this have now been elucidated.

When an atherosclerotic lesion develops within the intima, the distance between the deeper intimal layers and the luminal surface increases, producing hypoxia within the plaque once the oxygen diffusion threshold (250-500 μ m) is exceeded.⁴¹ This stimulates the release of pro-angiogenic factors (most notably hypoxia-inducible factor alpha [HIF- α]) that induce proliferation of the VV. This neovascularisation, an attempt to restore normal oxygen tension, also arborizes from the adventitia into the media and intima, growing within plaques, thus known as intra-plaque neovascularisation (IPN).⁴²

Date	Details
1799	English physician Caleb Hillier Parry ⁴³ notes during autopsy a hard and gritty material in the coronary arteries and “well remembered looking up to the ceiling, which was old and crumbling, conceiving that some plaster had fallen down”. He discovers, however, that the vessels had hardened, and states that “a principle cause of the syncope anginosa is to be looked for in disordered coronary arteries”.
1844	Fenger <i>et al</i> ⁴⁴ first describe “plaque rupture” during the autopsy of Danish artist Bertel Thorvaldsen, stating that the vessel wall “contained several atheromatous plaques, one of which quite clearly had ulcerated, pouring the atheromatous mass into the arterial lumen”.
1858	Rudolf Virchow ⁴⁵ describes “atheroma” as a dermal cyst, a fatty mass encapsulated within a fibrous cap
1876	Köster ⁴⁶ first alludes to a relationship between atherosclerosis and the vasa vasorum, noting that atherosclerotic vessels were associated with “ectopic vascularization” of the media and intima.
1938	Paterson ⁴⁷ and Winternitz ⁴⁸ separately describe the association between plaque haemorrhage and events, noting that plaque neovessels and haemorrhage were found in virtually all recent coronary thrombosis cases.
1983	Imparato <i>et al</i> ⁴⁹ report intraplaque haemorrhage in 31% of 376 carotid plaques studies and find it is the only characteristic associated with symptoms
1984	Barger <i>et al</i> ³⁹ directly link adventitial and intra-plaque neovascularisation to atherosclerosis in human coronary arteries
1984	English pathologist Michael Davies ⁵⁰ describes plaque rupture as the cause of coronary thrombosis in 90% sudden cardiac death cases
1987	Glagov <i>et al</i> ⁵¹ introduce the concept of outward remodelling of vessel walls, before luminal compromise occurs
1989	Muller <i>et al</i> ⁵² categorizes haemodynamically insignificant but dangerous lesions as “vulnerable plaques”
1996	Mann and Davies ⁵³ show that plaque cap thickness and size of the lipid core are not related to stenosis severity or plaque volume
2000	Virmani <i>et al</i> ⁵⁴ introduce a classification scheme for plaques, categorizing the vulnerable plaque as a thin-cap fibroatheroma (TCFA).

Table 2.1: Historical milestones in understanding of plaque biology

The on-going accumulation of plasma components perpetuates this cycle until, eventually, the plaque is enveloped in extensive VV and IPN, a hallmark of atherosclerosis. However, these neo-vessels are immature with a single endothelial layer in the wall and without matrix support. Thus, they are inherently leaky, with incomplete endothelial junctions and detached basement membranes noted⁵⁵ – and thought to be the primary cause of intraplaque haemorrhage (IPH). Presence of IPH has been linked with symptomatic plaques – erythrocyte cell membranes are rich in cholesterol and thus contribute to the lipid pool of the plaque core and free haemoglobin within the plaque is lysed resulting in generation of harmful reactive oxygen species, further increasing lipid peroxidation and macrophage activation. As a result, it is now widely thought that IPN is a pre-cursor for IPH, in itself a feature that increases risk of plaque rupture. Therefore, the presence of IPN is now considered as a surrogate marker of plaque vulnerability (see figures 2.1 & 2.2).

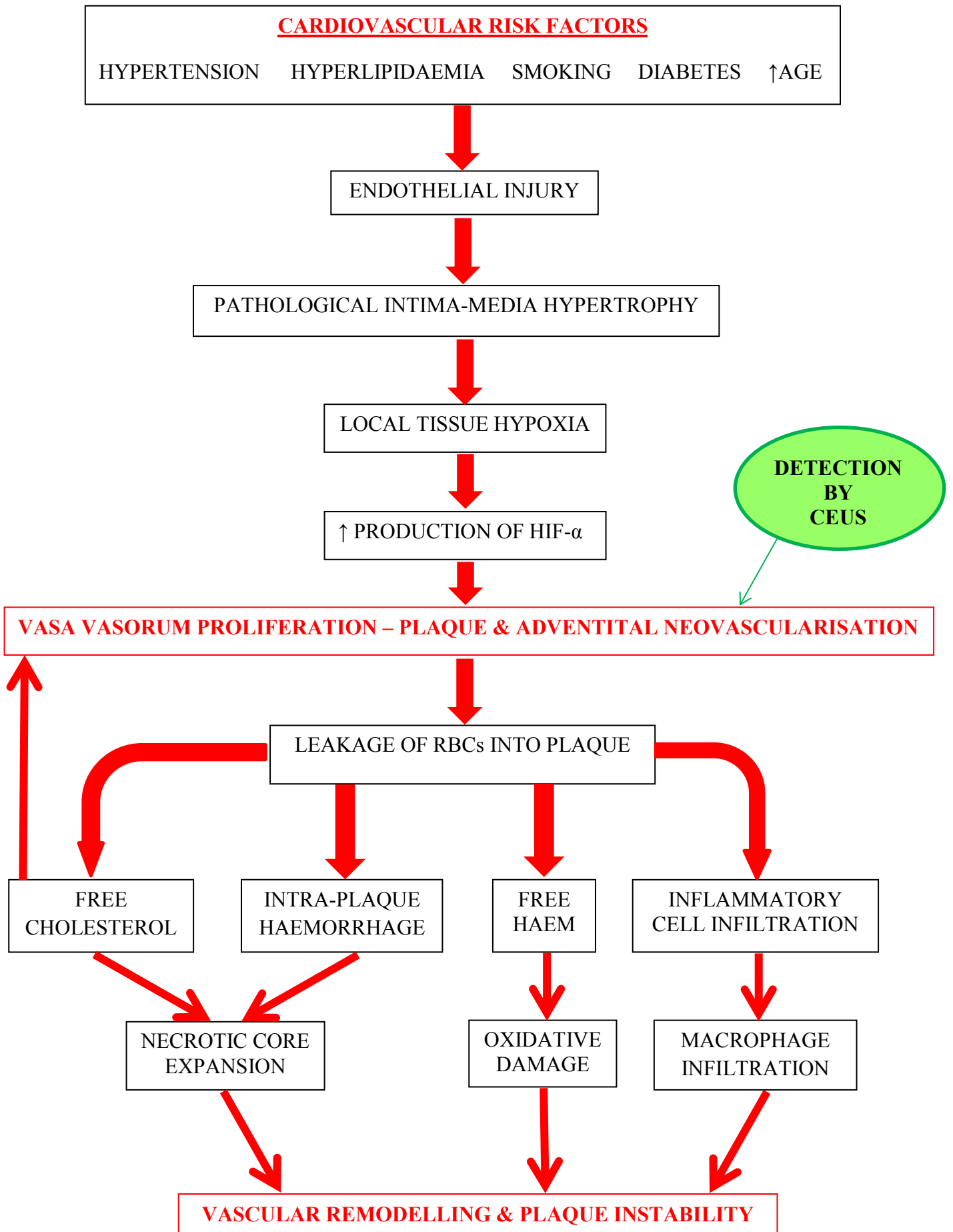
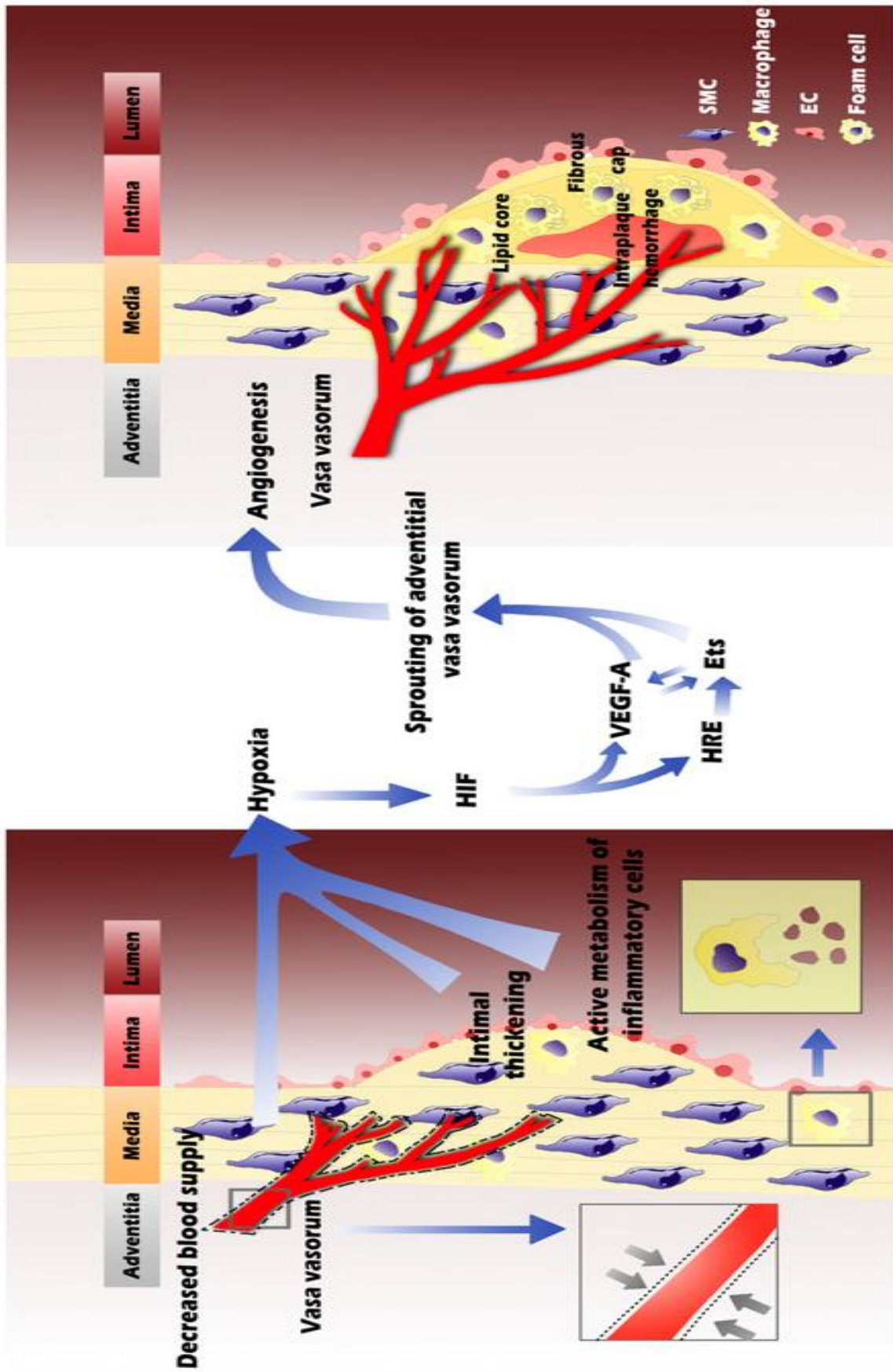


Figure 2.1 (previous page): Flow diagram illustrating the patho-aetiology of atherosclerotic plaque and intraplaque neovascularisation and the time-point within this pathological cascade at which contrast-enhanced ultrasound can detect plaque neovascularization. (HIF- α = Hypoxia Inducible Factor-alpha)

Figure 2.2 (following page): Left panel - Intimal thickening, a reduced blood supply (due to high pressure in parent vessel and the stimulated constriction of vasa vasorum [VV], represented by grey arrows in the left closed box) and active metabolism of inflammatory cells together contribute to hypoxia in atherosclerotic vessels. Right panel – The oxygen-insufficient microenvironment in inner layers of vessel wall further induces angiogenesis through activating HIF, VEGF-A and Ets signalling pathways. As a result, the formation of IPN originating from VV leads to the progression of atherosclerotic plaques, including intraplaque haemorrhage, lipid core enlargement, inflammatory cell infiltration, and ultimate rupture (Reproduced from Xu et al⁵⁶).



2.3 Intra-Plaque Neovascularization – a marker of plaque vulnerability?

A large amount of data has been gathered from observational studies on the association between IPN and plaque symptomatology and also patient outcomes. Initially these were predominantly pathological studies (post-mortem and ante-mortem) but recently, our ability to detect IPN has improved with imaging techniques, as listed in Table 2.

In a post-mortem study looking at the walls of the iliac, renal and carotid arteries, Fleiner *et al* compared 22 patients with symptomatic atherosclerosis with 27 patients free from CVD and found that patients with symptomatic atherosclerosis had a significantly denser network of VV than patients free from CVD.⁵⁷ These findings were supported by a UK study in 2007, in which Dunmore *et al* analysed carotid plaques from endarterectomy patients and compared the histological findings against presence or absence of related symptoms prior to surgery.⁵⁸ They found that only symptomatic plaques contained highly irregular, dysmorphic and immature vessels lacking smooth muscle cells. They concluded that these microvessels may be linked to plaque instability and symptoms.

Finally, in a landmark prospective prognostic study, Hellings *et al* published early results from the Dutch Athero-Express study, in which 818 patients undergoing carotid endarterectomy had plaques collected and analysed histologically for content and were then followed-up for 3 years.⁵⁹ The primary outcome was a vascular event (death, stroke or MI) or vascular intervention and this was significantly more common in patients whose plaques had contained IPH or marked IPN, thus concluding that local plaque composition is an independent predictor of future CVD events. Beyond pathological studies, however, recent advances in technology have allowed for non-invasive identification of plaque content / composition and these are discussed below.

2.4 Imaging the Vulnerable Plaque – Methods of Detection

Plaque characteristics may be assessed by several non-invasive imaging techniques, as described below.

2.4.1 Ultrasound

Carotid ultrasonography permits visualization of plaques – whilst location, size, area and volume can all be determined, the echogenicity of plaques can also be studied (figure 2.3). A number of studies have reported on the correlation between plaque echogenicity and composition on histological analysis – echo-bright plaques tend to have high calcium content and have been termed ‘hard plaques’ whilst echo-lucent plaques tend to have a low calcium content and thus are sometimes termed ‘soft plaques’.^{60, 61} The echolucent plaques also tend to contain a larger lipid pool, greater necrotic core and have been shown to have a higher proportion of macrophages,⁶² thus linking echolucency with plaque inflammation. However, the sensitivity and specificity of echolucency for prediction of plaque neovascularisation and / or plaque haemorrhage is only modest.⁶³

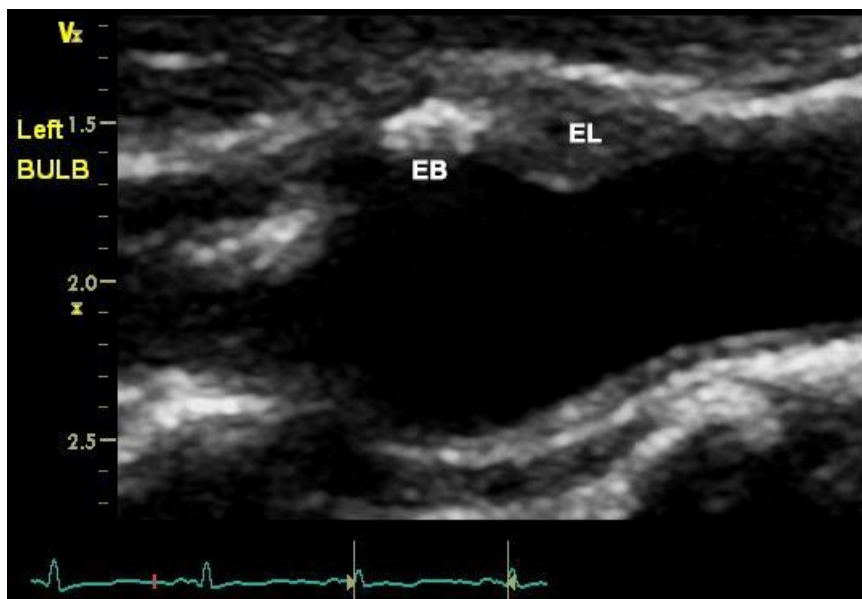


Figure 2.3: B-mode image showing echobright (EB) and echolucent (EL) regions of a near wall carotid plaque, corresponding to so-called 'hard' and 'soft' regions of a plaque respectively.

Plaque heterogeneity has also been investigated (with heterogeneous plaques reported to contain many more calcifications)⁶¹ and shown to improve the accuracy of predicting plaque haemorrhage over echolucency alone.⁶⁴ Plaque echolucency and heterogeneity have been combined for optimal sensitivity in the ultrasonic assessment of plaque composition, although specificity remained poor.⁶⁵

Contrast-enhanced ultrasound (CEUS) is the investigative technique employed in the studies presented in this Thesis. CEUS has gained attention in recent years after the first report, a decade ago, that carotid arteries could be assessed during contrast administration for improved image quality. Ultrasound contrast agents (UCAs) consist of gas-filled microbubbles that resonate when exposed to an ultrasound wave. Thus, their mechanism of improving image quality is separate from other contrast agents used in imaging, such as the iodine-based agents used in x-ray angiography and computed tomography (CT) and gadolinium-based agents used in magnetic resonance imaging (MRI). This is predominantly a non-linear oscillation (i.e. expansion and contraction of the bubble are not equal) at the ultrasound frequencies used in diagnostic imaging. Microbubbles are several million times more effective at scattering sound than red blood cells, resulting in a greatly enhanced “blood pool” signal.⁶⁶ The blood pool agents developed consist of a gaseous material encapsulated within a stabilizing outer shell. These microbubbles are typically slightly smaller than erythrocytes, allowing free passage within the circulation and effectively acting as red cell “tracers”.⁶⁷

These microbubbles are most frequently utilised during ultrasound imaging of the heart – echocardiography – to improve image quality. However, in 2004, American researchers reported the use of ultrasound contrast during carotid ultrasonography, demonstrating that the IMT of the near wall – frequently sub-optimally visualised on B-mode ultrasound – was more clearly defined after contrast (see figure 2.4).⁶⁸

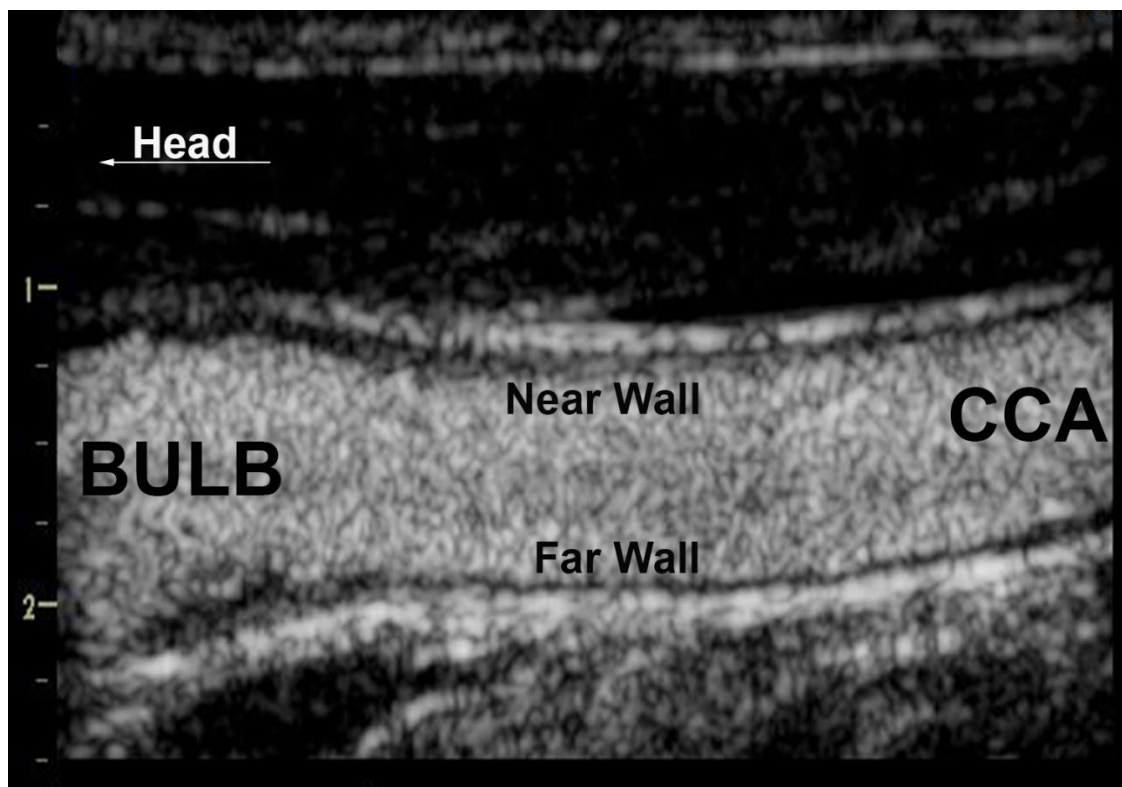


Figure 2.4: Contrast enhanced ultrasound image of a human common carotid artery (CCA). The tunica adventitia is seen as an echo-bright structure whilst the intima-media complex is black in CEUS imaging, providing clear definition against the white appearance of the contrast bubbles within the arterial lumen.

This study followed on from earlier experimental work by Sirlin *et al*, who showed that use of ultrasound contrast was superior to colour or power Doppler techniques for identifying

experimentally induced aortic plaques.⁶⁹ The same group then first demonstrated that CEUS could be used to identify IPN; as contrast bubbles travel wherever erythrocytes travel, contrast bubbles enter the neovessels within plaques, which was detected by CEUS (figure 2.5). They showed a good correlation with histological neovessel density.⁷⁰ A number of studies using CEUS for IPN identification have since been published (see Table 2.2).

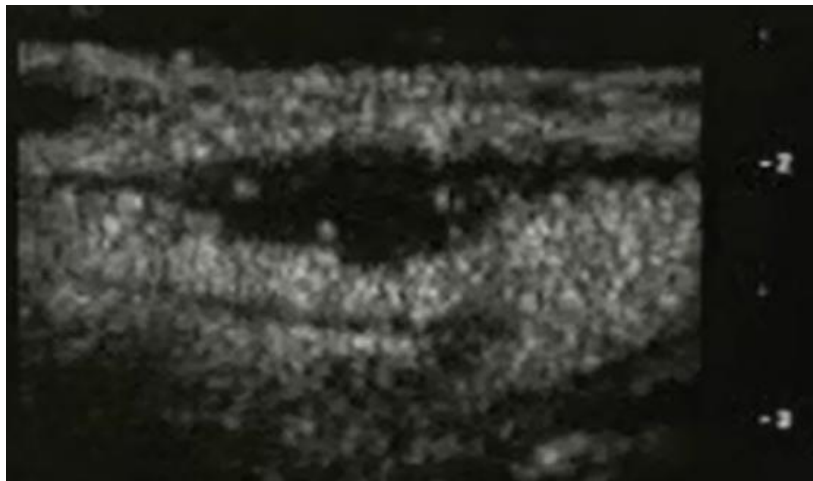


Figure 2.5: Early human CEUS scan demonstrating a large near wall plaque (black) with multiple neovessels (white spots) seen within [courtesy of Prof Steve Feinstein, USA].

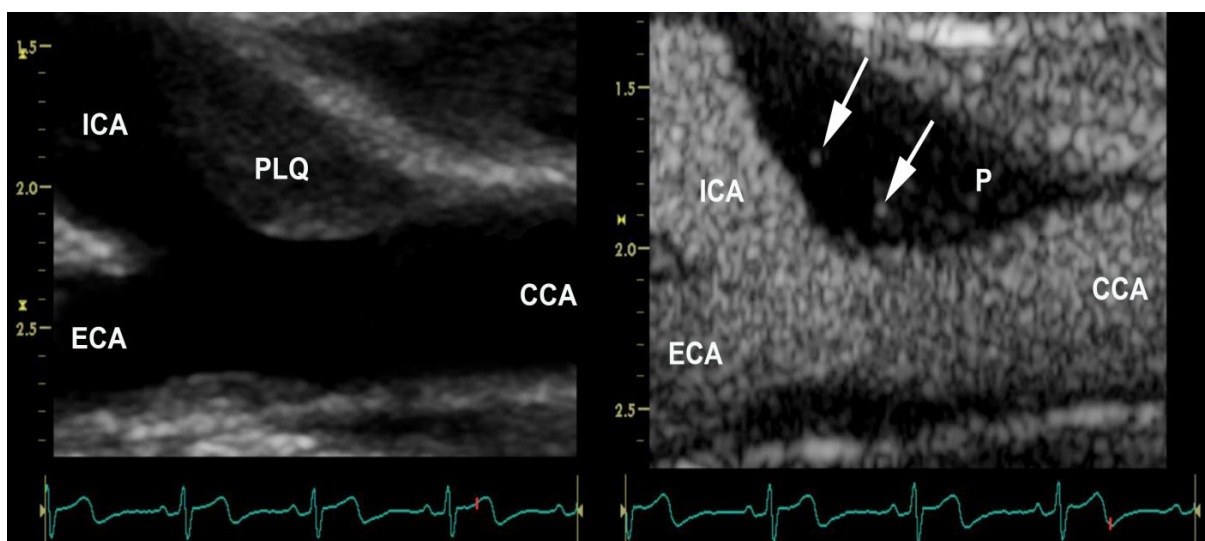


Figure 2.6: B-mode (left) and CEUS (right) images showing a large echolucent plaque (PLQ) at the carotid bifurcation with clear IPN noted during CEUS imaging (white arrows)

Table 2.2: Key studies in humans published to date regarding IPN as studied by CEUS

Author	Year	n	Contrast Agent	Findings
Shah <i>et al</i> ⁷⁰	2007	15	Optison	1 st validation study, showing that IPN on CEUS correlated with neovessel density on histology
Vicenzini <i>et al</i> ⁷¹	2007	23	Sonovue	IPN found in fibrous & fatty areas of plaques but not calcific or necrotic regions
Coli <i>et al</i> ⁷²	2008	32	Optison	CEUS findings correlated with histology. IPN more common in echolucent plaques, unrelated to stenosis severity.
Giannoni <i>et al</i> ⁷³	2009	77	Sonovue	IPN strongly associated with symptomatic plaques and infrequently seen in asymptomatic plaques
Xiong <i>et al</i> ⁷⁴	2009	104	Sonovue	IPN more commonly seen in symptomatic plaques than asymptomatic plaques (80% vs. 30%)
Huang <i>et al</i> ⁷⁵	2010	176	Sonovue	Greater plaque enhancement due to IPN was associated with risk of stroke
Staub <i>et al</i> ⁷⁶	2010	147	Opt / Def	IPN more frequent in patients with previous CVEs
Staub <i>et al</i> ⁷⁷	2011	175	Opt / Def	IPN correlated positively with degree of stenosis and inversely with plaque echogenicity (i.e. as plaque echogenicity ↑ ,IPN ↓)
Shalhoub <i>et al</i> ⁷⁸	2011	31	Sonovue	IPN identified on late phase CEUS associated with other plaque features of inflammation
Zhou <i>et al</i> ⁷⁹	2013	46	Sonovue	IPN associated with micro-embolic signals on trans-cranial Doppler
Van den Oord <i>et al</i> ⁸⁰	2013	69	Sonovue	Majority (90%) of asymptomatic patients with familial hypercholesterolaemia have plaques, and majority of plaques (86%) demonstrate IPN
Zhu <i>et al</i> ⁸¹	2013	312	Sonovue	IPN seen in 82% ACS patients vs. 44% with stable CHD (p < .001). IPN was a significant and independent predictor of future coronary events in patients with stable CHD

[NB – Def = Definity; Opt = Optison]

2.4.2 Cross-Sectional Imaging – CT & MRI

CT has been used for almost two decades for accurate detection of stenoses in both carotid and coronary vessels. The use of CT for assessing plaque morphology and composition is based upon density measurements, expressed in Hounsfield units (HUs), with all value normalized to the density of water (0 HU).⁶³ CT can be used to assess plaque ulceration⁸² and plaque calcification⁸³, although the correlation between CT findings and size of the plaque lipid core, even using more contemporary multi-slice CT scanners, remains sub-optimal.⁸⁴ This is since the soft tissue contrast of CT is low, producing weak correlations with ‘soft’ plaque components. Furthermore, several studies assessing accuracy of CT compared these findings against intravascular ultrasound (IVUS) findings,^{85, 86} itself an imaging technique and thus not a true gold standard for validation purposes.

MR angiography is increasingly used in clinical practice for evaluation of arterial stenosis, but the development of a number of MR sequences that permit multiple contrast weightings for individual plaque components has allowed their differentiation during imaging. MR imaging of the human carotid artery has been shown to allow measurement of fibrous cap thickness,⁸⁷ detection of cap ulceration and detection and measurement of the size of the lipid pool⁸⁸ and intraplaque haemorrhage⁸⁹, both recognised surrogate markers for plaque instability. It may also be feasible to estimate the age of intra-plaque haemorrhage using contrast-enhanced MRI.⁸⁹ Gadolinium-contrast enhanced MRI can also detect adventitial vasa vasorum⁹⁰ and, finally, studies using super para-magnetic iron oxide particles have facilitated detection of markers of plaque inflammation (e.g. macrophage accumulation.)^{91, 92}

2.4.3 Positron Emission Tomography (PET)

In positron emission tomography (PET) – the most advanced form of nuclear imaging – the scanner visualises the temporal and spatial distribution of tracers labelled with positron-emitting radionuclides, the most commonly used being 18-fluorodeoxyglucose (¹⁸FDG). FDG has been shown to accumulate in areas of inflammation and studies have now shown that PET imaging of the carotid artery reveals increased ¹⁸FDG uptake within atherosclerotic plaques⁹³ and that this correlates with macrophage density upon subsequent immunohistochemical staining of CEA specimens.⁹⁴ This is potentially of great clinical relevance – for example, a recent study in ischaemic stroke patients found that early stroke recurrence was higher in patients with increased FDG uptake in the ipsilateral plaques compared with patients without early stroke recurrence.⁹⁵

2.5 Intra-Plaque Neovascularization and CEUS – Current Status

The studies published to date using carotid CEUS have shown that CEUS allows improved visualisation of near-wall IMT, allows visualisation of vasa vasorum (VV) & IPN, that plaque enhancement during CEUS is due to a greater degree of IPN and that the presence & degree of VV and IPN correlates with plaque rupture and MACE.

In the following Chapter, the questions that have yet to be answered concerning CEUS are addressed, thus setting out the premise for the research studies contained within this Thesis.

CHAPTER 3 – THE UNKNOWNNS of PLAQUE NEOVASCULARIZATION

3.1 Impact of Ethnicity on Plaque Neovascularization in Asymptomatic Individuals

To date, almost all published reports have examined IPN either in post-mortem studies or in symptomatic patient groups (e.g. patients with stroke undergoing CEA). There are no studies that have examined the determinants of IPN (as detected non-invasively using CEUS) in a healthy asymptomatic cohort. As IPN appears to be an important component of the vulnerable plaque, and thus by definition a vulnerable *patient*, the possibility of early identification of important subclinical disease – namely plaque with IPN in asymptomatic subjects – raises the possibility of using CEUS to screen “at-risk” individuals. Almost 2000 participants in the Atherosclerosis Risk in Communities (ARIC) study underwent MRI in a sub-study to correlate baseline clinical variables with plaque characteristics, but unfortunately IPN was not evaluated.⁹⁶

Furthermore, in those studies that have assessed IPN in humans, these have been performed in one country, with no specific mention of ethnic origin of the patients and the relationship between incidence of IPN and ethnicity has not been well defined. As the incidence of CVD varies across the globe between individuals of different ethnic origin, the incidence of IPN between different ethnic groups may also vary.

3.1.1 Cardiovascular Risk and Asian Ethnicity

India is the second most populous nation on Earth, with a population in excess of 1 billion at the last census. Prior to partition under the British Empire, India also comprised the modern-day nations of Pakistan and Bangladesh, thus creating a land mass and population so large, it became known as the “sub-continent”, a phrase still widely used today. People that originate

from India, Pakistan and Bangladesh are often collectively referred to as of South Asian (SA) ethnic origin.

South Asians have migrated to many parts of the globe, initially through colonial systems and, later, to the United Kingdom (UK) when under British rule. As a result, in addition to the UK, a large number of South Asians are also to be found in many island countries such as the West Indies, Mauritius and Fiji as well as African countries including Tanzania, Kenya, Uganda and South Africa. It became clear, from a number of early studies, that these migrant SA populations carried a far greater CVD burden compared with the native populations.⁹⁷⁻⁹⁹

The excess burden of CVD amongst the SA migrants has long been the subject of study and research in the UK. National statistics derived from the census revealed, decades ago, an apparent difference between SA and native individuals with regards to CVD mortality.^{100, 101} Furthermore, studies conducted upon migrant families demonstrated that siblings that remained in the sub-continent had a *lower* CVD risk profile – assessed by surrogate markers such as blood glucose and cholesterol levels – than their siblings that had migrated to the UK.¹⁰²

3.1.2 Why are South Asians at Higher Cardiovascular Risk?

It has frequently been argued that the main reason for higher CVD risk in SA populations is related to cultural and life-style issues, ranging from food content (e.g. ghee versus olive oil) and methods of preparation (e.g. steamed vs. fried) to exercise habits (active vs. sedentary).¹⁰³ Although there is some truth to these stereotypes, they provide an incomplete explanation for the observed differences in CVD risk. Biomarker studies have shown greater levels of inflammatory markers such as C-reactive protein.¹⁰⁴ As atherosclerosis is now widely considered a chronic inflammatory condition, this finding has raised interest in the field but, to

date, the finding remains an observation with no definitive study demonstrating that there is a direct causal relationship between circulating CRP levels and CVD risk.¹⁰⁵

More recently, novel inflammatory markers such as lipoprotein A [LP(a)] and homocysteine have been the subject of much research and, although both these markers have been found in higher concentrations in South Asians^{102, 106}, their role in CVD causation – if any direct role – remains undetermined.

3.1.3 Risk Stratification: Are Risk Models Valid in South Asians?

The Framingham Study⁶ – initiated after the end of the Second World War to elucidate the reasons for CVD death amongst Americans – was conducted in the small eastern American town of Framingham, Massachusetts. The enrolled study cohort – just over 5000 individuals – were over-whelmingly homogenous in ethnic origin (native white) and this has led many to question the external validity of such a model. This is especially true in SA populations, where studies have shown that the Framingham Risk Score under-estimates CVD risk.^{107, 108}

This finding has also been observed using different scoring systems. Tillin *et al* presented data from a cohort study of almost 4000 multi-ethnic individuals living in west London.¹⁰⁹ Follow-up data revealed that both the Framingham and QRISK-2 scoring systems under-estimated CVD risk in SA individuals. Kanjilal *et al*¹¹⁰ published their results derived from a cohort enrolled between (2003-2005) into the Indian Atherosclerosis Research Study (IARS), a family-based genetic epidemiological study, with the aim of investigating the genetic factors associated with CAD and also their interaction with traditional risk factors in a SA cohort in their home country. The performances of the Framingham score, Joint British Societies (JBS) score and the European SCORE (Systematic Coronary Risk Evaluation) models were studied.

The authors found that the Framingham-based risk scores (Framingham and JBS) and the European SCORE underestimated the risk of CVD morbidity and mortality, both in men and women, from an estimated high risk SA cohort.¹¹⁰

The risk factor profile itself varies between SA and EW subjects. Smoking is less commonly seen in the SA community, especially amongst SA women. However, it is widely recognised that the age-standardised prevalence of diabetes is higher in people of SA origin compared with the EW population.^{103, 111, 112} Older studies have suggested that type 2 diabetes is 3-5 times more commonly observed in the SA community, though more recent studies suggest the gap is smaller,¹¹³ though still noticeably larger amongst SA individuals.

3.1.4 The London Life Sciences Prospective Population (LOLIPOP) Study

The LOLIPOP study is a large, community-based study initiated in west London in 2002. The principal aim of the study is to improve understanding of the reasons for development of CVD amongst South Asians in comparison with European Whites. Over 30,000 individuals aged 35-74 years, free from established CVD, were initially recruited into the study between 2002-2008. Individuals were classified as South Asian if all 4 grand-parents were born in the Indian sub-continent and European White if all 4 grand-parents were born in Northern Europe.

Following extensive baseline questionnaires and physical examination, a proportion of these participants (~2800) took part in the LOLIPOP-Atherosclerosis sub-study, in which patients underwent trans-thoracic echocardiography and carotid ultrasonography at Northwick Park Hospital, Harrow. The carotid arteries of 2288 healthy subjects free from CVD were analysed for IMT, plaque presence and plaque echogenicity. This data obtained from SA and EW subjects revealed that, after adjustment for cardiovascular risk factors, there were no significant

differences between SA and EW subjects in cIMT, plaque presence or plaque echogenicity.¹¹⁴ This led to the conclusion that the increased CVD risk observed in SA individuals cannot be attributed to a greater sub-clinical burden of atherosclerosis. This suggested that other mechanisms, yet to be elucidated, were at play.

In Chapter 5, we describe the results of a study in which some of these subjects returned to undergo CEUS imaging for determination of IPN frequency between EW and SA individuals. This project was undertaken in order to attempt to understand better the potential reasons for differing CVD burdens between EW and SA populations. As this has not previously been studied, we suggest that this data could be used to inform the planning of a significant large epidemiological study using non-invasive imaging to assess IPN in an asymptomatic community cohort and to examine the independent correlates of IPN formation and, prospectively, the impact of IPN upon outcome. Such a study would clearly require many thousands of patients but, as recently highlighted by Professor Renu Virmani,

*“the current technologies for carotid imaging like ultrasound, MRI and CT need to be carried out in a large cohort of asymptomatic individuals with non-critical stenosis with the goal of identifying high-risk plaques with systematic follow-up”.*⁶³

CEUS, by virtue of its ability to identify IPN as a marker of the high-risk plaque, would satisfy the criteria for such a study (wide availability, portable, safe, painless, no ionising radiation) and therefore this initial work will hopefully facilitate such a study in the future.

In addition, these images also allow us to examine the effectiveness of CEUS at improving visualisation of the carotid arterial tree. Although it has been shown that CEUS improves

visualisation of the near-wall IMT⁶⁸ and also results in fewer non-diagnostic scans,¹¹⁵ it is not known whether CEUS improves visualisation of carotid arterial segments and, therefore, whether a greater number of plaques are detected. The ICA is frequently incompletely seen on B-mode ultrasound – a recent analysis of the Framingham Offspring Cohort Study¹⁹ found that only ICA IMT and ICA plaque burden provided incremental risk stratification benefit over the Framingham Risk Score itself – and thus improved visualisation of the ICA by CEUS, if this is found, may be of significant clinical value. We therefore also propose to analyse the CEUS scans to determine whether CEUS results in superior arterial segments visualisation and plaque detection.

3.2 Intra-Plaque Neovascularization & Radiotherapy

3.2.1 Radiotherapy and the Vascular System

Globally, the incidence of most cancers is increasing each year. Radiotherapy (RT) remains a mainstay of therapy for a number of different malignancies. Cardiac toxicity is one of the most concerning side effects of anti-cancer therapy. The gain in life expectancy obtained with efficacious treatment can be compromised by increased morbidity and mortality associated with its cardiac complications.¹¹⁶ While radio-sensitivity of the heart was initially recognized in the 1970s, the heart is regarded in the current era as one of the most critical dose-limiting organs in RT.

Radiotherapy (RT) damages arterial walls and promotes atherosclerotic plaque formation. The carotid arteries frequently receive significant incidental doses of radiation during RT treatment of malignancies, especially head and neck cancers (HNC). Radiation vasculopathy had until recently been considered quite a rare entity, as patients would frequently succumb to their malignancy first. However, as cancer survival rates improve, patients are “outliving” their malignancies and presenting later with the long-term sequelae of cancer therapy.¹¹⁷

The patho-physiology of radiation-induced arterial damage remains incompletely understood. Over forty years ago, three distinct mechanisms for arterial vessel damage were proposed: ischaemic necrosis (due to occlusion of vasa vasorum), adventitial fibrosis (producing extrinsic compression) and accelerated atherosclerosis.¹¹⁸ Early radiation damage is thought to be characterised by an inflammatory process. What has remained unclear is the extent to which subsequent development of a “clinically significant” stenosis is under-pinned by a chronic

inflammatory process (with cytokine release and fibrosis) or a chronic ischaemic process (with vasa vasorum thrombosis and thus vessel wall ischaemic injury).¹¹⁹

Several studies have shown that RT of the carotid arteries is associated with increased intima-media thickness (IMT) and increased carotid plaque formation – the consequences of RT upon the carotid arteries (imaging studies) and future CV events (outcome studies) have recently been comprehensively reviewed.¹¹⁹ However, for a multitude of reasons, the literature displays marked heterogeneity in this field with a number of problems associated with these studies.

First, studies that have reported an increased relative risk of CVE after RT have either used non-matched control groups or have matched their HNC patients to geographically distinct and distant population data,^{120, 121} sometimes derived from another country. Studies have not always reported upon stroke sub-type (ischemic or haemorrhagic)¹²² and information on CVE has not always been judged by a clinician or by brain imaging, but by patient questionnaires.¹²³ Finally, and possibly most importantly, the majority of these studies did not provide data on the laterality of the stroke. For example, if the right carotid artery has been exposed to RT, a clinical ischaemic event would – in almost all but the rarest cases – be expected in the right cerebral hemisphere and thus produce left sided signs (e.g. paresis, reduced sensation). However, this level of detail is not available in many prior research papers; thus, although one would assume that an ischaemic CVE must be related to the RT-side carotid artery, the data confirming this are absent.

As a result of these short-comings in the existing data, several questions regarding radiation vasculopathy remain unanswered, most prominent of which is the mechanism by which RT affects the arterial wall and subsequently appears to increase stroke risk. Although the effects

of RT on carotid IMT and plaque burden have been documented, the effect of RT on plaque composition has not been studied in humans.

3.2.2 Expected effects of Radiotherapy upon angiogenesis

The published literature to date is heterogeneous on this issue. Prior research in animal models has suggested that irradiation dose-dependently induces the activation of the pro-angiogenic nitric oxide pathway in endothelial cells through increases in endothelial nitric oxide synthase activity.¹²⁴ Furthermore, the survival and subsequent recurrence of neovessels after RT has been proposed as a potential mechanism to explain tumour recurrence.¹²⁵

A recent review article has provided a comprehensive overview on the effects of radiation upon angiogenesis.¹²⁶ In summary, the effects of ionizing radiations on angiogenesis are more complex than previously thought and there are now at least three distinct ways in which radiation can affect vessel growth:

- 1) The photons of electromagnetic radiations stimulate vessel growth at least in part, by causing the increased expression of angiogenic factors.

- 2) Low Linear Energy Transfer (LET) charged particles, such as protons, inhibit angiogenesis by an unknown mechanism (decreased expression of angiogenic factors is implicated).

- 3) High LET heavy ions, such as iron [Fe] ions, also inhibit angiogenesis by an unknown mechanism that affects the later stages of tubulogenesis.¹²⁶

As a result, a collaborative study between the Royal Brompton (Cardiology) and Royal Marsden (Oncology) hospitals was planned in order to examine the effect of RT upon IPN further. As carotid arteries are inevitably exposed to RT during treatment of head and neck cancers, the study was designed to recruit survivors of such malignancies that had received RT as part of their treatment. Importantly, only patients with *unilateral* RT would be included, thus allowing use of the contra-lateral, non-irradiated artery to act as an internal self-control for each patient. The effect of RT upon the carotid arteries was thus studied by B-mode and CEUS imaging and this study forms the basis of Chapter 7.

3.3 Quantitative vs. Qualitative Assessment of Intra-Plaque Neovascularization

3.3.1 Quantification – The Holy Grail of Contrast Imaging

Technological advances in medical imaging over the past quarter century have facilitated significant improvements in the abilities to confirm diagnoses, estimate disease burden, perform risk stratification and estimate prognosis by non-invasive methods. A number of these imaging techniques – whether using ultrasound or cross-sectional modalities such as computed tomography (CT) and magnetic resonance imaging (MRI) – rely upon the use of contrast agents to enhance the diagnostic yield of imaging.

Iodine-based (CT) and gadolinium-based (MRI) contrast agents are widely used in daily practice and, over the past two decades, ultrasound contrast agents (UCAs) have also been used in clinical cardiology and, more recently, in diagnostic radiology laboratories as well. To date, the use of contrast has permitted visual – that is, *qualitative* – assessment of tissues but a more objective – that is, *quantitative* – measure is preferable to improve accuracy and reproducibility and reduce the intra- and inter-observer variability of these imaging techniques. Consequently, much research effort of late has focussed upon the ability to quantify contrast images in cardiovascular imaging.

CEUS has emerged in the past decade as a research tool of significant interest, permitting visualization of IPN and adventitial vasa vasorum and thus allowing insights into plaque composition. This is especially true in view of our ability to study the human carotid artery (owing to its superficial location that facilitates imaging) and then confirm these findings with histological specimens, given that such plaques are frequently excised during endarterectomy procedures.

3.3.2 CEUS Quantification – The Technical Challenges

There are several technical challenges that must be addressed in order to produce an accurate and robust tool for quantitative analysis of CEUS images. One of the most challenging problems is that of plaque motion. Motion of the plaque occurs inherently as the arteries are pulsatile, but also occurs additionally due to patient breathing, patient motion (including swallowing) and transducer motion, even if slight, by the operator. Thus, correcting for motion is an essential initial step in any quantification algorithm. Secondly, perfusion within plaques is weak and intermittent, unlike perfusion of larger organs such as the liver. Thus, conventional quantitative approaches, such as using average time-intensity curves, are most likely to be inappropriate for plaque assessment.¹²⁷ Thirdly, the region of interest (i.e. within plaques) is relatively small and surrounded by much larger structures with potential to cause significant artefact – namely, the lumen and adventitia. Fourthly, a large sample size is required to have greater confidence in the reproducibility of the results but this has proven challenging to date. Finally, the ‘validation’ of the newly developed quantification software should ideally be against a ‘gold standard’, which in this case would be histology. However, many studies have validated algorithms against visual accuracy, a false gold standard and thus real accuracy remains unknown.

3.3.3 CEUS Quantification – Limitations to Current Approaches

Since the first description of CEUS for assessment of plaque composition almost a decade ago⁷⁰, the vast majority of CEUS studies have reported on qualitative analysis of IPN, namely presence or absence of IPN. Although semi-quantitative scales have been proposed⁷², a universally-accepted and validated methodology for quantification of CEUS images is still awaited. A number of research groups have published in-house approaches to CEUS quantification (see table 3.1).

Author	Year	Human /Animal	n	Contrast Agent	Quantification Approach	Findings
Moguillansky <i>et al</i> ¹²⁸	2011	Animal	20	Definity	Contrast video-intensity curves	CEUS can quantify development of adventitial vasa vasorum associated with atherosclerosis
Hoogi <i>et al</i> ¹²⁹	2011	Human	27	Definity	In-house software using MatLab®	Ratio of IPN area: total plaque area showed good correlation between CEUS and histology ($R^2=0.79$)
Hoogi <i>et al</i> ¹³⁰	2012	Human	76	Sonovue	Bubble tracking algorithm using Matlab	In-house software shows very good agreement with visual analysis of presence and extent of IPN
Hjelmgren <i>et al</i> ¹³¹	2013	Human	30	Sonovue	In-house contrast quantification programme	In-house software shows very good agreement with visual analysis of presence and extent of IPN
Van den Oord <i>et al</i> ¹³²	2013	Human	62	Sonovue	In-house software using MevisLab	No direct comparisons made between quantitative analysis and visual analysis (no histology)
Akkus <i>et al</i> ¹²⁷	2014	Human	23	Definity	MevisLab-MATLAB quantification combination software package	IPN surface area shows good agreement ($r=0.71$) with visual analysis of IPN presence
Muller <i>et al</i> ¹³³	2014	Human	33	Sonovue	In-house software using MatLab®	In-house software shows very good agreement with visual analysis & histology for presence of IPN
Zhang <i>et al</i> ¹³⁴	2015	Humans	34	Sonovue	In-house software using MatLab®	In-house software showed good correlation between CEUS and histological mean vessel density ($R^2=0.85$)

Table 3.1: Published studies (human and animal) reporting on accuracy of quantification software. Of note, many studies ‘validated’ their algorithm(s) against visual analysis of CEUS images rather than against histological specimens

However, none of these software algorithms have been proven or validated external to their centre of development and none are available for wider commercial use. In addition, many of the “validation” studies of such software in fact only compared the newly developed quantification software against visual accuracy – rather than histology – and thus did not use a true “gold standard” for comparison. As alluded to above, the perfusion pattern of plaques is both intermittent and weak in nature, meaning that extrapolation of traditional quantitative methods used in solid organs, such as time intensity curve analysis, is unlikely to be valid. However, this has been the approach adopted in some prior studies.^{74, 135}

The methodology used for motion compensation is crucial to determining the accuracy of a quantification algorithm. In summary, two approaches can be used, namely rigid and non-rigid motion compensation. A number of studies have used a ‘block matching’ approach,^{80, 127, 136, 137} which is a form of rigid motion compensation – although simple to use, this approach cannot account for as many types of motion as non-rigid compensation (as may be encountered, for example, when a patient swallows or breathes during imaging). Rigid motion compensation can account for rotational and translational motion only, whereas non-rigid algorithms can account for affine, scaling and skew motion in addition.

Furthermore, the methods used to track bubble motion have potential for further improvement. The Multi Dynamic Programming (MDP) plus block matching approach favoured by some investigators^{127, 130} requires a pre-defined ‘bubble template’ and performs an ‘optimization’ to track the bubble path, which takes more computational time. An algorithm that does not require such a template would be more user-friendly if it was relatively fast.

Accordingly, the final goal of this research project was to assist in the development and validation of novel quantification software that could be used for analysis of CEUS images. This involved collaboration with a team of biomedical physicists from Imperial College London. The study planned to validate the novel software against histological specimens. In order to achieve this, ethical approval was sought to recruit patients from a district hospital in London, awaiting carotid endarterectomy, to a study that would allow CEUS imaging and also permit collection of the excised plaque from theatre for histopathological analysis. Estimated neovessel density, as determined quantitatively using the novel software, would then be compared against the true neovessel density as seen in histological assessment of the excised plaques.

THESIS AIMS and OBJECTIVES

This thesis explores the potential clinical value of contrast-enhanced carotid ultrasound (CEUS) of the carotid arteries for assessment of atherosclerotic plaque composition, in particular presence of intra-plaque neovascularisation (IPN). CEUS is a relatively new imaging technique and is at present a research tool. Translation of its use from the research arena to the clinical arena will require demonstration of potential incremental clinical value over existing practice.

This thesis describes scientific investigations that aimed to study diverse groups of individuals using CEUS to improve our mechanistic understandings regarding atherosclerosis and thus, hopefully, enhance the evidence base and provide new avenues for future research that may help CEUS become a relevant tool in clinical practice for improving patient care and patient outcomes.

The aims and objectives of this thesis were as follows:

- 1) To study the prevalence and determinants of intra-plaque neovascularisation, as detected by CEUS, in a healthy asymptomatic cohort of individuals derived from a large population study.
- 2) To study the prevalence and determinants of intra-plaque neovascularisation in irradiated carotid arteries from survivors of head and neck malignancies that had previously received radiotherapy.

3) To assist in the development of novel quantification software for the objective assessment of intra-plaque neovascularization during CEUS and validate this software against histology obtained from patients clinically scheduled for carotid endarterectomy.

4) To determine whether contrast-enhanced ultrasound can improve the visualization of carotid arterial tree segments and thereby improve the assessment of the extent of carotid arterial disease and sub-clinical atherosclerosis (i.e. improved visualization of IMT and number of plaques).

PART II

RESULTS of the RESEARCH STUDIES

CHAPTER 5

Contrast Enhanced Ultrasonography of Human Carotid Arteries Improves Intima-Media Thickness Visualization and Improves Carotid Plaque Detection.

5.1 ABSTRACT

Background

Carotid intima-media thickness (IMT) and plaque are recognised markers of increased risk for cerebrovascular events. Accurate visualization of the IMT complex and plaques is dependent upon clear image quality. Ultrasound contrast agents improve image quality during echocardiography, but whether contrast enhanced ultrasound (CEUS) improves carotid IMT visualization and plaque detection in an asymptomatic patient population is unknown.

Methods

Individuals free from known cardiovascular disease (CVD), enrolled in a community study, underwent B-mode and CEUS carotid imaging. Each carotid artery was divided into 10 segments (proximal, mid and distal segments of the common carotid artery [CCA], the carotid bulb and internal carotid artery [ICA]) and each segment had near and far walls assessed. The visualization of the IMT was scored semi-quantitatively as not clearly visualized (0), partially visualized (1) or clearly visualized (2), thus yielding a maximal possible visualization score of 20. Presence of plaque was defined as per the Mannheim consensus. IMT visualization and plaque assessments were made during both B-mode and CEUS imaging for all enrolled subjects.

Results

A total of 175 individuals underwent B-mode and CEUS imaging (mean age 65±9yrs). Visualization of the IMT was significantly improved during CEUS compared with B-mode imaging, in both near and far walls of the carotid arteries (% IMT visualization during B-mode vs. CEUS imaging: 61% vs. 94% and 66% vs. 95% for right and left carotid arteries, $p<0.001$ for both). Additionally, a greater number of plaques were detected during CEUS imaging compared with B-mode imaging (367 plaques vs. 350 plaques, $p=0.02$).

Conclusion

CEUS improves visualization of the intima-media complex, in both near and far walls, of the common and internal carotid arteries, and permits greater detection of carotid plaques. Further studies are required to determine if there is incremental clinical and prognostic benefit related to superior plaque detection by CEUS.

5.2 INTRODUCTION

The most common cause of mortality worldwide remains cardiovascular disease (CVD), an umbrella term encompassing myocardial infarction, stroke and peripheral vascular disease. A number of clinical risk scoring systems and imaging techniques have been investigated for their potential ability to identify individuals at higher risk of CVD outcomes. Following the initial description of use of high-resolution B-mode ultrasound to visualize the carotid arterial wall,¹⁴ a large number of longitudinal population studies have shown that the carotid intima-media thickness (IMT) is a surrogate marker of atherosclerosis and associated with cardiovascular risk factors¹³⁸ and CVD outcomes.¹³⁹⁻¹⁴² A pooled analysis of 8 population-based studies, with a total sample size of 37,197 subjects and mean follow-up of 5.5 years, found that for each absolute increase in carotid IMT of 0.1mm, there was a 10-15% increased risk of myocardial infarction and 13-18% increased risk of ischaemic stroke.¹⁵ Carotid IMT has also been shown to be a superior biomarker of stroke risk compared to coronary artery calcium score.^{18, 143}

The IMT, measured as the distance from the lumen-intima interface to the media-adventitia interface, consists almost entirely of media in healthy adolescents.²² This distance is approximately 0.6 - 0.7mm in health and increases with age. IMT varies with gender and is typically greater in men. Normal ranges for IMT, however, have proved challenging to provide as these vary depending upon which wall of the artery is used (near wall or far wall), which ultrasound system, which carotid segments are assessed (e.g. just common carotid artery [CCA] or internal carotid artery [ICA] also) and whether measurements were made using manual calipers or by automated edge-detection software.²²

The IMT can be difficult to visualize, especially in the proximal portion of the internal carotid artery, due to ultrasound artefacts. The IMT of the near wall, in particular, is frequently less clear than that of the far wall. Ultrasound contrast agents, comprising millions of acoustically-active gas-filled microspheres, improve ultrasound image quality and have been used in clinical echocardiography for a number of years. Over a decade ago, American investigators reported use of contrast-enhanced ultrasound (CEUS) to improve near-wall IMT visualization.⁶⁸ In 26 patients, they found that IMT measurements taken during CEUS imaging were significantly greater (12-25%) than those taken during B-mode imaging, consistent with an earlier report which had proven – using histological comparison as a gold standard – that near-wall IMT measurements were significantly under-estimated by B-mode ultrasound.¹⁴⁴

If improved visualization of the IMT permits superior detection of carotid plaques, then this potentially has very important clinical value. Since IMT increases with age can often be attributed to hypertension-induced thickening of the media due to smooth muscle hypertrophy, it has been suggested that arterial plaques are a more accurate marker of burden of atherosclerosis than IMT alone. Although it has been shown that CEUS improves visualisation of the carotid near-wall IMT⁶⁸ and also results in fewer non-diagnostic scans¹¹⁵, it is not known whether CEUS improves visualization of carotid arterial segments in asymptomatic individuals free of known CVD and, therefore, whether a greater number of plaques are detected. The internal carotid artery (ICA) is frequently incompletely seen on B-mode ultrasound and a recent analysis of the Framingham Offspring Cohort Study found that only ICA IMT and ICA plaque burden provided incremental risk stratification benefit over the Framingham Risk Score itself¹⁹ – and thus improved visualisation of the ICA by CEUS, if this is found, may be of significant clinical value. This study was therefore undertaken to determine the effect of CEUS upon IMT visualization and carotid plaque detection.

5.3 METHODS

B-mode and CEUS images were analysed from asymptomatic South Asian and European White individuals enrolled in the London Life Sciences Population (LOLIPOP) study, a large community-based study in west London undertaken to better understand the patho-biological mechanisms underlying the differences in CVD burden between Asian and Caucasian populations.

Patient Selection

Individuals initially underwent B-mode imaging and, of those with carotid arterial plaque detected, a randomly selected group of patients were invited to return for repeat carotid imaging, this time by B-mode and CEUS imaging. B-mode, colour Doppler and contrast enhanced carotid ultrasonography were performed using a high-resolution ultrasound system (Vivid-7; General Electric Healthcare, Chalfont, Bucks, UK) equipped with a broadband linear array (3-11 MHz) transducer. ECG monitoring was performed continuously throughout the scan and arterial blood pressure was recorded using an automated sphygmomanometer.

Carotid Imaging

In summary, the proximal, mid, and distal common carotid artery (CCA), bifurcation of the CCA and proximal portion of the internal and external carotid arteries were systematically interrogated in long-axis and short-axis views. After B-mode imaging, an intravenous cannula was inserted and two vials (8mL) of Sonovue ultrasound contrast (Bracco Diagnostics, Milan, Italy) were administered as a continuous intravenous infusion using a specific pump (Vueject, Bracco, Milan, Italy) at a standardized rate of 1.2 mL/min, providing approximately 6.5 minutes of contrast opacification. During this time, the right and left carotid arteries were re-imaged using a specific low MI contrast pre-set (MI 0.20).

Image Analysis

All images were stored on disc for off-line analysis, which was performed in random order after all patients had been scanned. The left and right carotid arteries consist of five distinct sections – namely, the proximal, mid and distal common carotid artery, the carotid bulb (point of bifurcation) and the internal carotid artery – each of which has a near wall and a far wall (thus a total of 10 segments). We employed a semi-quantitative scoring system to determine IMT visualization during B-mode and CEUS imaging. The scores assigned were as follows:

- 0 Carotid IMT poorly visualized along entire length of the segment
- 1 Carotid IMT partially visualized
- 2 Carotid IMT clearly visualized along entire length of the segment

Thus, as each artery had 10 segments to be scored (5 near wall and 5 far wall), a maximum possible visualization score was 20 (see figure 5.1 below).

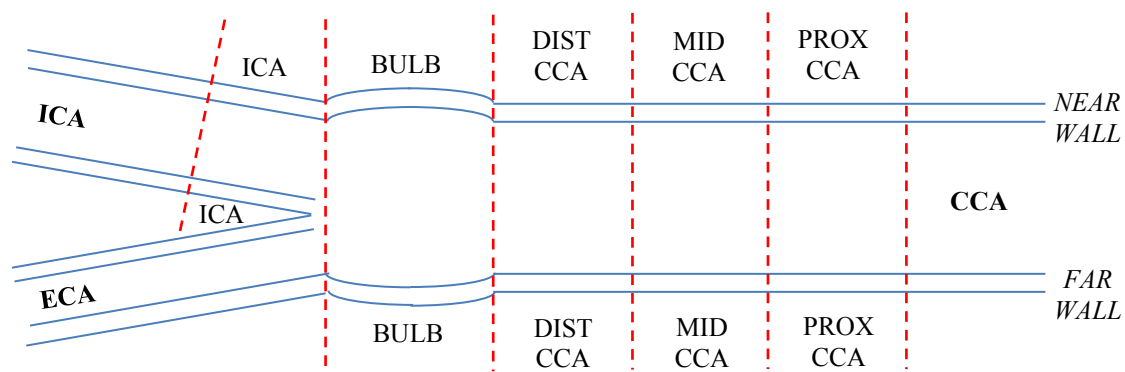


Figure 5.1: Illustration of a common carotid artery (CCA) with bifurcation into its internal (ICA) and external (ECA) branches. Ten segments were assigned for each carotid artery, five in each near wall and five in each far wall.

Plaque was defined as per the Mannheim consensus as a focal structure encroaching into the arterial lumen by >0.5 mm, a distinct area of IMT $>50\%$ greater than the adjacent wall or >1.5 mm in thickness.²⁶ The presence of plaque was judged in each of the ten segments of every carotid artery in all subjects and documented in a spreadsheet. Importantly, in an attempt to minimise observer bias, CEUS images were *not* interpreted immediately after the B-mode images of a particular individual. A random number generator was utilised and thus CEUS and B-mode images were analysed in random order and without viewing the B-mode and CEUS images of each individual ‘together’ as a ‘pair’ of studies. This was done to eliminate the possibility of viewing a plaque on CEUS images as the observer was ‘primed’ to its presence having just reviewed the B-mode images.

In cases when there was a discrepancy between B-mode and CEUS imaging, these scans were re-analysed with close attention paid to plaque echogenicity on the B-mode study. The most frequently used system for assessing plaque echogenicity is the Gray-Weale scoring system,¹⁴⁵ although prior studies have demonstrated only modest inter-observer reproducibility of this scale.¹⁴⁶ Consequently, in order to minimise the risks of such a problem, a simplified rating scale was devised for plaques on B-mode analysis, comprising:

- Predominantly echolucent ($>50\%$ plaque area has low echogenicity)
- Predominantly echogenic ($>50\%$ plaque area has high echogenicity)
- Mixed plaque ($\sim 50\%$ echolucent and 50% echogenic areas)

Reproducibility Studies

Intra-observer and inter-observer reproducibilities were assessed for both IMT visualization and plaque detection. Ten randomly selected patients had their B-mode and CEUS images re-

analysed segment-by-segment, documenting both IMT visualization score and presence/absence of plaque. This was done for both left and right carotid arteries, thus a total of 20 carotid segments were evaluated in each patient. Intra-observer analyses were performed >1 month after initial analysis. For inter-observer analysis, a second reader blinded to all clinical data of the subjects performed segmental analyses. Therefore, in total, reproducibility data were assessed as follows:

- 1) Intra-observer agreement on IMT visualization during B-mode imaging
- 2) Intra-observer agreement on IMT visualization during CEUS imaging

- 3) Intra-observer agreement on plaque presence during B-mode imaging
- 4) Intra-observer agreement on plaque presence during CEUS imaging

- 5) Inter-observer agreement on IMT visualization during B-mode imaging
- 6) Inter-observer agreement on IMT visualization during CEUS imaging

- 7) Inter-observer agreement on plaque presence during B-mode imaging
- 8) Inter-observer agreement on plaque presence during CEUS imaging

Random numbers were generated using a free online random number generator (Research Randomizer, www.randomizer.org).

Statistics

Continuous variables are expressed as mean \pm standard deviation and categorical variables as proportions. Data was tested for 'normalcy' – to determine whether parametric or non-

parametric tests were applicable – using the Shapiro-Wilk test and skewness & kurtosis parameters. However, as the distribution of the differences between the two methods was normal, a paired t-test was used to compare plaque detection between B-mode and CEUS imaging techniques. Inter-and intra-observer agreements were examined using Cohen’s kappa statistic. For all tests, a p value <0.05 was considered statistically significant. All analyses were conducted using SPSS version 19.0 (SPSS Inc, Illinois, USA).

5.4 RESULTS

A total of 175 patients were studied. The mean age was 64.7±8.9yrs and 140 (80%) were male. The complete baseline demographics of the patients are listed in table 6.1.

CHARACTERISTIC	TOTAL (/175) [%]
Mean Age (yrs ± SD)	64.6 ± 8.7
Male Gender	140 [80]
Hypertension	93 [53]
Hyperlipidaemia	89 [51]
Type 2 DM	36 [21]
Smoking History	12 [7]
Family History	58 [33]

Table 5.1: Baseline patient characteristics

Effect On IMT Visualization

On B-mode imaging, there was significantly better visualization of far wall IMT compared to near wall IMT in both left and right carotid arteries – figure 5.2 illustrates examples of clear far and near wall IMT and clear far wall but poor near wall IMT, respectively.

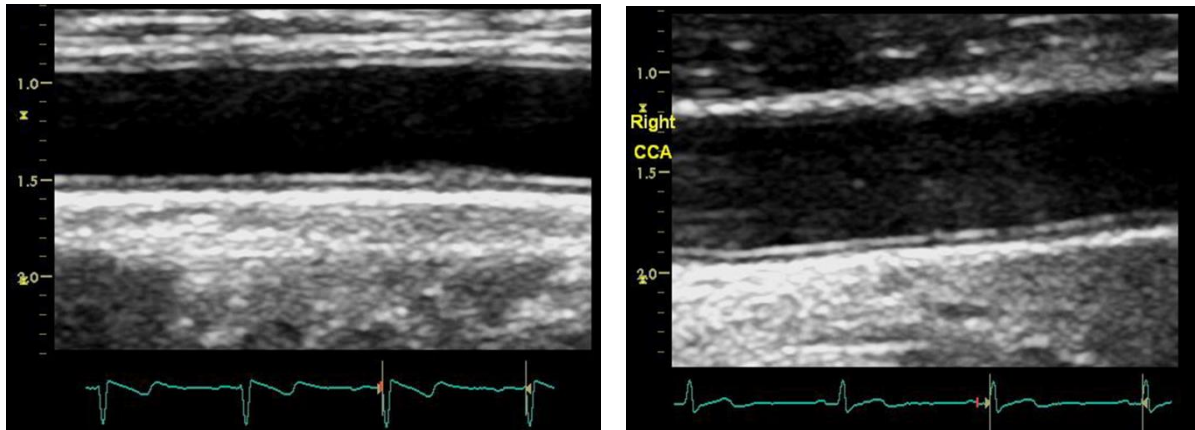


Figure 5.2: B-mode examples of clear IMT visualization in both near and far arterial walls (left) and an example of a clear far wall but poor near wall IMT visualization (right).

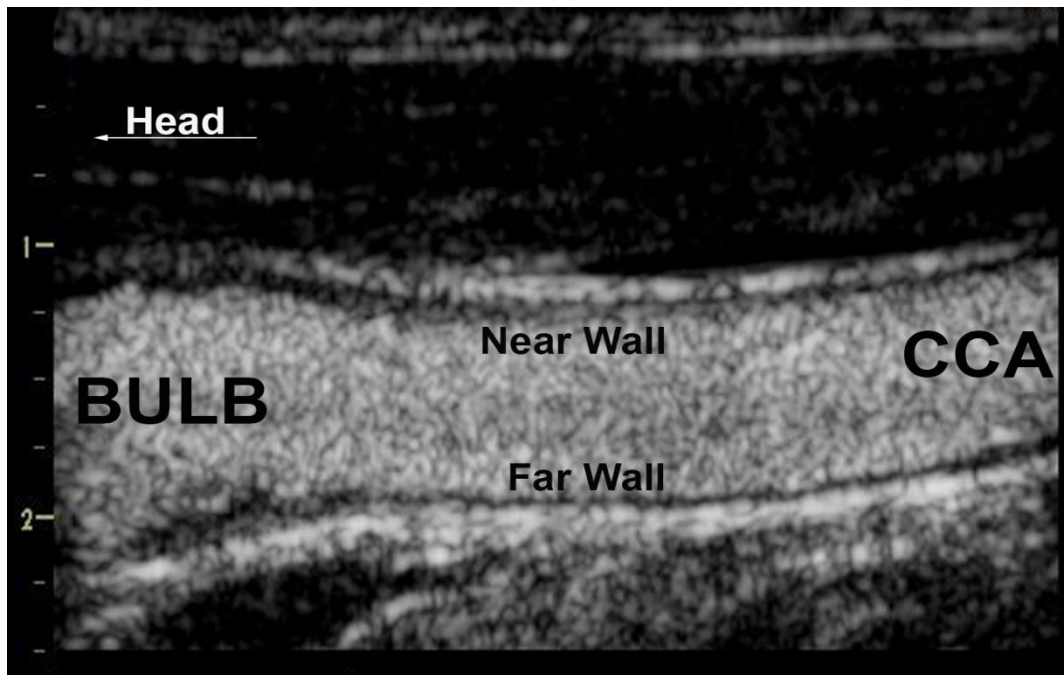


Figure 5.3: Example of near wall and far wall visualization during CEUS imaging.

CEUS significantly improved the percentage of segments in which IMT visualization was good (i.e. score = 2/2 – see figure 5.3), in all segments and also specifically in the ICA segments (see table 5.2).

Measurement	B-mode scan	CEUS scan	P value
Right IMT visualised (%)	61	94	<0.001
Left IMT visualised (%)	66	95	<0.001
Right ICA IMT visualised (%)	23	86	<0.001
Left ICA IMT visualised (%)	27	86	<0.001

Table 5.2: IMT visualization during B-mode and CEUS imaging, in all segments and in the ICA only.

The average visualization scores for the near wall and far wall of the right and left carotid arteries are presented in table 5.3. It should be noted that though CEUS improved IMT visualization compared with B-mode imaging, even during CEUS imaging there was a significantly greater IMT visualization of the far wall compared to the near wall.

	B-Mode Scan (/10)	CEUS Scan (/10)	P value
<i>RIGHT</i>			
Near Wall IMT Score	4.6±2.5	9.1±1.2	<0.001
Far Wall IMT Score	7.5±1.7	9.7±0.8	<0.001
P Value	<0.001	<0.001	
<i>LEFT</i>			
Near Wall IMT Score	5.4±2.4	9.3±1.0	<0.001
Far Wall IMT Score	7.7±1.7	9.7±0.8	<0.001
P Value	<0.001	<0.001	

Table 5.3: Mean near wall and far wall IMT visualization scores for the right and left carotid arteries during B-mode and CEUS imaging. Each score has a maximum possible value of 10 (5 segments per wall). IMT visualization was significantly improved by contrast in both near and far walls, but we also found that far wall IMT scores remained superior to near-wall IMT scores during CEUS.

Effect on Plaque Detection

A total of 350 plaques were detected on B-mode imaging and 367 during CEUS imaging. Figure 5.4 demonstrates that during both B-mode and CEUS imaging, by far the most common location for plaques was the carotid bulb, followed by the internal carotid artery whilst the common carotid artery was the least common location for plaque formation.

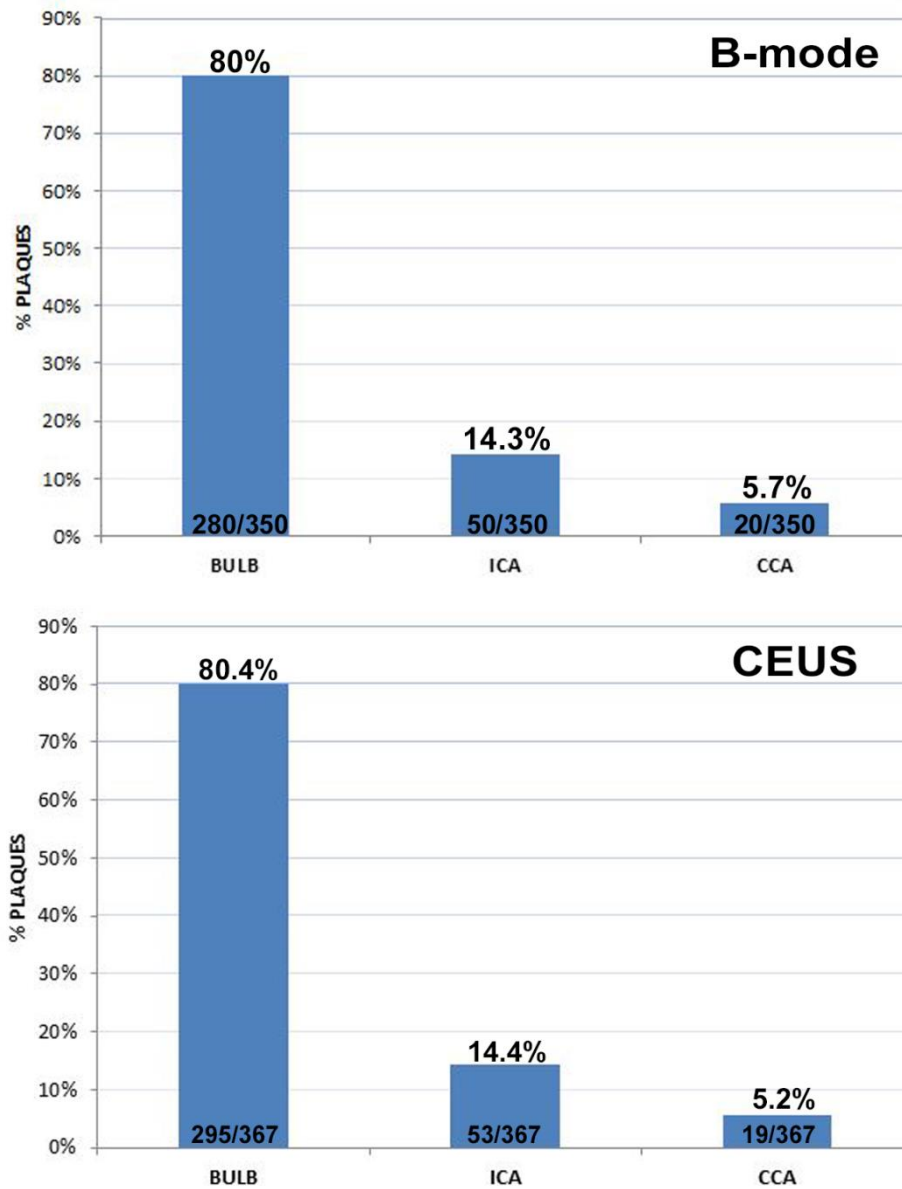
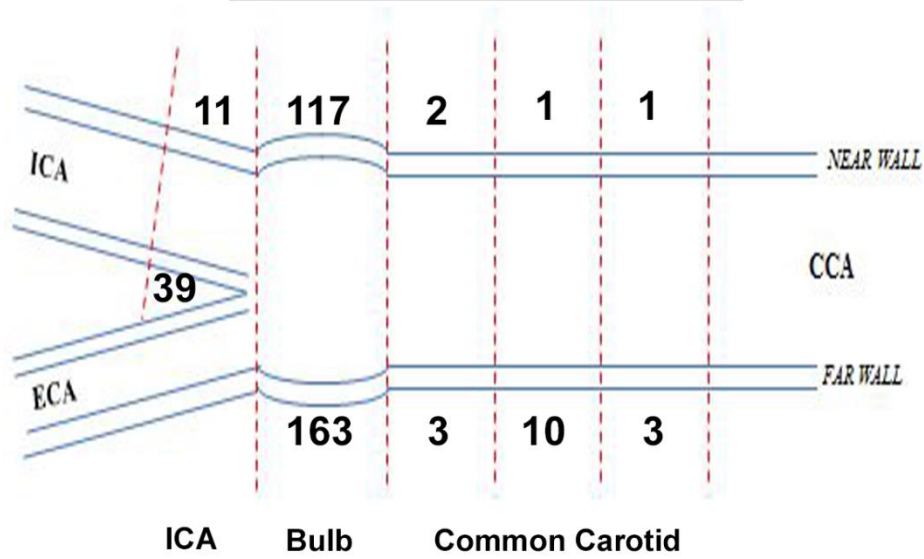


Figure 5.4: Distribution of plaques within the carotid arterial tree during B-mode and CEUS imaging.

The majority of plaques detected were in the far wall rather than the near wall, as shown in figure 5.5.

Plaque Distribution - B-mode



Plaque Distribution - CEUS

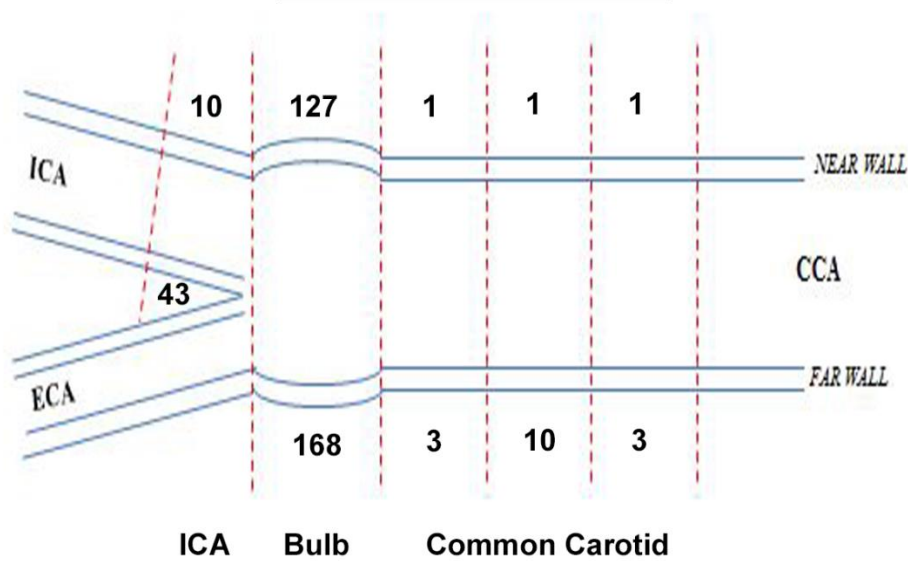


Figure 5.5: Number of plaques detected in each segment of the carotid artery during B-mode and CEUS imaging. A greater number of plaques were found in the far wall than in the near wall, in both B-mode and CEUS imaging. The CCA was the least common site for plaque formation.

Discrepancies between B-mode and CEUS imaging

There were a greater number of plaques detected during CEUS imaging than in B-mode imaging (367 vs. 350, $p=0.02$ by paired t-test). Table 5.4 demonstrates the categories of plaque detection between B-mode and CEUS imaging:

Row	Category	No. of patients (%)
1	B-mode plaque number = CEUS plaque number	131 (74.9)
2	No plaques on B-mode, Plaques on CEUS	4 (2.3)
3	No plaques on CEUS, Plaques on B-mode	4 (2.3)
4	CEUS plaque number > B-mode plaque number	27 (15.4)
5	B-mode plaque number > CEUS plaque number	9 (5.1)

Table 5.4: Categories of plaque detection between B-mode and CEUS imaging

In $\frac{3}{4}$ of the patients, the number of plaques detected on B-mode imaging was the same as during CEUS imaging. There were just 8 patients (4.6%) in whom plaques were seen during one modality (B-mode or CEUS) and not detected during the other. In a fifth of all patients (36/175), plaques were seen in both B-mode and CEUS imaging but the exact number detected differed.

There were 31 patients in whom plaques were seen on CEUS imaging that were not detected during B-mode imaging (rows 2 & 4 in table 5.4 above). In these 31 patients, 88 plaques were detected by CEUS imaging versus 56 plaques by B-mode imaging, thus a difference of 32

plaques. Of these 32 plaques, 15 were in the bulb near wall, 12 in the bulb far wall, 2 in the ICA near wall and 3 in the ICA far wall. Thus, all of the extra plaques detected by CEUS were in the carotid bulb (27/32, 84%) or proximal ICA (5/32, 16%). On the other hand, there were 13 patients in whom plaques were seen on B-mode imaging that were not detected during CEUS imaging (rows 3 & 5 in table 5.4 above). In these 13 patients, 30 plaques were detected by CEUS imaging versus 15 plaques by B-mode imaging, thus a difference of 15 plaques. Of these 15 plaques, 6 were in the bulb near wall, 7 in the bulb far wall, 1 in the ICA near wall and 1 in the distal CCA near wall. Thus, in summary, there were 32 extra plaques detected by CEUS but also 15 plaques missed by CEUS (detected by B-mode) thus yielding an overall difference of 17 extra plaques detected by CEUS.

Exploring these results in greater detail, of the 32 plaques detected on CEUS imaging but not seen on B-mode imaging, 25 (78%) were predominantly hypo-echoic with no or minimal calcium seen on B-mode imaging. Conversely, of the 15 plaques detected on B-mode imaging and not identified during CEUS imaging, 11/15 (73%) were predominantly echo-bright plaques (i.e. high calcium content) on B-mode imaging.

There were also 4 patients in whom there was diagnostic uncertainty whether shadowing in the carotid bulb represented plaque or ultrasound artefact (after assessment in both long and short axis views). Each of these instances referred to the carotid near wall. In all 4 cases, CEUS imaging revealed a normal bulb with no plaques visualized (see figure 5.6 below).

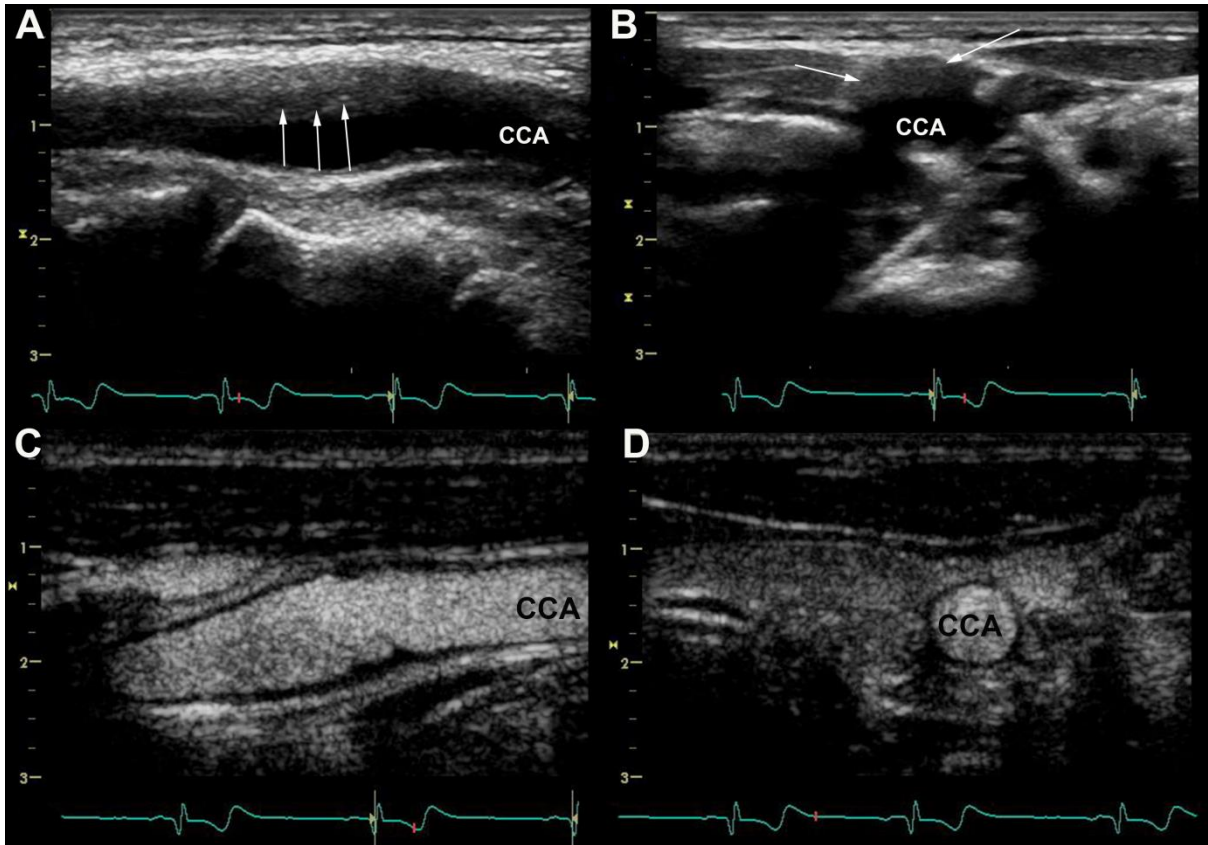


Figure 5.6: Suspicion of a large plaque (arrows) in long and short (panels A & B) axis images during B-mode imaging that were proven artefacts on CEUS imaging (panels C & D).

Reproducibility Studies

Intra-observer and inter-observer reproducibilities were assessed for IMT visualization and plaque detection in both carotid arteries of 10 randomly selected patients (thus 20 arteries in total). This was done for both the B-mode and CEUS images in each patient. The full segment-by-segment results are illustrated in Appendix 2. However, in summary, excellent agreement was observed in both intra- and inter-observer agreement during both B-mode and CEUS imaging with respect to both IMT visualization and plaque detection.

Intra-observer agreement for plaque presence or absence was 100% ($k = 1.0$) in the common carotid artery segments and either 90%, 95% or 100% agreement in the bulb and ICA segments.

Inter-observer agreement for plaque detection was also excellent, with 100% agreement in all CCA segments except the distal CCA near wall (in which there was 95% agreement) and 85-95% agreement in the bulb and ICA segments.

6.5 DISCUSSION

The principal findings of this study are firstly that CEUS improves carotid IMT visualization compared with B-mode imaging, secondly that even in CEUS imaging, far-wall IMT visualization remains superior to near-wall IMT and thirdly that CEUS imaging permitted detection of a significantly greater number of carotid plaques.

The conventional approach to CVD risk stratification involves identification and quantification of the presence of CVD risk factors and then estimating the future risk of a CVD event using a recognised scoring model.¹⁴⁷ In the UK, this is the lifetime CVD risk using the 3rd Joint British Societies' (JBS-3) system and, in the US, the 10-year CVD risk using the Framingham Risk Score (FRS). The FRS has several well-described limitations, including estimation of 10-year rather than lifetime risk, failure to account for ethnicity and family history of CAD and a binary (present or absent) approach to risk factors such as diabetes mellitus and smoking, whereas a continuous relationship may be more appropriate.¹⁴⁷ Furthermore, chronological age is the predominant determinant of the FRS, thus potentially adversely skewing risk prediction in a number of elderly but otherwise healthy individuals.¹⁴⁸

As a result, it is hypothesized that patients in the intermediate risk group may benefit most from measurement of subclinical atherosclerosis to help refine risk stratification further.¹⁴⁹ Increased IMT has been associated with a higher risk of stroke, myocardial infarction and CVD death in

several large (>1000 subjects) longitudinal prospective studies of healthy asymptomatic individuals.^{139-141, 150-154} Studies have also revealed a high prevalence of carotid atherosclerosis (including raised IMT) in individuals with low FRS scores.¹⁷ IMT has been shown to be more likely than coronary artery calcium score to revise the FRS.¹⁷ Indeed, a recent large analysis from the Multi-Ethnic Study of Atherosclerosis (MESA study), involving 6562 subjects, found that ultrasound-derived plaque metrics independently predicted CVD events and improved risk stratification in addition to Framingham risk factors, with the mean maximal IMT measurement showing greatest Net Reclassification Improvement.¹⁵⁵

Against this background, our results that IMT visualization is significantly improved by CEUS imaging – in both common and internal carotid arteries – potentially has great utility. CEUS improved visualization of near wall IMT, in keeping with previous studies,⁶⁸ but also far wall IMT. The facilitation of accurate IMT measurement may help identify patients in whom risk reduction therapies may be helpful but also may help exclude sub-clinical disease in patients whose B-mode images are sub-optimal, thus potentially sparing them pharmacological agents such as statins and anti-platelet drugs.

Our results also demonstrate that even during CEUS imaging, optimal far wall IMT visualization is superior to optimal near wall IMT visualization. The near wall in carotid imaging frequently suffers from ultrasound artefacts, indeed our findings extend those of Macioch et al,⁶⁸ who first reported use of CEUS to improve near wall IMT visualization, because in addition to improving near wall IMT visualization in the common carotid artery, we also found superior IMT visualization in both near and far walls of the internal carotid artery. As subclinical atherosclerosis in the ICA has been suggested as a superior marker of adverse risk as opposed to the CCA,¹⁹ this finding, we hypothesized, would permit superior plaque

detection. Thus, the ability to improve IMT visualization by CEUS in itself will permit more accurate IMT assessment.

A significantly greater number of plaques were detected by CEUS imaging compared to B-mode imaging. The results show that although some plaques were detected by B-mode imaging that were missed by CEUS, a far greater number were missed by B-mode but detected by CEUS, thus resulting in a net benefit of CEUS imaging. Although this difference did reach statistical significance, the overall difference in plaque detection between B-mode and CEUS imaging was small. As a result, the incremental clinical benefit of such an approach is yet to be determined.

Our findings are in keeping with a recent Dutch study¹³² that assessed the presence of sub-clinical atherosclerosis using CEUS of carotid arteries in 100 asymptomatic patients with cardiovascular risk factors but no known CVD. They found plaques in 77% patients using B-mode imaging only and reported that this increased to 88% using CEUS as well. The authors concluded that incorporation of CEUS significantly increased detection of sub-clinical atherosclerosis compared to B-mode imaging alone.

There are a number of differences between the present study and the study of van den Oord *et al.*¹³² Firstly – and most importantly – the methodology of the Dutch group suggests that CEUS images were interpreted immediately after B-mode images were obtained. Although this may be considered more ‘natural,’ as this is what might be done if CEUS were utilized in a clinical setting, seeing the B-mode images first would inform an interpreter of the presence of plaques, thus the individual would be ‘primed’ to seek these out on CEUS imaging. As a result, a plaque may be seen on CEUS imaging that may have been missed had the B-mode images not been

seen prior to the CEUS images. Indeed, despite imaging 200 carotid arteries, the authors did not report a single case of detecting a plaque on B-mode imaging which was not seen on CEUS imaging. One potential explanation is the prior review of B-mode images prior to analysing the CEUS images. Therefore, the present findings extend those of the Dutch group as these results indicate that even when CEUS images and B-mode images of patients were not reviewed together as a 'pair', CEUS allowed greater plaque detection.

We found that 15 plaques were seen during B-mode imaging that were not seen during CEUS imaging. The majority (11/15, 73%) of these plaques were echo-bright. The echo-bright nature meant that they were difficult to visualize when the lumen was opacified with contrast and this is the likely explanation for CEUS 'missing' these plaques. Conversely, most plaques (25/32, 84%) not detected on B-mode imaging but seen on CEUS were predominantly echolucent. These observations on plaque characteristics during B-mode and CEUS imaging are consistent with the findings of van den Oord *et al.*¹³²

CEUS is an excellent technique for optimal visualization of the carotid arterial tree and can help distinguish between ultrasound artefacts and plaques. In addition to enabling improved plaque detection, CEUS also helped to prevent 'false positive' reporting of plaques during B-mode imaging. It may prove that CEUS is clinically most helpful in combination with B-mode imaging for distinguishing between plaques and artefacts (especially in the near wall), permitting optimal IMT visualization and optimal plaque visualization.

Study Strengths and Limitations

There are certain study strengths and limitations which merit discussion. The use of a continuous intravenous infusion of contrast is a strength of the study design as it permitted

excellent and homogeneous arterial opacification. Furthermore, the superior value of CEUS over B-mode imaging for plaque detection has also been shown in a study in which contrast bolus doses were given,¹³² thus suggesting that method of contrast administration is not a significant factor in plaque detection. The number of subjects' studies is small and from a single centre; a larger and multi-centre study assessing CEUS in asymptomatic individuals with elevated CVD risk would be of benefit. A potential limitation of this study is the question over incremental clinical value of the data obtained during CEUS. If a patient already qualifies for primary prevention therapy, then the presence or absence of carotid atherosclerosis is unimportant. However, a recent study in symptomatic patients undergoing stress testing found that almost 20% patients that did not qualify for primary prevention drugs (e.g. statins) had sub-clinical carotid atherosclerosis.¹⁵⁶ There is, therefore, the possibility that optimal detection of carotid atherosclerosis – by B-mode & CEUS imaging – may lead to better identification of patients requiring primary prevention strategies, although a large scale study proving this hypothesis is required.

Conclusions

CEUS significantly improves visualization of the intima-media thickness in common carotid and internal carotid artery segments compared with B-mode imaging and also permits detection of a significantly greater number of carotid plaques. A combination of B-mode and CEUS imaging will allow for excellent IMT visualization and accurate plaque detection, as well as distinguishing between ultrasound artefacts and genuine arterial plaques.

CHAPTER 6

Higher Prevalence of Plaque Neovascularisation – a Marker of Plaque Vulnerability – in South Asians versus Northern European Asymptomatic Subjects: Implications for a Possible Mechanism for Differential Ethnic Outcome

6.1 ABSTRACT

Background

Individuals of South Asian (SA) ethnic origin have a considerably greater risk of suffering cardiovascular events compared with European White (EW) individuals. Although a number of explanations have been proposed, the underlying reasons for this difference remain incompletely defined. A difference in plaque composition – specifically, presence or absence of intraplaque neovascularisation (IPN) – may help explain the underlying mechanisms.

Objective

To determine the frequency in which IPN is observed in carotid plaques from asymptomatic SA and EW subjects free of known cardiovascular disease.

Methods

Individuals were recruited from the London Life Sciences Population (LOLIPOP) study. Men and women found to have carotid plaques during initial carotid imaging were invited for repeat

imaging by B-mode and contrast-enhanced ultrasound (CEUS). Plaques were interrogated in long and short axis views for presence of IPN during CEUS imaging.

Results

Of 175 patients that were studied by B-mode and CEUS carotid ultrasonography, there were 96 Northern European subjects (55%) and 79 South Asian subjects (45%), in whom 197 and 170 plaques were identified respectively. The mean age was 64.7 ± 8.9 yrs and 140 (80%) were male. IPN was detected in approximately 50% of all plaques.

On a per-patient basis, IPN was detected in 56/79 (71%) Asian subjects and 55/96 (57%) European subjects. After adjustment for clinical variables by multi-variable logistic regression (including age, gender and conventional cardiovascular risk factors), South Asian ethnicity was the only independent predictor of presence of IPN (Odds Ratio 2.8, 95% C.I. 1.36 – 5.92, $p=0.006$).

Conclusions

This is the first study to identify a differential incidence on IPN based upon ethnicity and may help explain, at least in part, the greater CVD burden amongst SA populations.

6.2 INTRODUCTION

Recently, much research has focused upon predicting which atherosclerotic plaques will ‘rupture’ – triggering events such as myocardial infarction or stroke – and which plaques will not rupture, leading to the concept of the ‘vulnerable’ (or unstable) plaque.¹⁵⁷ Emerging key features of such plaques are intra-plaque neovessels. These neovessels are fragile, leaky and prone to bleeding, leading to intra-plaque haemorrhage, which contributes to the necrotic core of plaques and is believed to increase risk of plaque rupture.¹⁵⁸ Consequently, the presence of intra-plaque neovascularisation (IPN) has been postulated as a pre-cursor to the vulnerable plaque. A number of imaging and histological studies have revealed a clear association between presence and extent of IPN and subsequent cardiovascular events, including mortality.^{57, 59, 76} Contrast enhanced ultrasound (CEUS), a non-invasive technique that utilizes trans-pulmonary ultrasound contrast agents, can be used to visualize IPN during carotid ultrasonography.¹⁵⁹

South Asians (people of Indian, Pakistani and Bangladeshi origin) living in the United Kingdom have a greater than 50% higher risk of death from cardiovascular disease (CVD) compared with native European whites.¹⁶⁰ The mechanisms underlying their excess mortality are not clear. The burden of subclinical atherosclerosis detected in the carotid arteries is an established prognosticator for major CVD events. However, our group has recently shown that there were no significant differences in intima-media thickness, plaque prevalence or plaque echogenicity between asymptomatic South Asian and European populations.¹¹⁴ We therefore hypothesized that a difference in plaque vulnerability may account for the observed increased CVD events and thus performed this study to determine whether there are significant differences in IPN prevalence between SA and EW individuals.

6.3 METHODS

Patient Selection

Individuals were drawn from the London Life Sciences Population (LOLIPOP) study, a community-based study comparing EW and SA individuals, free from known cardiovascular and cerebrovascular disease, in an attempt to better understand the mechanisms underlying the increased CVD burden amongst the SA community. Subjects were considered of SA ethnicity if all four grand-parents were born in the Indian sub-continent, whilst EW subjects had grand-parents that were all born in Northern Europe. The LOLIPOP study recruited over 30,000 subjects, of whom approximately 2400 took part in the LOLIPOP-Atherosclerosis sub-study. The imaging findings in these individuals have been previously published.^{114, 161} In the Atherosclerosis sub-study, just over 1000 individuals had carotid plaques detected on B-mode carotid ultrasonography. We randomly selected 200 patients from this group and invited them to return for carotid B-mode and CEUS imaging.

Carotid Ultrasonography

B-mode, colour Doppler and contrast enhanced carotid ultrasonography were performed using a high-resolution ultrasound system (Vivid-7; General Electric Healthcare, Chalfont, Bucks, UK) equipped with a broadband linear array (3-11 MHz) transducer. ECG monitoring was performed continuously throughout the scan and arterial blood pressure was recorded using an automated sphygmomanometer.

In summary, the proximal, mid, and distal common carotid artery (CCA), bifurcation of the CCA and proximal portion of the internal and external carotid arteries were systematically interrogated in long-axis and short-axis views. Colour Doppler imaging was used to identify

flow and spectral Doppler used to measure flow velocities. After B-mode imaging, an intravenous cannula was inserted and two vials (8mL) of Sonovue ultrasound contrast (Bracco Diagnostics, Milan, Italy) was administered as a continuous intravenous infusion using a specific pump (Vueject, Bracco, Milan, Italy) at a standardized rate of 1.2 mL/min, providing approximately 6.5 minutes of contrast opacification. During this time, the right and left carotid arteries were re-imaged using a specific low MI contrast pre-set (MI 0.20), with special focus upon areas of abnormality (i.e. plaques) identified during the B-mode scan.

Image Analysis

All images were subsequently stored on disc for off-line analysis, which was performed in random order after all patients had been scanned. In an attempt to minimize the risks of bias in the study, all carotid images were analysed by a cardiologist that did not perform the scans and who was blinded from the subject's ethnicity (as scans were identified by study number only). Plaque was defined as per the Mannheim consensus as a focal structure encroaching into the arterial lumen by >0.5 mm, a distinct area of IMT $>50\%$ greater than the adjacent wall or >1.5 mm in thickness.²⁶ Presence of IPN was graded semi-quantitatively as absent (Grade 0), limited to the adventitia / plaque base (Grade 1) or extensive and/or extending into the plaque body (Grade 2).⁷²

Statistics

Continuous variables are expressed as mean \pm standard deviation and categorical variables as proportions. Continuous variables between EW and SA subjects were compared using the unpaired Student's t-test and categorical variables using the chi-squared test. Logistic regression was used to identify independent predictors of the presence of IPN after adjustment for clinical variables. For all tests, a p value <0.05 was considered statistically significant. All

analyses were conducted using SPSS version 19.0 (SPSS Inc, Illinois, USA).

6.4 RESULTS

Of the 200 individuals invited for repeat carotid imaging, 17 had suffered a (first) cardiovascular event since the initial scan, 3 patients did not have CEUS imaging performed (inability to obtain IV access) and 5 patients had incomplete data sets, leaving a final total of 175 patients that were studied by B-mode and CEUS carotid ultrasonography. The mean age was 64.7 ± 8.9 yrs and 140 (80%) were male. The complete baseline demographics of the patients are listed in table 6.1. There were 96 Northern European subjects (55%) and 79 South Asian subjects (45%), in whom 197 and 170 plaques were identified respectively. IPN was detected in approximately 50% of all plaques, with no significant difference between plaques detected in the left (95/192, 49%) and right (88/175, 50%) carotid arteries ($p=0.88$).

CHARACTERISTIC	SOUTH ASIAN (/79) [%]	EUROPEAN WHITE (/96) [%]	TOTAL (/175) [%]	P value
Mean Age (yrs \pm SD)	63.2 \pm 9.4	65.7 \pm 7.9	64.6 \pm 8.7	0.055
Male Gender	60 [76]	80 [83]	140 [80]	0.224
Hypertension	48 [61]	45 [47]	93 [53]	0.067
Hyperlipidaemia	42 [53]	47 [49]	89 [51]	0.580
Type 2 DM	23 [29]	13 [14]	36 [21]	0.011
Smoking History	3 [4]	9 [9]	12 [7]	0.146
Family History	31 [39]	27 [28]	58 [33]	0.120

Table 6.1: Baseline characteristics of the study patients.

Per-Patient Analysis

On a per-patient basis, at least one plaque containing IPN was detected in 56/79 (71%) Asian subjects and 55/96 (57%) European subjects ($p=0.06$) – see figure 6.1. However, after adjustment for clinical variables (age, gender, hypertension, hyperlipidaemia diabetes mellitus and smoking status) – by multi-variable logistic regression – South Asian ethnicity was the only independent predictor of the presence of IPN (Odds Ratio 2.8, 95% C.I. 1.36 – 5.92, $p=0.006$).

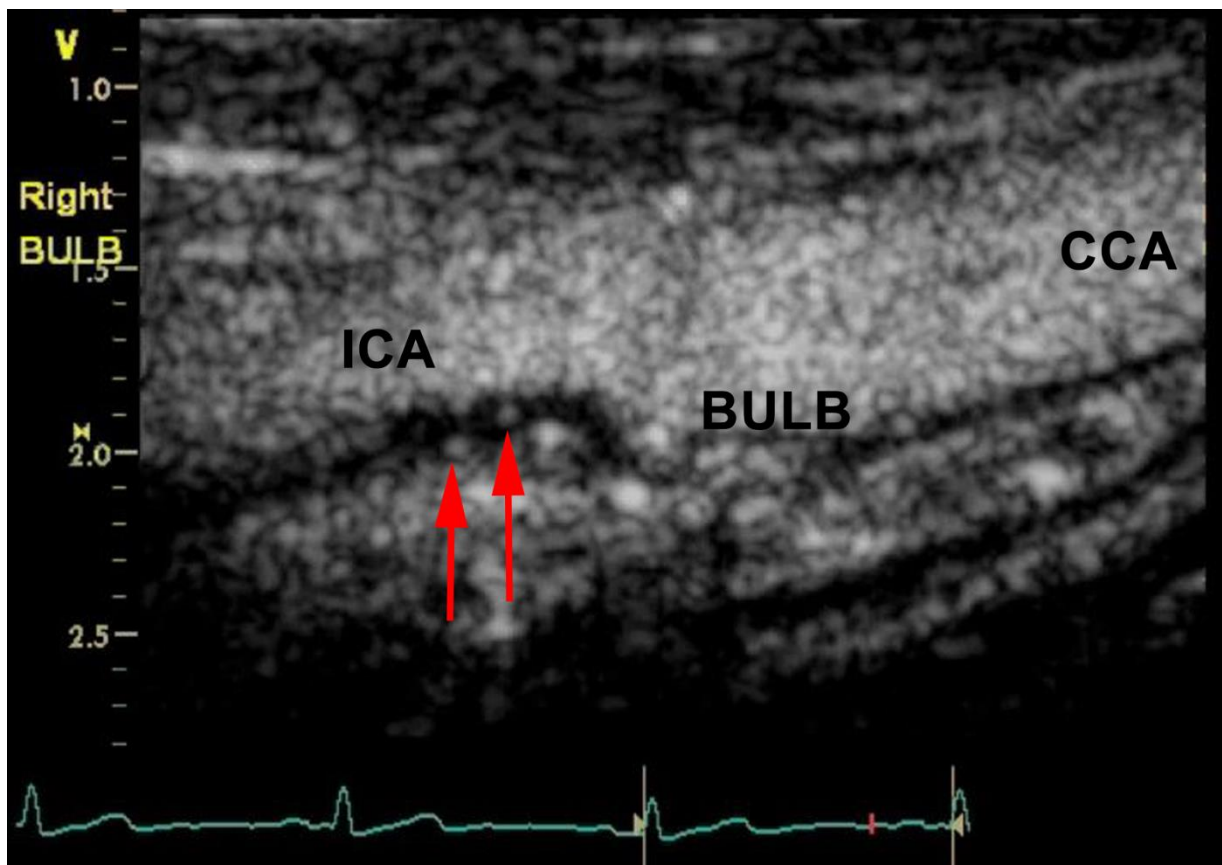
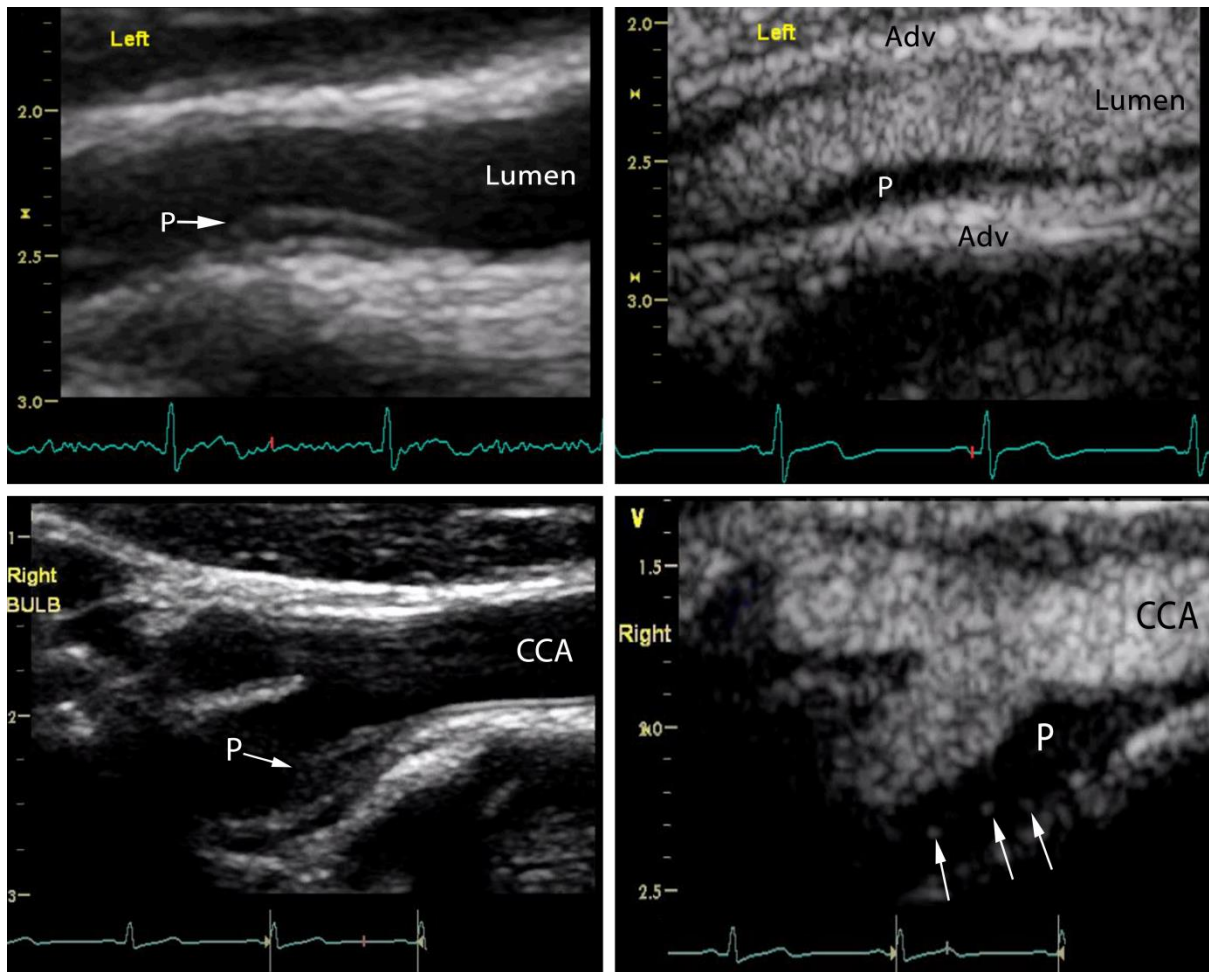


Figure 6.1: CEUS still image showing a plaque in the carotid bulb, extending into the origin of the internal carotid artery (ICA) with clearly seen contrast bubbles within the plaque (red arrows) representing IPN.



*Figure 6.2: B-mode and carotid CEUS images. **Top left** – B-mode image of a plaque (P) in the left internal carotid artery (ICA). **Top right** – The same left ICA plaque (P) on CEUS with no bubbles seen within it (Adv = Adventitia). **Bottom left** – a plaque just distal to the right common carotid artery (CCA) bifurcation. **Bottom right** – the same plaque with multiple contrast bubbles within (arrows) indicative of IPN.*

Per-Plaque Analysis

In total, there were 367 plaques visualized during CEUS imaging, of which 170 were in SA subjects and 197 in EW subjects (see example in figure 6.2). Almost exactly half of the plaques (184/367, 51%) contained IPN. Amongst SA subjects, 94/170 (55%) plaques contained IPN whereas amongst EW subjects 90/197 (46%) plaques contained IPN. Again, by multi-variable

logistic regression, South Asian ethnicity was an independent predictor of the presence of IPN (Odds Ratio 1.8, 95% C.I. 1.18 – 2.87, p=0.007).

Reproducibility Studies

In order to determine the inter- and intra-observer reproducibility of the technique, 20 CEUS studies were selected at random for analysis by a second observer and re-analysis one month after initial analysis, respectively. Inter- and intra-observer agreements were 85% and 95% yielding kappa values of 0.85 and 0.95, respectively. Full tables are provided in Appendix 1.

6.5 DISCUSSION

This is the first study to detect a significant difference in plaque neovascularisation based upon ethnicity. Our results have shown that IPN is associated with SA ethnic origin independent of conventional cardiovascular risk factors, including those typically more prevalent in SA individuals such as diabetes mellitus, hypertension and hypercholesterolaemia. As a marker of plaque vulnerability, this finding may in part account for higher CVD risk observed in South Asians vs. Europeans. However, larger studies are required to confirm these preliminary findings.

Migrant South Asians in the UK have a considerably increased risk of CVD mortality compared to native whites.¹⁶⁰ Though much of this risk is thought attributable to modifiable risk factors such as diabetes mellitus and hypertension, conventional risk scoring systems (e.g. Framingham) incompletely assess this risk and thus under-estimate CVD risk in Asians.¹⁶²

Plaque neovascularisation has emerged recently as the likely pre-cursor to intra-plaque haemorrhage, which is believed to contribute to the necrotic core of plaques and thus may be a marker of plaque vulnerability.⁴⁰ Prior studies have shown an association between IPN and adverse CVD outcomes.⁵⁹ Our preliminary results suggest that a difference in IPN may explain the greater CVD risk in South Asians compared with European whites.

The exact mechanisms that may underpin this difference between plaque neovascularisation in SA and EW individuals are yet to be defined. A genetic contribution is one possibility. The tunica intima and media are dependent upon diffusion of oxygen from the lumen and, in disease conditions when the IMT complex thickness, local hypoxia triggers release of Hypoxia Inducible Factor (HIF). HIF- α is released from the arterial wall once a diffusion threshold of oxygen tension is reached and one hypothesis is that this diffusion threshold is lower in SA individuals compared to EW subjects, although currently this is unproven.

Clinical Implications

Observational data suggests that IPN is associated with a greater rate of adverse cardiovascular events. If follow-up of such a patient cohort were to confirm that the difference noted in IPN during an asymptomatic period translated into adverse outcome later in life, this may have significant implications for clinical practice and may fuel research interests further to identify interventions in the sub-clinical stage of disease that may improve longer term outcomes. Large scale, multi-country trials are likely to be required for this purpose.

Statins have been used in clinical practice for lowering of low density lipoprotein (LDL) cholesterol for over two decades. High dose statin therapy has been shown to induce a reduction in plaque volume,¹⁶³ principally by reducing cholesterol and thus the size of the lipid core of

‘vulnerable’ plaques. A more recent study has also shown that high dose statin treatment can in fact increase the thickness of the fibrous cap of atherosclerotic plaques,¹⁶⁴ another potential feature of vulnerable plaques. Clinical trials are required to determine whether high-dose statin therapy, for example, could be used for plaque stabilization specifically in IPN-containing plaques. Anti-angiogenic therapy for normalization of atherosclerotic plaque vessels is also an attractive potential therapeutic strategy,¹⁶⁵ though data in this field are at present lacking.

Strengths & Limitations

There are certain strengths and limitations of this study that should be acknowledged. Strengths include use of contemporary ultrasound equipment, use of a continuous intravenous infusion of ultrasound contrast and ability to study a well-characterized and ethnically unambiguous population. The principal limitation of the study is the small sample size. Larger studies are required to confirm the results of our initial data and demonstrate reproducibility of the CEUS technique prior to widespread use. Follow-up of this patient cohort will also clarify the prognostic impact of IPN amongst South Asians.

Conclusions

Plaque neovascularisation, a putative pre-cursor to intra-plaque haemorrhage and thus a surrogate marker of plaque vulnerability, is increased in SA compared to EW individuals free from cardiovascular disease. This finding may help explain the greater CVD burden amongst SA populations. Larger studies are required to ratify these findings and determine associated prognostic implications.

CHAPTER 7

Plaque Neovascularization is Increased in Human Carotid Atherosclerosis Related to Prior Neck Radiotherapy

7.1 ABSTRACT

Background

Patients with a malignancy in the head or neck region frequently receive radiotherapy (RT) during treatment of their cancer. Consequently, the carotid artery is frequently exposed – unavoidably – to irradiation. Exposure of the carotid arteries to RT, during treatment for head and neck cancer (HNC), is associated with an increased risk of stroke. However, the effect of RT upon plaque composition has not previously been studied. Specifically, the effect of RT upon intraplaque neovascularization (IPN) – a pre-cursor to intraplaque haemorrhage and, thus, a surrogate marker of plaque vulnerability – is unknown.

Objectives

To determine the effect of radiotherapy (RT) upon IPN in human carotid arteries.

Methods

In this cross-sectional study, patients who had undergone unilateral RT for HNC ≥ 2 years previously underwent B-mode and contrast-enhanced ultrasonography (CEUS) of both RT-side and non-RT side carotid arteries. As only patients that received unilateral RT were studied, by scanning both the left and right carotid arteries, each patient acted as their own internal ‘self-control’. The presence of IPN during CEUS was judged semi-quantitatively as grade 0 (absent), grade 1 (present but limited to plaque base) or grade 2 (extensive and noted within plaque

body). CEUS images were interpreted by an individual blinded to the side of RT in each patient. The presence of IPN was compared against baseline patient characteristics, including laterality of RT.

Results

Of 49 patients studied, 38 (78%) had plaques. The number of plaques was significantly greater in the RT versus the non-RT arteries. Overall, 48/64 (75%) of all RT-side plaques had IPN vs. 9/23 (39%) of the non-RT side plaques ($p=0.002$). Amongst patients with plaques, IPN was present in 81% patients with RT-side plaques vs. 41% patients with non-RT side plaques ($p=0.004$). Grade 0 IPN was significantly more common in patients with non-RT side plaques (25% vs. 61%, $p=0.002$) whereas Grade 2 plaques were more common on the RT side (31% vs. 9%, $p=0.03$). The only clinical variable which predicted presence or absence of IPN was RT laterality.

Conclusion

This is the first study in humans to report upon the relationship between prior RT and plaque neovascularization. A significant association between RT and presence and extent of IPN was found in this study. This may provide insights into the mechanisms underlying the increased stroke risk amongst HNC survivors treated by RT.

7.2 INTRODUCTION

Atherosclerosis is the underlying patho-biological substrate that accounts for most cardiovascular events. However, not all patients with atherosclerosis experience such outcomes. In recent years, much research has focused upon predicting which atherosclerotic plaques will ‘rupture’ – triggering events such as myocardial infarction or stroke – and which plaques do not rupture, leading to the concept of the ‘vulnerable’ (or unstable) plaque.¹⁵⁷

An emerging key feature of such plaques is intra-plaque neovessels. These neovessels are fragile, leaky and prone to bleeding, leading to intra-plaque haemorrhage, which contributes to the necrotic core of plaques and is believed to increase risk of plaque rupture.¹⁶⁶ Consequently, the presence of intra-plaque neovascularization (IPN) has been postulated as a pre-cursor to the vulnerable plaque.^{158, 167} A number of imaging and histological studies have revealed a clear association between presence and extent of IPN and subsequent cardiovascular events (CVE), including mortality.^{57, 59, 76} Much of this research in humans has focused upon the carotid arteries, owing to their superficial location (favours non-invasive imaging), the association with stroke and because patients undergoing carotid endarterectomy provide a suitable model for histological comparisons.

IPN can be visualized by several imaging techniques, including contrast-enhanced ultrasound (CEUS). CEUS utilizes trans-pulmonary ultrasound contrast agents, which remain intravascular at all times, effectively acting as red cell “tracers”. Carotid ultrasonography performed following administration of contrast permits visualization of IPN⁷⁰ and comparisons with histological neovessel density have validated the technique’s accuracy.⁷²

Radiotherapy (RT) damages arterial walls and promotes atherosclerosis. The carotid arteries frequently receive significant incidental doses of radiation during RT treatment of head and neck cancers (HNC). Radiation vasculopathy had until recently been considered quite a rare entity, as patients would frequently succumb to their malignancy first. However, as cancer survival rates improve, patients are “outliving” their malignancies and presenting later with the long-term sequelae of cancer therapy.¹¹⁷

Several studies have shown that RT of the carotid arteries is associated with increased intima-media thickness (IMT), increased carotid plaque formation and overall an increased risk of stroke.^{168, 169} However, the effect of RT on plaque composition – specifically IPN – has not been studied in humans. This study was thus performed to assess the effects of RT upon IPN in survivors of HNC who had previously received RT.

7.3 METHODS

Study Design

This was a cross-sectional study of patients previously treated with RT for HNC. Ethical approval was obtained and all patients provided informed written consent. The inclusion criteria were as follows:

- Age >18 years
- Histologically confirmed cancer treated with hemi-neck RT to ≥ 50 Gray (Gy)
- Radiotherapy administered > 24 months previously
- Patient able to provide written informed consent.

The exclusion criteria were:

- Patients with active HNC
- Patients with a prior history of carotid endarterectomy or carotid angioplasty
- Patients with bilateral RT
- Patients with known allergy to sulphur / sulphur-containing drugs.

HNC patients who had received unilateral RT prior to December 2009 were identified via the RT database. The requirement for RT to have been ≥ 2 years previously was chosen for two reasons: firstly, such patients are likely to be cured of their cancer and therefore live long enough to develop atherosclerosis. Secondly, plaques need time to develop after RT and thus recruiting patients after a shorter time duration may have resulted in many more normal studies. Eligible patients agreeable to participation (only three patients declined) were invited to attend for a baseline questionnaire (for confirmation of study eligibility and determination of risk factor profile), physical examination, routine blood tests and carotid ultrasonography. Each patient had their height (in metres) and weight (in kilograms) recorded in order to calculate the body mass index (BMI).

Patient Clinical Variables

The presence of cardiovascular risk factors was defined as follows:

Diabetes mellitus: random serum glucose ≥ 11.1 mmol/L, a glycosylate haemoglobin A1c (HbA1c) $\geq 5.8\%$ or current use of glucose-lowering agents or insulin

Hypertension: systolic blood pressure ≥ 140 mmHg and/or diastolic blood pressure ≥ 90 mmHg or current use of anti-hypertensive agents)

Hyperlipidemia: fasting serum low density lipoprotein (LDL) ≥ 2.6 mmol/L, high density lipoprotein (HDL) < 2.3 mmol/L or triglycerides (TG) ≥ 2.3 mmol/L, or current use of cholesterol-lowering agents

Smoking History: Ever smoker

Family history of premature CAD: First degree relative suffered myocardial infarction or stroke, < 55 yrs (men) or < 65 yrs (women)).

Carotid Ultrasonography

B-mode, colour Doppler and contrast enhanced carotid ultrasonography (see figure 7.1) were performed using a high-resolution ultrasound system (Vivid-7; General Electric Healthcare, Chalfont, Bucks, UK) equipped with a broadband (3-11 MHz) transducer. All scans were performed by a cardiologist blinded to the patient's history including the laterality of RT (as RT had been delivered > 2 yrs previously, potential markers of treatment such as erythema, telangiectasiae and skin tenderness were no longer present). ECG monitoring was performed continuously throughout the scan and arterial blood pressure was recorded using an automated sphygmomanometer. In summary, the proximal, mid, and distal common carotid artery (CCA), bifurcation of the CCA and proximal portion of the internal and external carotid arteries were systematically interrogated in long-axis and short-axis views. Colour Doppler imaging was used to identify flow and spectral Doppler used to measure flow velocities.

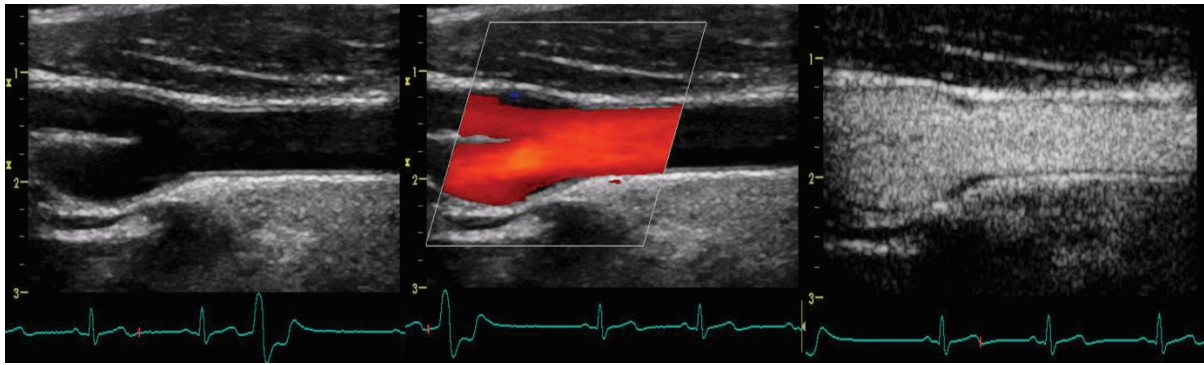


Figure 7.1: Examples of B-mode (left), colour Doppler (centre) and CEUS (right) imaging of the carotid arterial tree. The figures show a long-axis view of the common carotid artery with bifurcation into internal and external carotid arteries.

Plaque was defined as per the Mannheim consensus as a focal structure encroaching into the arterial lumen by >0.5 mm, a distinct area of IMT $>50\%$ greater than the adjacent wall or >1.5 mm in thickness²⁶ (see figure 7.2). IMT measurements were taken at the far wall of the distal CCA at end-diastole using a semi-automated edge detection algorithm (EchoPAC version 8.0, GE Healthcare) and the mean value obtained was an average of 3 measurements. Plaque area was calculated by tracing around the plaque edges in end-diastolic long axis still images and was also expressed as an average of three measurements.

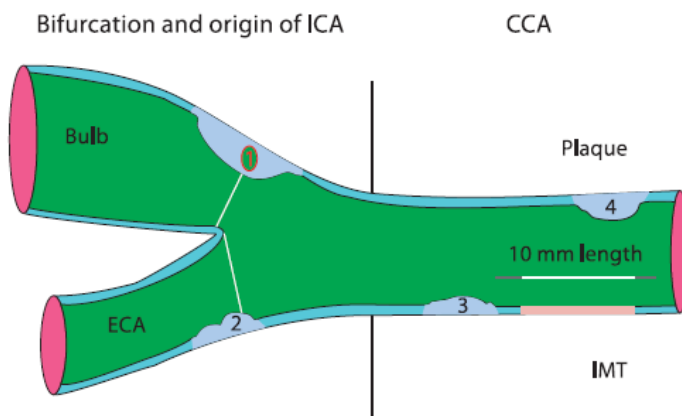


Figure 7.2: Drawn representation of carotid tree, with plaque and IMT measurements according to Mannheim consensus:

- 1: thickness > 1.5 mm*
- 2: lumen encroaching > 0.5 mm*
- 3, 4: $>50\%$ of the surrounding IMT value*

After B-mode imaging, an intravenous cannula was inserted and two vials (8mL) of Sonovue ultrasound contrast (Bracco Diagnostics, Milan, Italy) were administered as a continuous intravenous infusion at a standardized rate of 1.2 mL/min, providing approximately 6.5 minutes of contrast opacification. During this time, the right and left carotid arteries were re-imaged using a specific low MI contrast pre-set (MI 0.20), with special focus upon areas of abnormality (i.e. plaques) identified during the B-mode scan. All images were subsequently transferred to the EchoPAC database and also stored on disc for off-line analysis, which was performed in random order (after all patients had been scanned) and blinded to the patient's clinical details. IPN was graded semi-quantitatively as absent (Grade 0), limited to the adventitia / plaque base (Grade 1) or extensive and/or extending into the plaque body (Grade 2) by a doctor blinded to the side of RT.⁷²

Statistics

The primary aim of this study was to compare the incidence of IPN within carotid plaques in irradiated arteries to un-irradiated internal controls. However, the expected prevalence of IPN within such plaques-required for the ample size calculation – was entirely unknown as this question has never previously been the subject of a research study. Consequently, the advice from a medical statistician in this case was to use the expected prevalence of carotid plaque as the nearest estimate for prevalence of IPN in order to perform a sample size calculation.

As previously reported, the expected absolute difference in the prevalence of carotid artery stenosis due to plaque is around 25-30%.^{170, 171} With a Type I error set at 95% ($\alpha = 0.05$) and a type II error set at 10% ($\beta = 0.10$), a minimum of 80 patients would be required. As patients treated with unilateral RT were evaluated (the contralateral carotid artery served as an internal

control), a total of 40 patients were therefore required for this study. In order to account for unexpected loss of subjects (e.g. poor ultrasound windows), the study aimed to recruit 50 patients. As increased prevalence of carotid plaque was expected on the RT-side, we hypothesized that there may also be an accompanying increased incidence of IPN.

Continuous variables are presented as mean \pm standard deviation and categorical variables as proportions. Data was analyzed on a per-patient basis and a per-plaque basis. The per-patient analyses represent paired data (two data sets obtained from each patient, one from the RT-side artery and one from the non-RT side artery) whereas the per-plaque analyses represent unpaired data, as there were a different number of plaques between the RT and non-RT sides (thus these were unmatched groups). Therefore, the per-patient analyses were conducted using the paired t-test (continuous data) and McNemar's test (categorical data) and the per-plaque analyses were conducted with the Student's t-test (continuous data) and chi-squared test (categorical data). All statistical calculations were performed using SPSS version 19.0. A p value <0.05 was taken as statistically significant for all tests.

For determination of intra-observer and inter-observer variability, Cohen's kappa statistic was used to measure agreement between two different assessments – at least 1 month apart – by one reader and two different readers, respectively, of 15 randomly selected CEUS cine images. For inter-observer assessment, we used two readers to compare against the first author – one with experience in CEUS imaging and a second cardiologist with no prior experience of CEUS imaging.

7.4 RESULTS

Patient Variables

Of 50 patients that consented for the study, 49 underwent B-mode and contrast-enhanced carotid ultrasound studies (in one patient intravenous access proved impossible and thus contrast could not be administered). The baseline demographics of these 49 patients are detailed in Table 7.1. Mean age was 57 ± 8 yrs, 69% were male and mean BMI was 26.3 ± 4.4 kg/m².

The histological tumour type was squamous cell carcinoma in the majority of patients (38/49, 78%). There were 42 patients with oropharyngeal (tonsillar) tumours and 7 patients with parotid tumours. All patients had 3D conformal RT to the section of the carotid artery we studied (i.e. from the bifurcation to the proximal CCA). Some patients would have received intensity-modulated radiotherapy (IMRT) to the cranial part of the ICA/ECA, but we did not examine these segments in this study. The average maximum dose to the irradiated side was 53 ± 13 Gy and to the un-irradiated side was 1.9 ± 3.7 Gy. The dose to the un-irradiated side would be considered clinically negligible.

Almost half the cohort (22/49, 45%) had also received platinum-based chemotherapy drugs for treatment of their HNC. The mean time duration from RT to carotid imaging was 5.4 ± 2.5 years (range 2.1 – 12.6 yrs). Routine full blood count was normal in all patients. Mean serum creatinine value was 75 ± 19 mmol/L (range 46-128 mmol/L). The mean total, HDL and LDL cholesterol levels were 5.3 mmol/L, 1.5 mmol/L and 3.2 mmol/L respectively. All patients had normal serum calcium concentration (mean 2.2 ± 0.1 mmol/L).

Patient characteristics	Total (%) (n = 49)	Plaque (%) (n = 38)	No plaque (%) (n=11)	P value
<u>Demographics</u>				
Mean age (yrs±SD)	57±8	59±7	50±8	0.001
Male gender	34 (69.0)	28 (73.7)	6 (54.5)	0.23
Diabetes	4 (8.2)	3 (7.9)	1 (9.1)	0.90
Hypertension	13 (26.5)	12 (31.6)	1 (9.1)	0.14
Smoker	26 (53)	20 (52.6)	6 (54.5)	0.91
Hyperlipidemia	11 (22.4)	10 (26.3)	1 (9.1)	0.23
Mean BMI (±SD)	26.3±4.4	26.6±4.4	25.1±4.2	0.34
Mean time from RT (years)	5.4±2.5	5.9±2.6	3.6±1.4	0.006
<u>Medications</u>				
Anti-hypertensive drugs	13 (26.5)	12 (31.6)	1 (9.1)	0.14
Anti-diabetic drugs	4 (8.2)	3 (7.9)	1 (9.1)	0.90
HMG Co-A reductase inhibitors (Statins)	11 (22.4)	10 (26.3)	1 (9.1)	0.23
Aspirin	13 (26.5)	10 (26.3)	3 (27.3)	0.95

Table 7.1: Baseline characteristics of the 49 enrolled patients

Carotid Ultrasonography

Of the 49 patients examined, plaques were detected in 38 (78%) with bilateral plaques in 15 patients and unilateral plaques in 23 patients. Patients with bilateral plaques more frequently had a history of smoking than those with unilateral plaques, but all other variables were similar between the groups (see table 7.2). The data presented in Table 7.3 demonstrate the differences in plaque number, area and prevalence of IPN from the RT and non-RT carotid arteries. There were a greater number of plaques on the RT side although mean plaque area and total plaque burden by area were similar between RT and non-RT arteries. A total of 87 plaques were detected, with 41 plaques in the right carotid artery and 46 in the left carotid artery. On a per-plaque basis, there was no significant difference in the frequency of IPN between plaques from the left and right sided arteries (27/41 [66%] vs. 30/46 [65%], $p=0.95$).

IPN was analyzed on a per-patient as well as per-plaque basis, but in both cases, IPN was more commonly seen on the RT side than the non-RT side. Of all 49 patients, 29 (59%) had at least 1 plaque containing IPN on the RT-side versus just 7 patients (14%) that had ≥ 1 plaque containing IPN on the non-RT side ($p<0.001$). Amongst the 38 patients with plaque, 36 (95%) had plaque on the RT-side whereas 17 patients (45%) had plaque on the non-RT side ($p<0.001$ – see figure 7.3). Thus, analyzing only those patients with IPN, 29/36 patients had at least 1 plaque containing IPN on the RT-side versus 7/17 patients that had ≥ 1 plaque containing IPN on the non-RT side (81% vs. 41%, $p<0.001$). Similarly, at a patient level, the absence of IPN (i.e. Grade 0) was significantly more frequent in non-RT plaques than RT plaques. Conversely, Grade 2 IPN – the highest grade and indicative of the most extensive IPN – was significantly more commonly identified in RT plaques than in non-RT plaques. Figure 7.4 shows examples of grade 0, grade 1 and grade 2 IPN during CEUS imaging.

Patient characteristics	All patients with PLQ (n = 38)	Bilateral PLQ (%) (n = 15)	Unilateral PLQ (%) (n=23)	P value
<i>Demographics</i>				
Mean age (yrs±SD)	59±7	60±6	57±8	0.21
Male gender	28 (73.7)	12 (80.0)	16 (69.6)	0.48
Diabetes	3 (7.9)	2 (13.3)	1 (4.3)	0.32
Hypertension	12 (31.6)	6 (40.0)	6 (26.1)	0.37
Smoker	20 (52.6)	5 (33.3)	5 (21.7)	0.04
Hyperlipidemia	10 (26.3)	11 (73.3)	9 (39.1)	0.23
Mean BMI (±SD)	26.6±4.4	26.1±5.0	26.9±4.1	0.60
Mean time from RT (yrs)	5.9±2.6	4.8±2.0	6.7±2.7	0.67
<i>Medications</i>				
Anti-hypertensive drugs	12 (31.6)	6 (40.0)	6 (26.1)	0.37
Anti-diabetic drugs	3 (7.9)	2 (13.3)	1 (4.3)	0.32
HMG Co-A reductase inhibitors (Statins)	10 (26.3)	11 (73.3)	9 (39.1)	0.23
Aspirin	10 (26.3)	6 (26.3)	4 (27.3)	0.12

Table 7.2: Comparison of patients with bilateral versus unilateral plaques

[PLQ = Plaque]

Statistical comparisons performed using Student's t-tests [continuous variables] and chi-squared tests [categorical variables]

VARIABLE	RT SIDE	NON-RT SIDE	P VALUE
	n (%)	n (%)	
Total Number of Plaques	64/87 (74)	23/87 (26)	<0.001
<i>Per-Patient Analyses</i>			
Mean Intima-Media Thickness (mm)	0.77±0.20	0.68±0.16	0.02
Mean Total Plaque Area (mm ²)	39.1±33.2	28.5±24.2	0.25
IPN detected?	29/49 (59)	7/49 (14)	<0.001
Grade 2 IPN detected?	14/49 (29)	2/49 (4)	0.001
<i>Per-Plaque Analyses</i>			
Mean Area per Plaque (mm ²)	23.1±13.8	21.0±14.5	0.57
No. of plaques with IPN category:			
Grade 0	16/64 (25)	14/23 (61)	
Grade 1	28/64 (44)	7/23 (30)	
Grade 2	20/64 (31)	2/23 (9)	0.002

Table 7.3: Per-patient and per-plaque data analyses of B-mode and CEUS imaging in RT-side and non-RT side arteries

ALL PATIENTS**RT-SIDE ONLY**

Variable	IPN	No IPN	p value	IPN	No IPN	p value
	N=30	N=19		N=29	N=7	
	(%)	(%)		(%)	(%)	
<i>Male Gender</i>	23 (77)	11 (58)	0.17	22 (76)	4 (57)	0.58
<i>Smoking</i>	18 (60)	8 (42)	0.22	18 (62)	2 (29)	0.13
<i>Aspirin use</i>	9 (30)	4 (21)	0.49	8 (28)	2 (29)	0.95
<i>Statin use</i>	7 (23)	4 (21)	0.85	6 (21)	4 (57)	0.05
<i>BMI >25kg/m²</i>	17 (57)	6 (32)	0.80	19 (66)	5 (71)	0.77
<i>RT >5yrs</i>	17 (57)	6 (32)	0.09	17 (59)	3 (33)	0.15
<i>Chemotherapy</i>	13 (43)	9 (47)	0.78	12 (41)	2 (29)	0.53

All comparisons made using chi-squared tests

Table 7.4: Relationship between presence or absence of IPN and patient variables in all patients (n=49, left side of table) and RT-side only plaques (n=36, right side of table)

We examined the impact of patient variables on presence or absence of IPN, both in all patients and the patients with IPN on the RT side plaques only (see table 7.4). In summary, there was no statistical relationship between presence or absence of IPN and any clinical variable. There was a trend towards greater IPN presence in those with a smoking history and those with RT >5yrs previously, but these did not reach statistical significance (possibly due to the small numbers of patients).

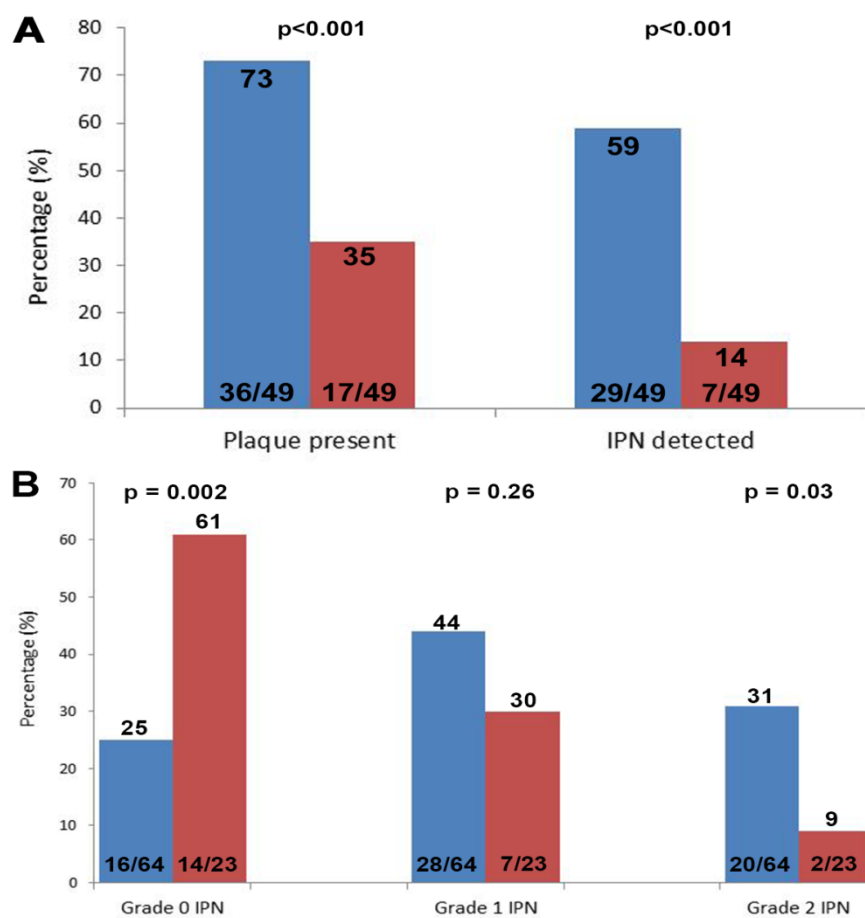


Figure 7.3: Graphs illustrating the differences between RT (blue) and non RT (red) carotid arteries. Panel A (top) shows the difference in incidence of plaques and IPN on a per-patient basis, whereas panel B (bottom) illustrates these differences on a per-plaque basis.

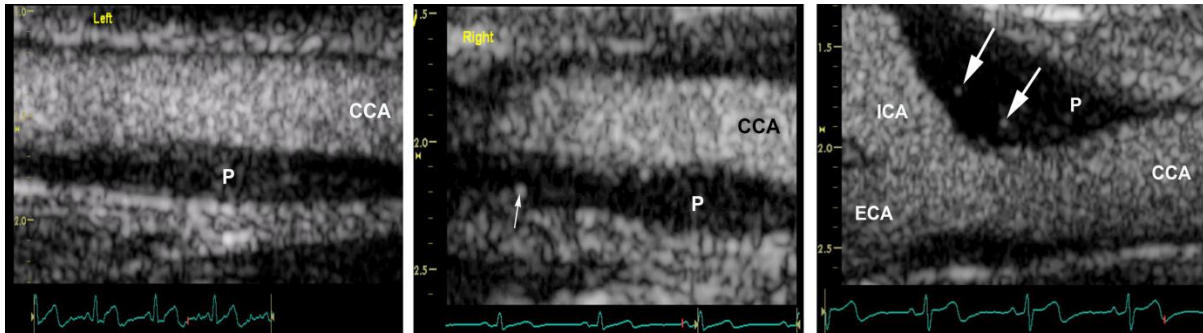


Figure 7.4: Long axis examples of plaques with grade 0 IPN (left), grade 1 IPN (centre) and grade 2 IPN (right). Contrast bubbles within plaques (P) are indicated by arrows.

Variability Assessments

Intra-observer agreement and inter-observer agreement between the first author and another cardiologist familiar with the CEUS technique were both excellent (100% agreement, kappa = 1.0). Inter-observer agreement between the first author and a CEUS novice reader was good (80% agreement, kappa = 0.60). This level of agreement is comparable with reports from other CEUS research studies.⁷⁶ The tables showing agreement between observers are listed in Appendix 3.

7.5 DISCUSSION

This is the first study to assess the impact of RT upon plaque neovascularization. Our results show that IPN is significantly increased in plaques within arteries exposed to RT compared to arteries that did not receive RT. On a per-patient and per-plaque basis, IPN was more common in RT-side plaques and extensive IPN – Grade 2 – was also significantly more frequent on the RT side than non-RT side. These findings were independent of all clinical variables – indeed, the only variable associated with presence of IPN was RT laterality.

The pathophysiology of radiation vasculopathy is poorly understood, in large part due to the lack of a definitive clinicopathologic study in humans. Three mechanisms have been proposed – ischemic necrosis (due to occlusion of the vasa vasorum), adventitial fibrosis (leading to external arterial compression) and accelerated atherosclerosis.¹⁷² Animal studies have given an insight into the changes seen in arterial walls with time following RT, progressing from initial endothelial damage and then thickening to adventitial fibrosis and necrosis of the media.

It is widely believed that the initial injury to the vasa vasorum is a key feature of RT-related arterial disease (radiation vasculopathy), though it has remained unclear whether this process is predominantly inflammatory or ischemic in nature.¹⁷² However, our results show that the vasa vasorum have proliferated markedly into the plaques (IPN), rather than being reduced, favouring an inflammatory process. In ‘conventional’ (i.e. non-RT related) atherosclerosis, proliferation of the adventitial vasa vasorum is triggered by increased production of hypoxia inducible factor (HIF- α), a response to reduced local oxygen tension due to increased thickness of the intima-media complex. As RT is known to cause increased IMT – as we also observed in this study – it is not surprising that a greater degree of IPN was observed on the RT side.

Limitations of Current Evidence

Many groups have investigated the effects of head and/or neck RT upon carotid arteries (imaging studies) and future CVE (outcome studies), which have recently been comprehensively reviewed.¹¹⁹ However, for multiple reasons, the literature displays marked heterogeneity in this field with a number of problems associated with these studies. First, studies that have reported an increased relative risk of CVE after RT have either used non-matched control groups or have matched their HNC patients to geographically distinct and

distant population data.^{120, 121} Studies have not always reported upon stroke sub-type (ischemic or haemorrhagic)¹²² and information on CVE has not always been judged by a clinician or by brain imaging, but by patient questionnaires.¹²³ Finally, and possibly most importantly, the majority of these studies did not provide data on the laterality of the stroke. For example, if the right carotid artery has been exposed to RT, a clinically ischemic event would – in almost all but the rarest cases – be expected in the right cerebral hemisphere and thus produce left sided signs. However, this level of detail is not available in most papers;^{120, 122, 123} thus, although one might assume that an ischemic CVE must be related to the RT-side carotid artery, the data confirming this are absent.

Consequently, several questions regarding radiation vasculopathy remain unanswered, most prominent of which is the mechanism by which RT affects the arterial wall and subsequently increases stroke risk. The increased frequency of IPN we observed strongly implicates an inflammatory reaction, in keeping with conventional models of atherosclerosis. Indeed, IPN is one of several initial defence mechanisms in response to atherosclerosis.¹⁷³ Of the three layers of the arterial wall, the tunica media and adventitia receive blood supply from the vasa vasorum, whereas the tunica intima is dependent upon diffusion of oxygen directly from the lumen. With development of an atherosclerotic plaque within the intima, the distance between the deeper intimal layers and the luminal surface increases, producing hypoxia within the plaque. This stimulates release of pro-angiogenic factors that induces proliferation of the adventitial vasa vasorum and growth of neo-vessels in an attempt to restore normal oxygen tension. Eventually, the plaque is enveloped in extensive vasa vasorum and IPN, a hallmark of atherosclerosis.³⁹

Finally, it should be acknowledged that an *association* has been made between intra-plaque neovascularization, intra-plaque haemorrhage and adverse cardiovascular outcomes. This association has arisen from observational data. However, association does not imply *causation* – we hypothesize that intra-plaque haemorrhage is secondary to IPN rupture and the cause of increased stroke risk. However, there are no studies to date in vivo of carotid plaques in which increased IPN has been detected and with prospective longitudinal follow-up to determine the exact contribution of plaque haemorrhage to plaque vulnerability. Such studies in the future would be of considerable value, in particular to help determine if outcomes (i.e. clinical events) can be prevented by (earlier) treatment (e.g. surgical excision) of IPN-containing plaques.

Clinical Implications

There is increasing evidence that plaque composition is clinically important – independent of stenosis severity – in relation to outcome.^{174, 175} As a result of large international trials, carotid endarterectomy is reserved for patients with symptomatic arterial plaques with stenosis severity >70-80% as judged by Doppler ultrasound.^{173, 176} However, it is not known whether superior risk stratification could be achieved by accounting for novel markers of plaque vulnerability, such as presence or absence of IPN, rather than stenosis severity alone.

Our results demonstrate that patients with RT-related carotid disease have a significant increase in IPN, a putative surrogate marker of plaque instability. One could, therefore, hypothesize that these patients with increased IPN are at increased risk of CVE. It is unknown whether surgical removal of these plaques, even if only causing mild or moderate stenosis, is preferable to medical therapy alone. Intuitively, one may conclude that the mere increased presence of

plaques on the RT side could account for the higher risk of stroke. However, studies published to date have already demonstrated an independent association between IPN and symptomatic plaques and cardiovascular events including stroke; thus, a randomized controlled trial examining whether surgical plaque removal should be based upon plaque composition would be the logical next step on the basis of our findings.

Our data implies that radiation increases neo-angiogenesis, though prior studies have shown RT to be anti-angiogenic. However, the literature is heterogeneous on this issue. Prior research in animal models revealed that irradiation dose-dependently induces the activation of the pro-angiogenic nitric oxide pathway in endothelial cells through increases in endothelial nitric oxide synthase activity.¹²⁴ Furthermore, the survival and subsequent recurrence of neovessels after RT has been postulated as a possible mechanism to explain tumour recurrence.¹²⁵

Multiple prior studies have shown that RT increases plaque formation and thus one may have expected a greater plaque burden on the RT-side. There was a non-significant trend towards greater plaque burden on the RT side (39.1mm² vs. 28.5mm², p=0.25). A possible explanation for this concerns methodology; discrete plaques can have their circumference traced to derive an area, but diffuse thickening of (the IMT of) an entire segment may preclude tracing an area. We were unable to calculate areas for 12 such segments – which were then excluded from the comparison between RT and non-RT sides – all of which were from the RT-side vessel. It is possible that, had it been possible to measure a plaque area in these cases, the difference between RT and non-RT side plaque burdens may have increased.

Finally, the high levels of intra- and inter-observer reproducibility are not surprising given the excellent spatial resolution achieved during CEUS. We believe this is largely explained by our

use of a continuous infusion of contrast, as opposed to bolus injections, as an infusion provides a steady-state concentration of contrast in the artery and thus reduces swirling artefacts that can increase difficulty of IPN assessment. The subsequent clarity of image obtained, together with the clear distinction between the moving white appearances of a contrast bubble against the black background of a plaque, is likely to explain the high reproducibility of the technique. However, this was in a small study and larger studies, using different ultrasound systems and/or alternative methods of contrast delivery may yield different results.

Strengths and Limitations

Our study has certain strengths and limitations. Strengths include a well-defined patient population, blinding of the carotid scanner from side of RT treatment, use of the contra-lateral artery as an ‘internal’ self-control and, uniquely, use of a continuous intravenous infusion of contrast which, unlike multiple bolus injections, produces a constant concentration of microbubbles within the bloodstream.

Limitations include a small sample size, lack of another imaging modality for comparison, the lack of histology for verification and lack of baseline carotid data (prior to RT). Regarding imaging, CEUS has been shown as an accurate technique and carotid MRI, for example, has not been shown to be superior for identification of IPN. Carotid MRI can assess more features of a plaque’s composition than CEUS, including size of the lipid core and thickness of the fibrous cap. However, these aspects of plaque composition were not the primary focus of this research. Further studies using multi-modality imaging (e.g. both carotid MRI and CEUS) would be of scientific benefit. Regarding histology, these patients had no clinical indication for carotid surgery. Thus, histology was impossible to obtain, though previous studies have

verified the accuracy of CEUS for identification of presence and extent of IPN. With regard to baseline carotid data, this was unavailable as patients were recruited following RT and, for many patients, RT had been administered several years previously. Thus, data on IPN (and plaque) prevalence prior to RT was not available, though prior to RT one might have expected to detect far fewer plaques (and thus less IPN).

Conclusions

Plaque neovascularization – a putative surrogate marker for plaque instability – is significantly increased in arteries exposed to RT during treatment of HNC, including age, gender and previous treatment with chemotherapy. This effect of RT upon IPN is independent of all other clinical variables. These results suggest that the atherosclerotic plaques of radiation vasculopathy may demonstrate increased vulnerability and this may help to explain the greater risk of CVE in this patient population.

CHAPTER 8: CEUS Quantification

Development of a novel software package for quantitative analysis of intra-plaque neovascularization during contrast-enhanced ultrasound (CEUS) imaging

8.1 ABSTRACT

Background

Contrast-enhanced ultrasound (CEUS) has emerged as a promising technique for detection of intra-plaque neovascularization (IPN), a surrogate marker of plaque vulnerability. Quantification of CEUS images has proven challenging and a widely-available, reliable and accurate quantification algorithm is still required.

Methods

This collaborative study aimed to develop a novel and reproducible tool for quantitative analysis of CEUS images. Attenuation correction, motion compensation and bubble contrast detection were identified as key steps in development of the algorithm. Validation of this algorithm would be against histology, obtained by recruiting patients with significant carotid arterial plaques that were scheduled to undergo carotid endarterectomy. Neovessel density on quantitative CEUS analysis would be compared against histological neovessel density using Bland-Altman agreement methods.

Results

An algorithm was developed incorporating methods for attenuation correction, motion compensation and bubble detection. Over a 9 month period, 10 patients with significant carotid

stenosis were recruited, of whom 9 underwent CEA. CEUS image analysis was considerably limited by attenuation from heavily calcified plaques and proved impossible to analyse using the novel quantification software tool.

Conclusions

It did not prove possible to analyse CEUS images obtained from patients with significant stenosis awaiting CEA in view of extensive calcification in all subjects. Furthermore, it did not prove possible to recruit a sufficient number of patients within the study time period.

8.2 INTRODUCTION

Technological advances in medical imaging over the past quarter century have facilitated significant improvements in our abilities to confirm diagnoses, estimate disease burden, perform risk stratification and even estimate prognosis by non-invasive methods. A number of these imaging techniques – whether using ultrasound or cross-sectional modalities such as computed tomography (CT) and magnetic resonance imaging (MRI) – rely upon the use of contrast agents to enhance the diagnostic yield of imaging.

Iodine-based (x-ray angiography and CT) and gadolinium-based (MRI) contrast agents are widely used in daily practice and, over the past two decades, ultrasound contrast agents (UCAs) have also been used in clinical cardiology and, more recently, in diagnostic radiology laboratories as well. UCAs are most frequently used in echocardiography to improve endocardial border definition and thus allow accurate assessment of global and regional systolic function.¹⁷⁷ However, their presence within myocardial capillaries permits assessment of myocardial perfusion.¹⁷⁸ Whilst this can be done by visual or qualitative analysis, quantification of myocardial perfusion is also feasible¹⁷⁹ and has been reported in numerous prior research publications.¹⁸⁰⁻¹⁸²

To date, the use of contrast has permitted visual – that is, *qualitative* – assessment of carotid plaques but a more objective – that is, *quantitative* – measure is preferable to improve accuracy and reproducibility and reduce the intra- and inter-observer variability of these imaging techniques. Consequently, much research effort of late has focussed upon the ability to quantify contrast images in cardiovascular imaging.

CEUS has emerged in the past decade as a research tool of significant interest, permitting visualization of IPN and adventitial vasa vasorum and thus allowing insights into plaque composition. This is especially true in view of our ability to study the human carotid artery (owing to its superficial location that facilitates imaging) and then confirm these findings with histological specimens, given that such plaques are frequently excised during endarterectomy procedures. Although several in-house quantification attempts have been published (see table 3.1 on page 62), none of these software algorithms have been proven or validated external to their centre of development and none are available for widespread use.

In view of the above, we collaborated with biophysicists at Imperial College, led by Dr Mengxing Tang, to develop quantification software with the specific aim of improving the objectivity of CEUS. Dr Tang and his group agreed to assist in the development of computer image analysis tools for reliable quantification of contrast enhancement within plaques and the vessel wall. Specifically, we aimed to develop techniques for computer assisted image segmentation of regions of interest (e.g. plaques, vessel wall, lumen etc.), automatic imaging artefact removal including attenuation and nonlinear artefacts (which are common in CEUS images) and automatic quantification of perfusion within regions of interest. Therefore, a cross-sectional study was designed to validate the novel quantification software against plaque histology obtained from patients scheduled to undergo carotid endarterectomy (CEA) for clinical reasons.

8.3 METHODS

Development of Quantification Software

A number of steps were identified that would need to be addressed in order to create a reliable quantification tool. These included addressing attenuation artefacts, motion artefacts and non-linear imaging artefacts, followed by development of the microbubble detection & quantification software. In this section, the steps taken to address each of these will be briefly discussed.

Attenuation Correction

Ultrasound images are affected by attenuation, the reduction in an ultrasound beam's intensity as it passes through a medium. Reflection, refraction, absorption and scatter all contribute to attenuation. If this attenuation is not corrected for, it would have a significant impact upon the reliability of techniques developed to quantify a contrast-enhanced image. The degree of attenuation depends upon the medium through which sound waves are travelling, as shown in table 8.1:

Medium	Attenuation Coefficient
Bone	5.0
Muscle	1.5-3.5
Fat	0.65
Blood	0.18
Water	0.002

Table 8.1: Attenuation coefficient of different tissues at a frequency of 1MHz (these values should be multiplied for different transducer frequencies – e.g. for 5MHz multiply by 5).

Time gain compensation (TGC) is commonly used for correcting attenuation (where echo signals are amplified as a function of time, so the further the echoes come from, the higher the signal gain is). However, TGC cannot account for spatially heterogeneous attenuation caused by either heterogeneous tissue distribution or non-uniform contact between the probe and skin.¹⁸³ It is also difficult for TGC to account for variations in tissue attenuating properties across patient populations. Consequently, it is quite common to see firstly, shadowing in vascular ultrasound images a manifestation of spatially heterogeneous attenuation; and secondly, variations in image intensity between patients, a manifestation of population variation.¹⁸³ It is important to note that attenuation may not necessarily be visually identifiable because of image compression at the point of image display, but could still be the cause of major errors in quantification based upon image intensity and this would subsequently limit the clinical utility of CEUS quantification.

Therefore, an attenuation correction algorithm for CEUS carotid artery images was developed. An assumption was made that, since the contrast was to be administered by a continuous intravenous infusion, the image intensity within the vessel lumen should be homogeneous. On the basis of this assumption, the algorithm initially estimates and corrects for the attenuation within the carotid lumen and then extends the correction at the lumen boundary to the vessel wall next to the lumen.¹⁸³ Furthermore, the images are normalised so that quantification of contrast enhancement is less affected by variations in the dose of contrast agent or patient variations. A block matching (rigid) algorithm was developed.

The first step of linear data conversion was performed by taking the exponential of log-compressed data. Using the lumen as a reference, a 2-D Gaussian filter was applied to estimate the attenuation profile within the lumen. Once the attenuation profile had been estimated,

attenuation correction was achieved by performing a numerical division of the original image and the estimated attenuation profile within the lumen. If the attenuation effect is corrected within lumen, the intensity of lumen should be more homogenous. The compensated image was then converted back to compressed data by taking the logarithm of the corrected image. To avoid the problem of division by zero, a regulariser was added to each pixel of the corrected image. The value of the regulariser was estimated by minimising the normalised intensity fluctuation within corrected lumen. Finally, the intensity of the compensated image was rescaled in such a way that the peak intensity within the lumen was located at exactly one (1.0).

Analysis of CEUS video sequences was performed off-line using in-house software developed using MATLAB (The MathWorks, Natick, USA). Regions of interest (ROIs) were selected manually, one to segment the lumen and the others to include regions within plaques, within which quantitative analysis was desired.

Motion Compensation

There are two main sources of motion artefacts:

- (1) Inherent arterial wall movement caused by the pumping motion of the heart
- (2) Human motion of the ultrasound probe

In order to correct these motion artefacts, a block-matching algorithm was employed. Firstly, a region-of-interest (ROI) was defined (by the clinician) in the first frame. Then, the algorithm was set to search the position of a block of the reference ROI from the second frame to the last frame to determine accurate ROI movement (figure 8.1). The block was referred to as an image template. The image template was shifted over the search region and a similarity measure

calculated for each possible shift. The shift where the largest similarity measure was achieved was the position where the template was most likely to be in the subsequent frame.

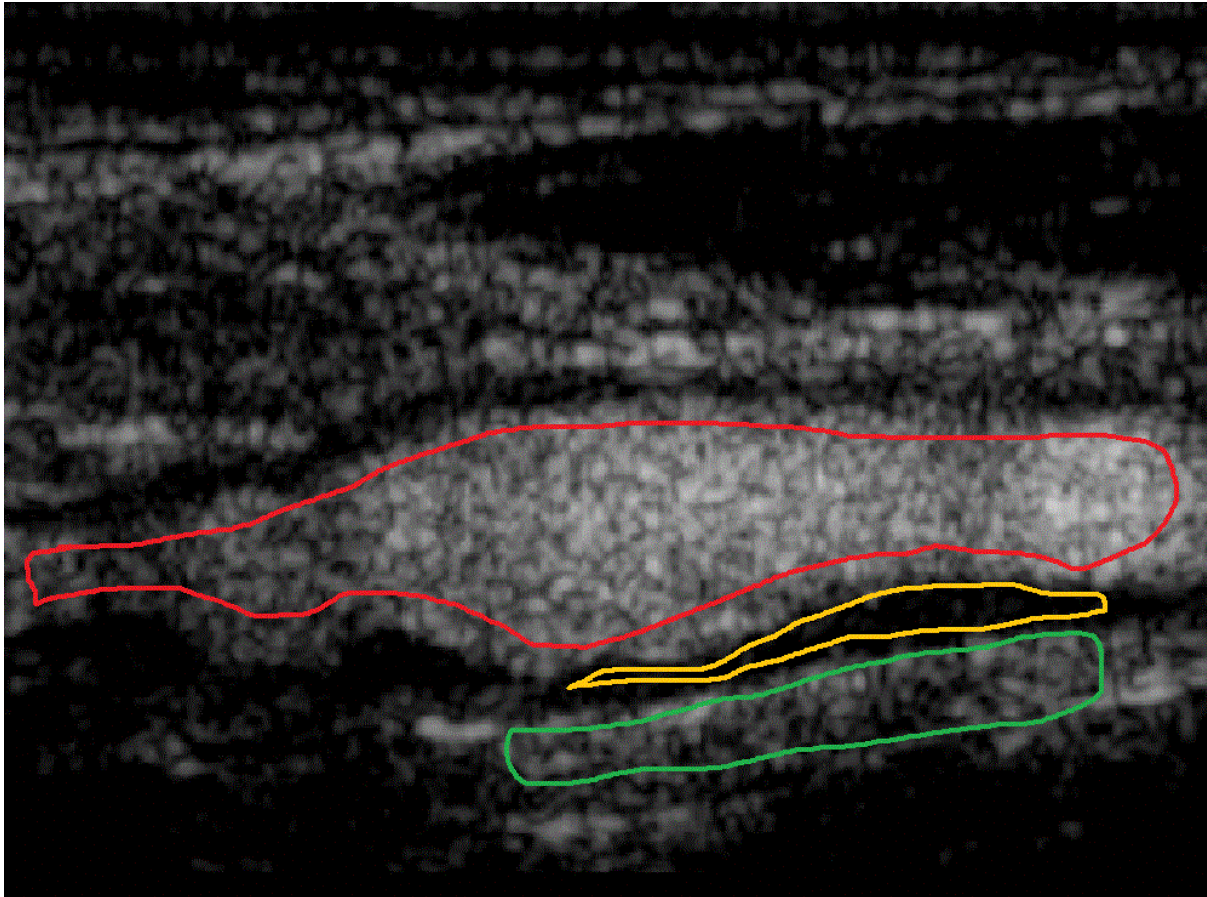


Figure 8.1: Regions of interest drawn on a CEUS image within the lumen (red), a plaque (yellow) and the adventitia (green). The pixel intensity, after correction algorithms were applied, was used to help determine the threshold used to differentiate bubbles from tissue in the algorithm.

Non-rigid motion compensation was used to compensate for movement of the carotid artery and comprises global and local motion models. The global model described the overall motion of carotid artery and an affine transformation was adapted to calculate the scaling and shearing of the artery. An affine transformation is any transformation that preserves co-linearity (i.e. all points lying on a line initially still lie on a line after transformation) and ratios of distances (e.g.

the midpoint of a line segment remains the midpoint after transformation).¹⁸⁴ For local motion correction, a spline-based free form model was chosen. The principle was to deform an object by manipulating an underlying mesh of control points.

The physicists' with whom we collaborated on this project validated these algorithms firstly in a phantom model and then against visual interpretation of previous CEUS images, the results of which have recently been published.¹⁸³ In summary, the results demonstrated that the overall image quality was improved by the attenuation correction algorithm, in particular the vessel lumen appeared brighter and more homogenous throughout its length in terms of pixel intensity.

Bubble Detection

In order to distinguish a bubble from tissue from 'noise' (i.e. artefact), thresholds of pixel intensity needed to be determined. Histograms were plotted to identify pixel intensities typical of microbubbles (from the lumen) and of tissue (e.g. from the vessel wall and adjacent tissues). The average and peak intensity and normalized variance were calculated at each pixel location to quantify tissue activity and noise. Consequently, the number of pixels due to bubbles in any given ROI was calculated as the number of pixels in the ROI less the number of pixels assigned to tissue and assigned to noise. For each CEUS data set, a ROI was drawn within the plaque and contrast variation over time (CVOT) was calculated for each pixel within the ROI. The number of pixels displaying CVOT was expressed relative to the total number of pixels in the ROI, giving a ratio termed the relative active area, a surrogate marker for plaque neovascularization.

We planned to assess the accuracy of the novel quantification software, which would use attenuation correction and motion correction algorithms to optimize image quality before

analysing pixel intensities within the lumen and ROI (i.e. plaque), by comparison against the histological neovessel density.

Patient identification and consent

Patients were identified and initially approached either in the Vascular Surgery Outpatient Clinic at Northwick Park Hospital – by their responsible doctor – or, more frequently, on the hospital stroke ward if awaiting CEA as an in-patient. If agreeable to discussing participation, the purpose of the study, aims and objectives and what enrolment would involve were all discussed. Consent to enter the study was sought from each participant only after a full explanation was given, an information leaflet offered and sufficient time allowed for consideration. Written and signed participant consent forms were obtained for all subjects that enrolled in the study. The right of the participant to refuse to participate without giving reasons was respected. Entry into the study did not hinder the responsible clinicians from recommending alternative treatment to that specified in the protocol at any stage if he/she felt it was in the participant's best interests. All participants were free to withdraw at any time from the protocol treatment without giving reasons and without prejudicing further treatment.

Patient specific data / variables were collected from the medical notes as well as by consulting the electronic patient records of the hospital and, where necessary, primary care databases also. These were collated on a pre-designed specific Case Report Form (CRF). The following data were documented on each patient's CRF:

Cardiovascular risk factors

- Known diagnosis of hypertension

- Known diagnosis of hyperlipidaemia
- Known diagnosis of Type I or Type II diabetes mellitus
- Family history of premature cardiovascular disease (defined as a myocardial infarction or ischaemic stroke in a male first degree relative <55yrs or a female first degree relative <65yrs) & smoking status

Medication history

- Use of cardiovascular drugs (e.g. aspirin, statins, ACE inhibitors, beta-adrenoceptor antagonists and diuretics) as well as anti-diabetic medications were all documented

Past medical history

- Previous myocardial infarction or stroke
- Previous percutaneous coronary intervention (PCI) or bypass surgery (CABG)
- Other medical illnesses / conditions

Body mass index

- Height (in metres)
- Weight (in kilograms)

Blood results

- Full blood count
- Serum biochemistry (including renal and liver function)
- Fasting lipid profile

Study procedures

Following informed written consent, patients underwent carotid ultrasonography (with and without Sonovue ultrasound contrast agent) prior to their scheduled date of surgical carotid endarterectomy. All ultrasound studies were undertaken in a standardized fashion using a commercially available ultrasound system (Vivid 7, GE Healthcare). The total time for the carotid ultrasound scan was approximately 30-45 minutes. In order to give the contrast agent, an intravenous cannula was inserted prior to imaging (the majority of in-patients already had a cannula in situ).

Carotid ultrasonography (B-mode and CEUS imaging)

Carotid duplex scans were all performed by myself in the echocardiography department at Northwick Park hospital. All patients had blood pressure measured by an automated sphygmomanometer prior to commencing the scan and had ECG monitoring throughout the scan. The common carotid (CCA), internal carotid (ICA) and external carotid (ECA) arteries on both left and right sides of the neck were examined with the patient supine on an examination couch during both B-mode and CEUS carotid imaging, which were both performed as described in previous Chapters.

Histological Analysis

Specimens were collected from General Theatres in Northwick Park Hospital at the time of endarterectomy. Excised plaques were placed in specimen jars containing formalin and immediately taken to the Pathology department for processing, which was performed by a

pathologist, blinded to the CEUS findings, experienced in plaque analysis. In brief, CEA specimens were fixed in formalin, sliced into 5µm longitudinal sections, embedded in paraffin and stained with Movat's pentachrome. Immunohistochemical staining, with CD31 and CD34 markers for endothelial cells of neo-vessels, were used to identify IPN. The proposed methodology for this aspect of the study was to derive a ratio of the neovascularisation area to total plaque area by dividing the IPN areas by the mean plaque area on each cardiac cycle, as previously described¹²⁹, which would allow expression of IPN as a ratio of neo-vessel area to total plaque area. The degree of agreement between these ratios on CEUS and corresponding findings on histology would thus be compared using Bland-Altman plots to assess agreement.

Statistics – Sample Size Calculation

The prevalence of IPN was estimated to be very high in these patients. Hoogi *et al*¹²⁹ found that 86% patients undergoing CEA had IPN, whereas Giannoni *et al*⁷³ found IPN in 100% of patients. A prevalence of IPN of 90% amongst these patients was therefore assumed.

The sensitivity and specificity of CEUS to detect IPN were estimated at 85% and 90% respectively (values used in a multi-centre CEUS study using Optison, sponsored by GE Healthcare). The degree of agreement between the ratios of neovessels area: total plaque area obtained by CEUS and histology (gold standard) would be judged by Bland-Altman analysis.

Bland-Altman analysis is an *estimation* problem; it estimates a prediction interval for a difference between two measurements by different methods – the limits of agreement. If one knows how accurately one wants to estimate the limits of agreement, this can be used to work out the sample size. However, in order to do this for our study, we would need to know the standard deviation of the measurements made by the quantification software, which is unknown

as this is currently in development. Consequently, the advice from the medical statistician was to make the sample size calculation on the basis of the expected correlation coefficient that might be obtained between the two parameters.

Using a 2-sided alpha of 0.05 and beta 0.1 (i.e. 90% power), the table below illustrates the sample sizes we would need (Stata 10.0, StataCorp LP, Texas, USA):

Alternate Rho (r) [Null Rho = 0]	Sample size (N)
0.80	12
0.75	15
0.70	17
0.65	21
0.60	25
0.55	31
0.50	38

Table 8.2: Sample sizes with corresponding strengths of correlation

The study thus aimed to recruit *at least 25 patients* to this study, to allow detection of a correlation of 0.60 and higher with sufficient confidence.

8.4 RESULTS

Over an eight month period (April-December 2013), ten patients consented to participate in the study. All ten patients had been hospitalized following either TIA or CVA, had a significant carotid stenosis identified on clinically-requested carotid ultrasonography and had been referred to the vascular surgeons for consideration of CEA.

The baseline characteristics of these 10 patients are shown in table 8.3:

Patient Characteristic	N (%)
Mean Age \pm SD (yrs)	72 \pm 8
Male Gender	7 (70%)
Hypertension	8 (80%)
Hyperlipidaemia	7 (70%)
Diabetes Mellitus	5 (50%)
Smoker	2 (20%)
Positive Family History	1 (10%)
Known Ischaemic Heart Disease	2 (20%)
Mean Body Mass Index (kg/m ²)	24.2 \pm 4.4

Table 8.3: Baseline patient characteristics

All patients underwent carotid imaging, although one patient changed his mind following B-mode imaging, stating that he did not wish to continue with CEUS imaging or remain in the study and so contrast imaging was not performed and a surgical specimen was thus also not collected from theatres, as there would be no comparison possible in this patient between CEUS images and histology. B-mode and CEUS images were stored for off-line analysis for the remaining 9 patients and the plaques were collected from theatres and promptly delivered to the Pathology department for these patients also.

Imaging revealed large, calcified plaques in all 9 patients, most frequently in the carotid bulb or at the origin of the internal carotid artery (see figure 8.2). Figures 8.3 and 8.4 show B-mode and CEUS images of large plaques, which created significant shadowing artefacts in the far

wall and which made image analysis for IPN detection very challenging. Image analysis was further hindered by motion artefact and excessive plaque calcifications.

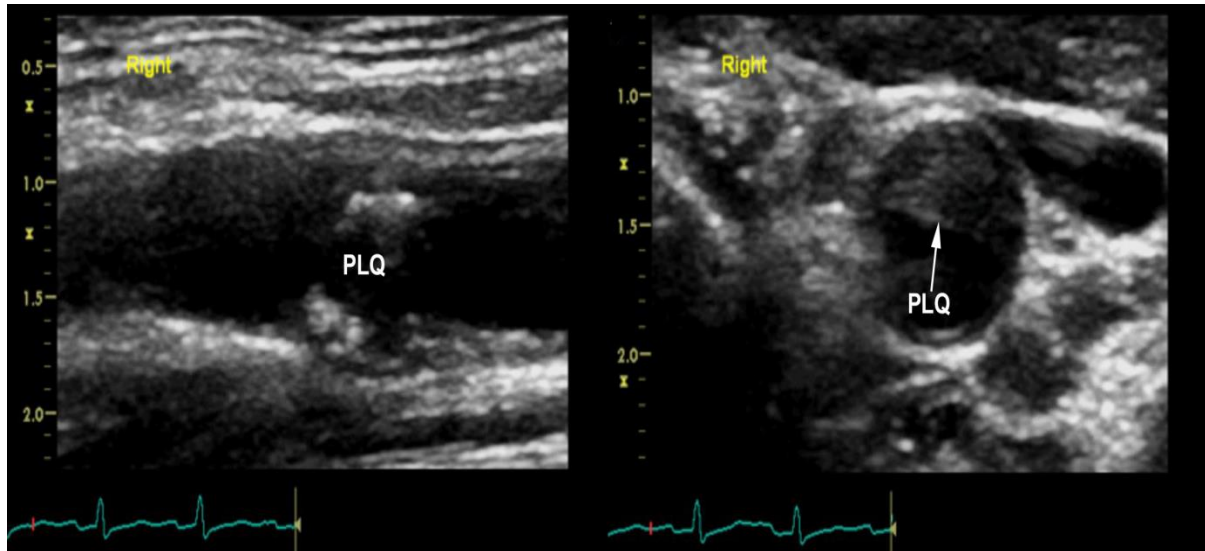


Figure 8.2: Long-axis (left) and short axis (right) B-mode images from a right carotid artery showing a large flow-limiting plaque (PLQ) in the carotid bulb.

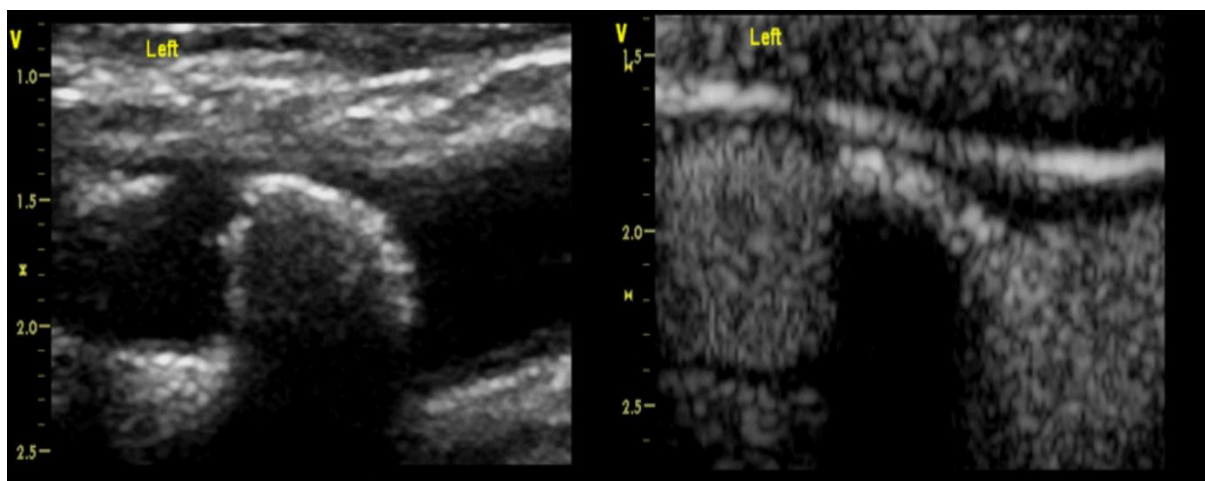


Figure 8.3: Long axis B-mode (left) and CEUS (right) images of a large plaque. Note the significant shadowing artefact seen in the CEUS image as a result of the echo-bright calcium in the near wall. This shadowing obscures the remainder of the plaque.

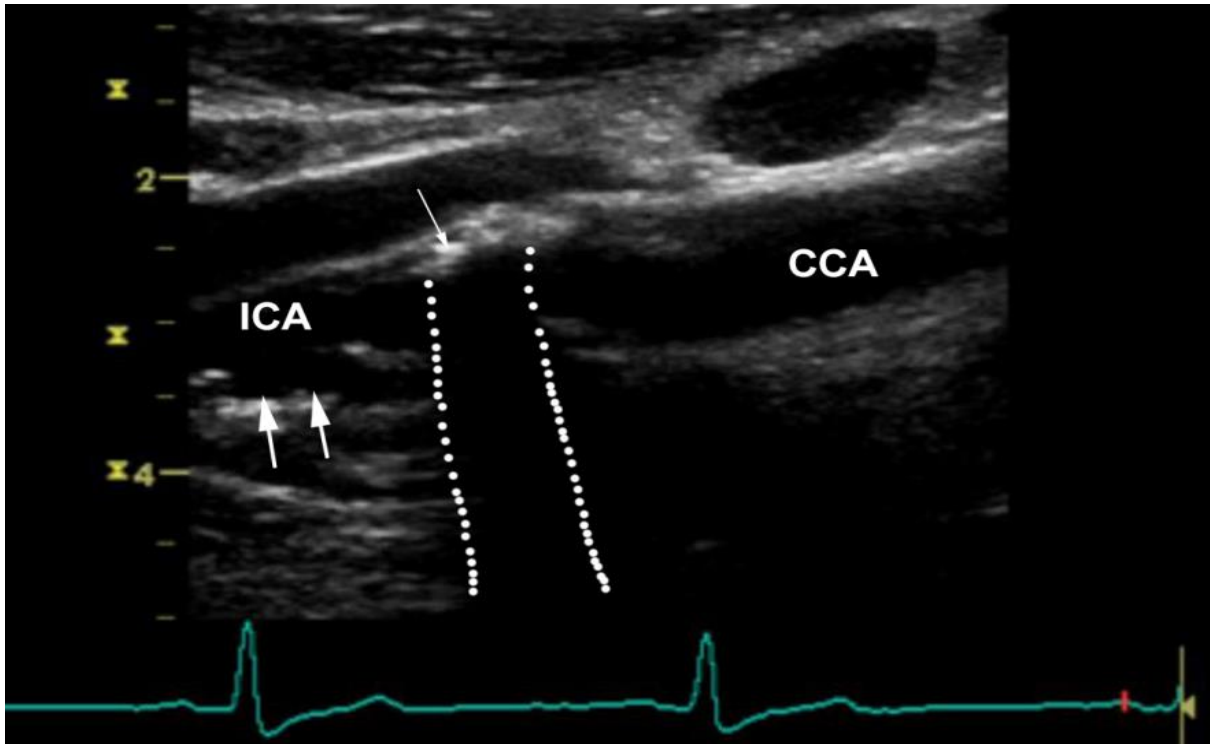


Figure 8.4: An example of significant attenuation / shadowing artefact (outlined between white dotted lines) caused by a near wall plaque (single arrow) which obscured a far wall plaque which extended into the ICA also (two white arrows).

It did not prove feasible to analyse any of the CEUS data obtained in this study using the novel quantification software for the above reasons. It had also proven impossible to recruit the required number of patients as per the sample size calculation and therefore, in combination with the inability of our quantification software to analyse the data, the decision was taken not to analyse the histological samples obtained (as no comparisons would be feasible with CEUS data).

8.5 DISCUSSION

In this study, the intended objective of validating novel quantification software for future use in quantitative analysis of CEUS images from human carotid arteries was not fulfilled. This arose from challenges in obtaining tissue specimens, challenges in analysing the CEUS images and challenges also with the quantification software itself. Each of these merits further discussion in turn.

Challenges in obtaining sufficient numbers of patients

As clinical medicine has evolved over time, the practice of elective excision of carotid plaques in asymptomatic individuals has declined, such that the majority of CEA procedures are now confined to patients hospitalized following acute neurological events. This reduced the number of potential study participants and, in fact, during the study period of 8 months there were no CEA operations performed on elective outpatients in this large centre, one of only 8 designated hyper-acute stroke units in Greater London.

Additionally, there was the predictable but nevertheless challenging issue of obtaining informed consent from patients that had recently suffered a stroke. There were some patients that clearly lacked capacity to consent to participate in the study and therefore could not be enrolled. There were also other patients who, even if able to consent, were unlikely to be capable of laying supine for 30-40 minutes to enable high quality images to be obtained with minimal motion and respiratory artefact.

Thirdly, there were a number of patients hospitalized with acute stroke who were thought to have significant stenosis on clinical Duplex scanning but who in fact, upon CT imaging, were

shown to have complete ICA occlusion and these patients were managed conservatively. As a result, after one such patient had been entered into this study but then subsequently not had surgery, none of these subsequent patients could be enrolled into the study as obtaining histology would not be possible (as surgery was not planned).

Each of the above factors combined to reduce the number of patients available to consent for the study and thus contributed to the small number of patients recruited. Previous studies have also reported low patient numbers across lengthy time periods, for example Müller et al¹³³ required 3 years (2008-2011) to recruit 33 patients for their study, a rate of recruitment consistent with the present study.

Challenges in CEUS image interpretation

Unlike the asymptomatic patients that had been scanned in the cardio-oncological collaborative study reported on in Chapter 7, the images obtained from these symptomatic patients were significantly different. The most striking and important difference related to the degree of calcification seen in the plaques in the present study. The large echo-bright masses seen in these patients unfortunately created large shadowing ultrasound artefacts, such that heavily calcified plaques in the near wall – and thus near field on imaging – cast a shadow over the far wall of the vessel, thus obscuring plaques that been identified on the B-mode scan and therefore preventing image analysis. This was true in almost all the CEUS images obtained, in both long axis and short axis views.

Furthermore, the heavily calcified plaques, which were echo-bright on the B-mode scan, became less clearly seen during CEUS imaging – an example of this is provided in figure 8.5.

During B-mode imaging, the echo-bright nature of calcium contrasts sharply with the black appearance of the vessel lumen (i.e. bloodpool signal) resulting in very easy identification of calcium. However, during contrast imaging, the echo-bright signal of calcium can become obscured by the white appearance of contrast bubbles within the vessel lumen, making such plaques harder to see and indeed, in some cases, almost making very large, calcific plaques virtually impossible to detect (see figure 8.5). This problem thus precluded close inspection of the plaques for IPN assessment.

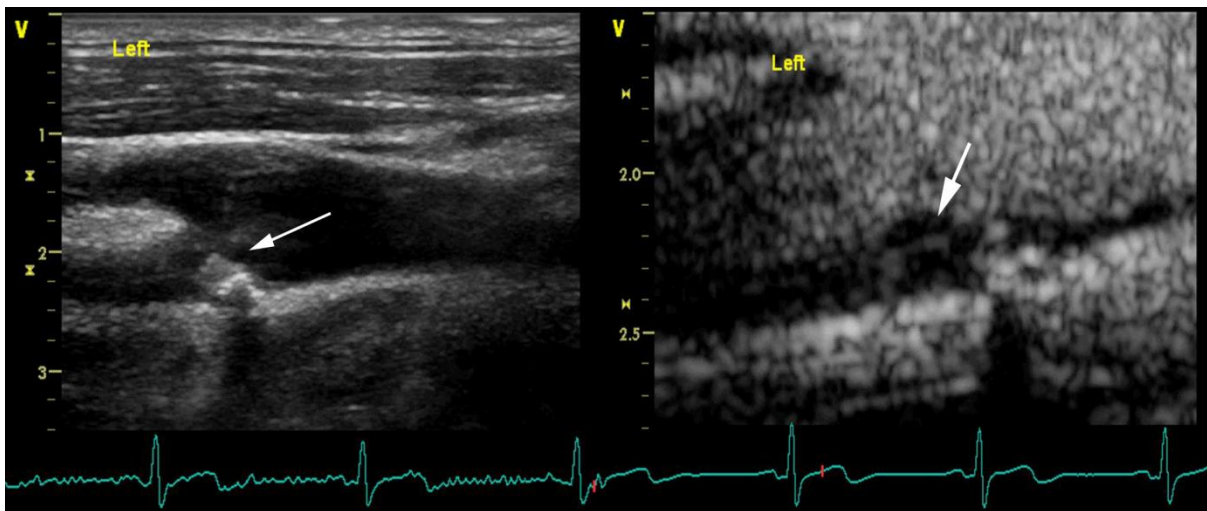


Figure 8.5: A large plaque was seen on B-mode imaging (arrow, left panel) in the carotid bulb but this became less clearly seen on CEUS imaging (arrow, right panel) as the calcified regions of plaque were seemingly washed out by the contrast opacification in the lumen.

Challenges with the Quantification Software

A literature search suggests that this is the first study to attempt quantification of CEUS using only CEUS images without simultaneous B-mode data. All other studies in this field to date have used dual-mode imaging systems, which permit side-by-side simultaneous display of B-mode and CEUS images (see figure 8.6). This significantly increases the difficulty for

designing the software, as the simultaneous B-mode data is used to determine if changes in intensity of a pixel are due to motion and to help distinguish between tissue and a contrast bubble. As it happened, without the simultaneous B-mode data, it turned out to be considerably more challenging to develop and write algorithms that could compensate for the lack of B-mode data.

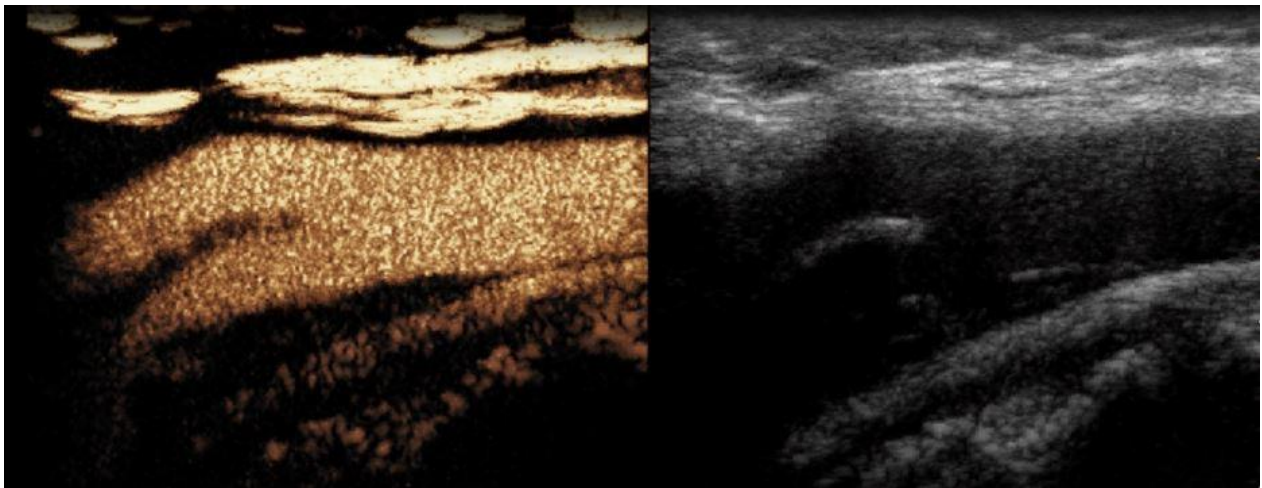


Figure 8.6: Simultaneous side-by-side CEUS (left) and B-mode (right) imaging, acquired using a radiology (rather than cardiology) ultrasound system [Philips iu22]. *Image courtesy of Dr Mengxing Tang, Imperial College, London.*

We were aware of the preference of our collaborating physicists' to have simultaneous B-mode data; however, this was not possible on the ultrasound system available to us. Many of the published studies using dual-screen images have been performed on a radiological (rather than cardiological) ultrasound system (e.g. Philips iu22 system rather than ie33 system) and therefore we had to accept CEUS images without simultaneous grey-scale images. The challenges in developing the quantification software against this backdrop affected our ability to analyse the CEUS images obtained from the patients enrolled in this study.

Future Work

In the absence of our ability to test our novel quantification software against histology, the true gold standard, the carotid CEUS images obtained from the radiotherapy patient cohort (described in Chapter 7) were analysed by the quantification software and compared against visual interpretation of IPN presence. This would allow some assessment of the feasibility and accuracy of the novel quantification tool. This further study forms the basis of Chapter 9.

Future work in this field will need to overcome the problems created by heavy calcification within plaques, although this may prove challenging as the artefacts generated by calcium are frequently large and difficult to eliminate completely.

Conclusions

In this study, a combination of challenges with patient recruitment, with CEUS image quality and with the quantification software culminated in an inability to validate novel software for the quantitative analysis of plaque neovascularization. As outlined above, several hurdles would need to be overcome to achieve this objective.

As a result of the above, a separate study was undertaken to compare the accuracy of the novel quantification software against the accuracy of visual analysis and this is described in the following section (Chapter 9).

CHAPTER 9

Assessment of Quantitative Analysis of Plaque Neovascularization During Contrast-Enhanced Ultrasound – A Comparison with Visual Assessment.

9.1 ABSTRACT

Background

Quantification of contrast signal within plaques is a desirable scientific goal for optimizing accuracy of detection of intraplaque neovascularization (IPN), a pre-cursor of plaque haemorrhage and putative surrogate marker of plaque instability. Novel quantification software can be compared against visual analysis in cases where direct histological comparison is not feasible.

Methods

Images obtained from the cardio-oncological collaborative study (described in Chapter 7) were analysed using the novel quantification software, described in Chapter 8. Quantification was performed by a biophysicist blinded to the visual interpretation results. Visual assessment of IPN was based upon a semi-quantitative scale – Grade 0 (no neovessels), Grade 1 (neovessels confined to plaque base) and grade 2 (extensive neovessels or vessels running through plaque body). Contrast variation over time (CVOT) and the percentage relative active area (RAA) were quantitative markers of plaque neovascularization. Agreement was assessed between visual analysis and quantitative analysis.

Results

CEUS images of 31 plaques, from 23 patients, were analysed using the newly-developed quantification software. The mean age of these patients was 58 ± 7 yrs and 57% were male. Although there was a numerical increase in CVOT and RAA between plaques in Grades 0, 1 and 2 IPN categories, this failed to reach statistical significance. Additionally, there was a broad range of values obtained within each category, such that no clear range could be identified that discriminated between plaques containing and those not containing neovessels.

Conclusions

The novel quantification software has shown only moderate ability to detect IPN, as seen on visual analysis. Additionally, at present this quantification algorithm cannot be used to reliably identify the presence and extent of IPN. Further work is required to improve the accuracy of this software before it is suitable for use in a large research study.

9.2 INTRODUCTION

Quantification of contrast-enhanced ultrasound images is a desirable goal, in order to improve the diagnostic accuracy as well as reproducibility of the technique. In the last Chapter, the project whose purpose was to assist in development – and subsequent validation – of novel quantification software was presented. As a result of challenges in patient recruitment, CEUS imaging and quantification of the obtained images, this project did not achieve its desired objectives.

Although quantification of contrast remains the gold standard, qualitative (i.e. visual) assessment of contrast images can still yield important and clinically meaningful results. Qualitative interpretation of contrast images is widely used, for example, in contrast-enhanced cardiac MRI scans for determining presence or absence of myocardial viability, based upon $<50\%$ or $>50\%$ thickness of contrast (reflecting scar tissue) signal within the myocardium.¹⁸⁵ Qualitative assessment of contrast signal within the myocardium during stress echocardiography, denoting myocardial perfusion, has also been widely reported upon and is also used clinically.¹⁸⁶

Several studies reporting upon the accuracy of newly developed (in-house) quantification packages for CEUS imaging have ‘validated’ their software by comparison against visual analysis.¹³³ Although this is not a true gold standard, it does permit some assessment of the software’s accuracy. Comparison of CEUS images against visual interpretation was not an original goal of this research thesis; however in view of the inability to validate against histology, this present study was undertaken with the aim of providing some insights into the

accuracy of the novel quantification software as it was anticipated that this might provide valuable data on the performance of the quantification software.

9.3 METHODS

The CEUS images obtained from the pre-endarterectomy in-patients (in Northwick Park Hospital) proved unsuitable for quantitative analysis in view of very heavy calcification. As a result, we decided to use the CEUS images obtained from the radiotherapy patient cohort that were described in Chapter 7. The majority of these patients did not have heavy calcification and thus the hypothesis was that it would prove more feasible to analyse using the quantification software. The methods for carotid imaging, by B-mode and CEUS techniques, for these patients are detailed in the Methods section (7.3) of Chapter 7.

Carotid plaques may be small or large in size and this can affect the ability of the software to detect IPN. Prior studies have restricted validation of their quantification software packages to arterial plaques of a certain size or height (e.g. although one part of the Mannheim consensus defines plaques as an area of IMT $>1.5\text{mm}$ in thickness,²⁶ Hjelmgren *et al* required a plaque height of $>2.5\text{mm}$ for inclusion in their study assessing a novel contrast quantification program).¹³¹ Accordingly, in this study, only plaques of height $>2.0\text{mm}$ were selected, in order to minimise the chances of errors with the quantification program due to an excessively small ROI for analysis. Preliminary data from such a study would, it was anticipated, be used to improve the robustness of the software in the future, thus allowing quantification of IPN in plaques of all sizes.

The CEUS cine loops were loaded into the quantification software. Regions of interest (ROIs) were drawn within the lumen, within the plaque and within the adventitia to denote these segments and then followed through the entire cine-loop, with manual adjustment of the ROIs where necessary in order to ensure that no areas of the lumen were within the plaque ROI and vice-versa. As outlined in the previous Chapter, the software produces a value for contrast variation over time (CVOT) of each pixel within the ROI, which ought to be zero – or close to zero – in a ROI in which there is no contrast seen, such as a plaque without IPN. Conversely, CVOT will be high in a ROI in which a large amount of contrast is seen, such as a ROI within a plaque with dense IPN. The number of pixels showing contrast variation is normalized by dividing by the total number of pixels within the ROI to produce the relative active area (RAA), a measure directly reflecting the extent of IPN within the ROI (i.e. the plaque).

9.4 RESULTS

The CEUS cine images of 31 carotid plaques, from 23 patients, were analysed using the quantification software. There were 13 (57%) men and the mean age was 58 ± 7 yrs. Overall, visual analysis of these plaques graded IPN as follows:

Grade 0 IPN	13 plaques
Grade 1 IPN	13 plaques
Grade 2 IPN	5 plaques

In the 13 plaques with no IPN by visual analysis (Grade 0), the mean and median CVOT values obtained were 296 and 19, respectively (range 0-2276). Only 4 plaques (31%) had a CVOT value of 0. In the 13 plaques with Grade 1 IPN, the mean and median CVOT values were 532 and 63, respectively (range 0-2417). Finally, in the 5 plaques with Grade 2 IPN, the mean and

median CVOT values were 1363 and 864, respectively (range 280-3051). Thus, there was a stepwise increase in both mean and median CVOT values with increasing IPN. However, there was also considerable overlap between the CVOT values obtained. A CVOT value of zero was detected in both Grade 0 and Grade 1 IPN plaques. A similar trend as observed with the RAA, as shown below:

IPN Grade	CVOT	RAA (%)	RAA Range
Grade 0	296	4.8	0 - 42
Grade 1	532	6.3	0 - 44
Grade 2	1363	18.1	1.8 - 51

Table 9.1: Mean CVOT and % RAA values stratified by IPN Grade (judged by visual analysis)

However, there was not a statistically significant difference in CVOT or RAA values between the 3 grades of IPN ($p=0.46$ [CVOT] and $p=0.76$ [RAA]). As the grading of IPN presence between grade 1 and grade 2 is subjective, the data for grades 1 and 2 IPN were also combined, creating just two categories (i.e. IPN absent [Grade 0] or IPN present [Grades 1 & 2]). However, again, there was not a statistically significant difference between these two groups for either mean CVOT values (296 vs. 763, $p=0.16$) or mean % RAA values (4.8 vs. 9.6, $p=0.35$).

There was also considerable overlap between values obtained across all 3 groups, as illustrated in figure 9.1:

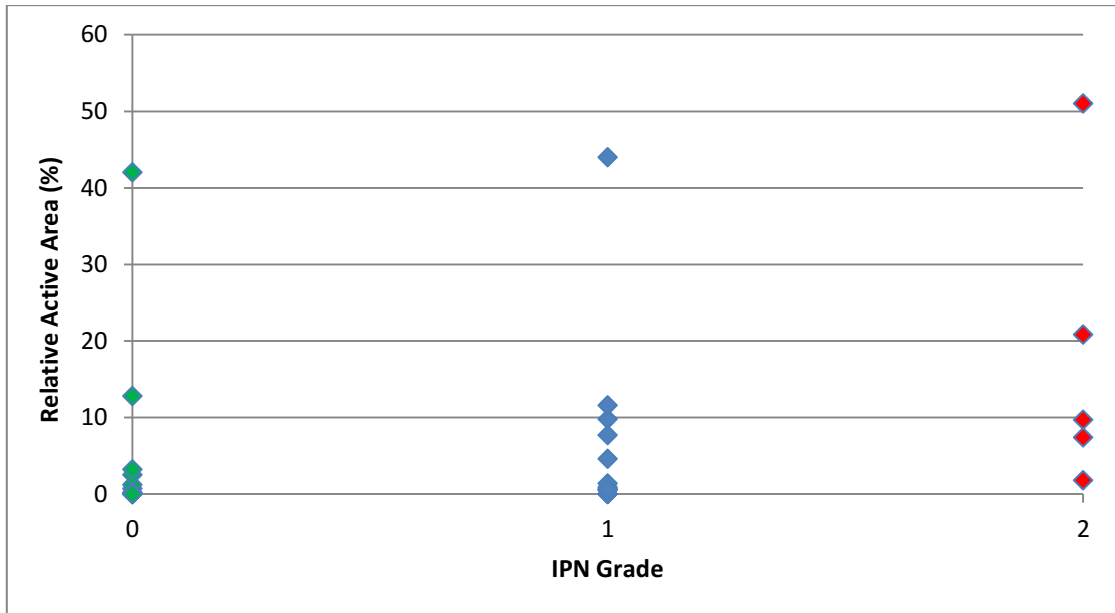
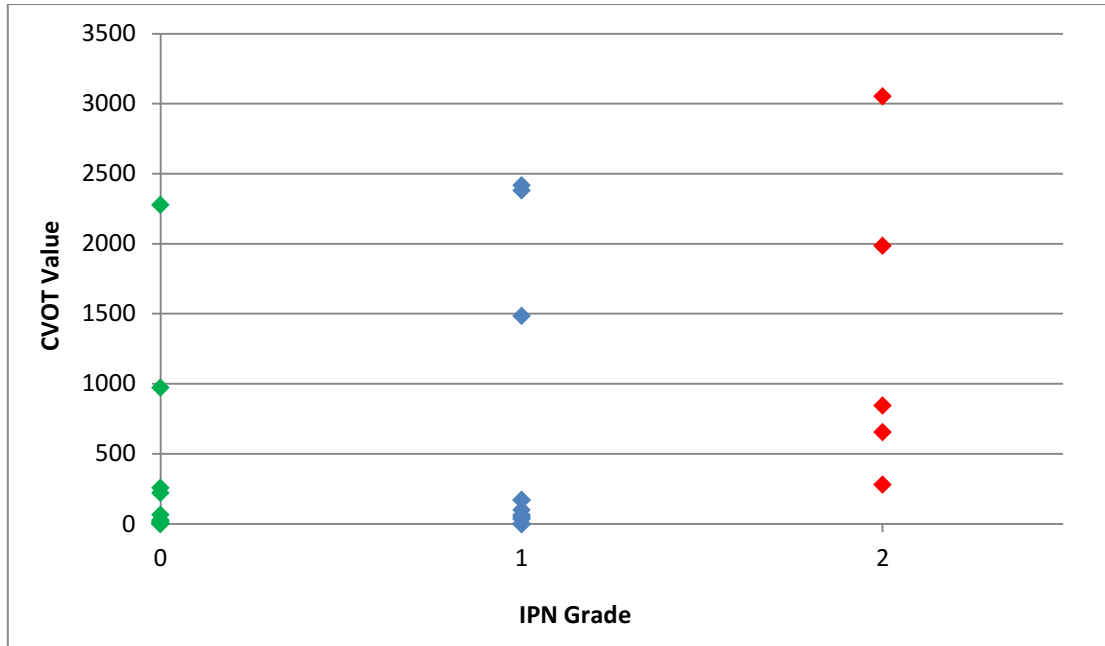
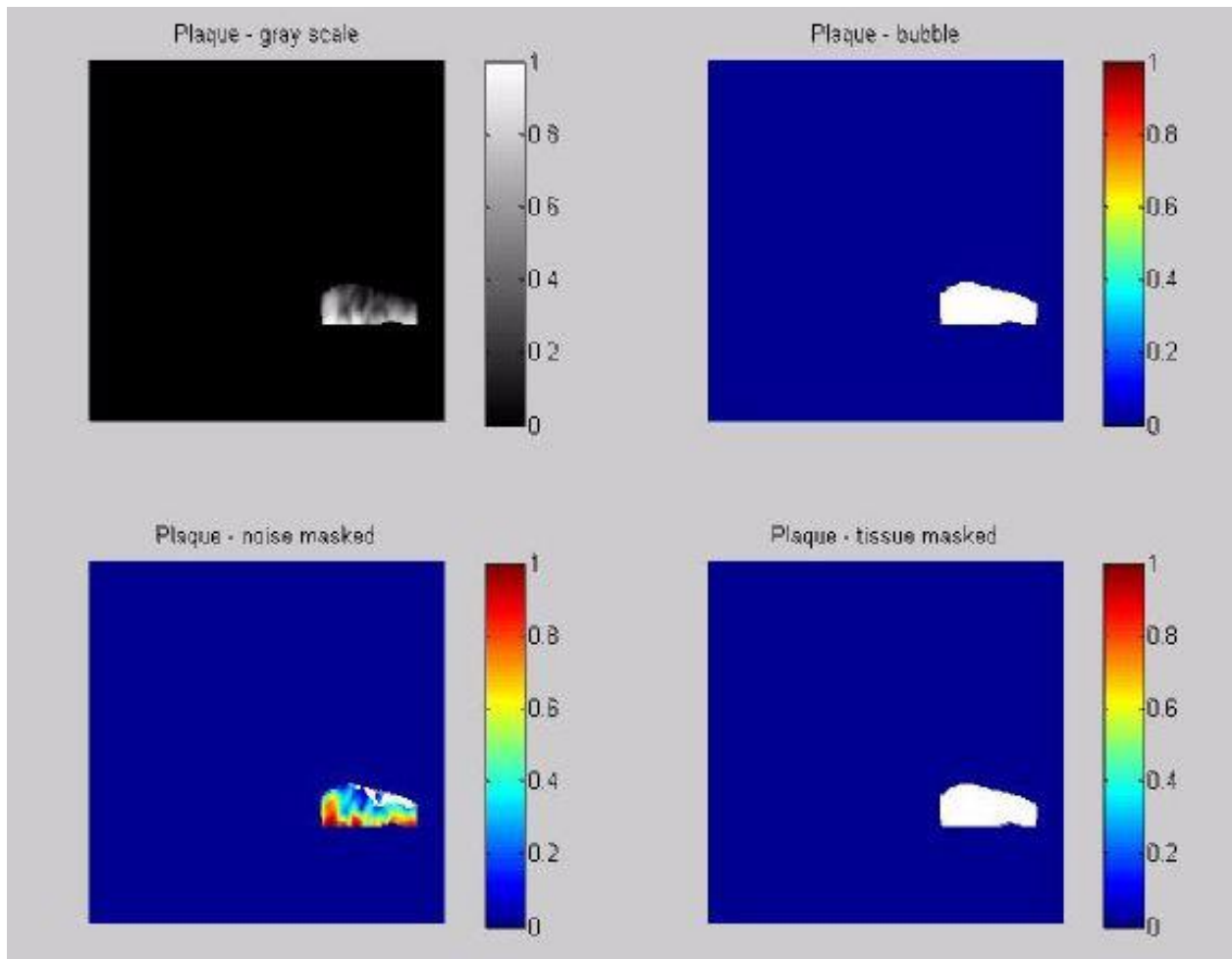
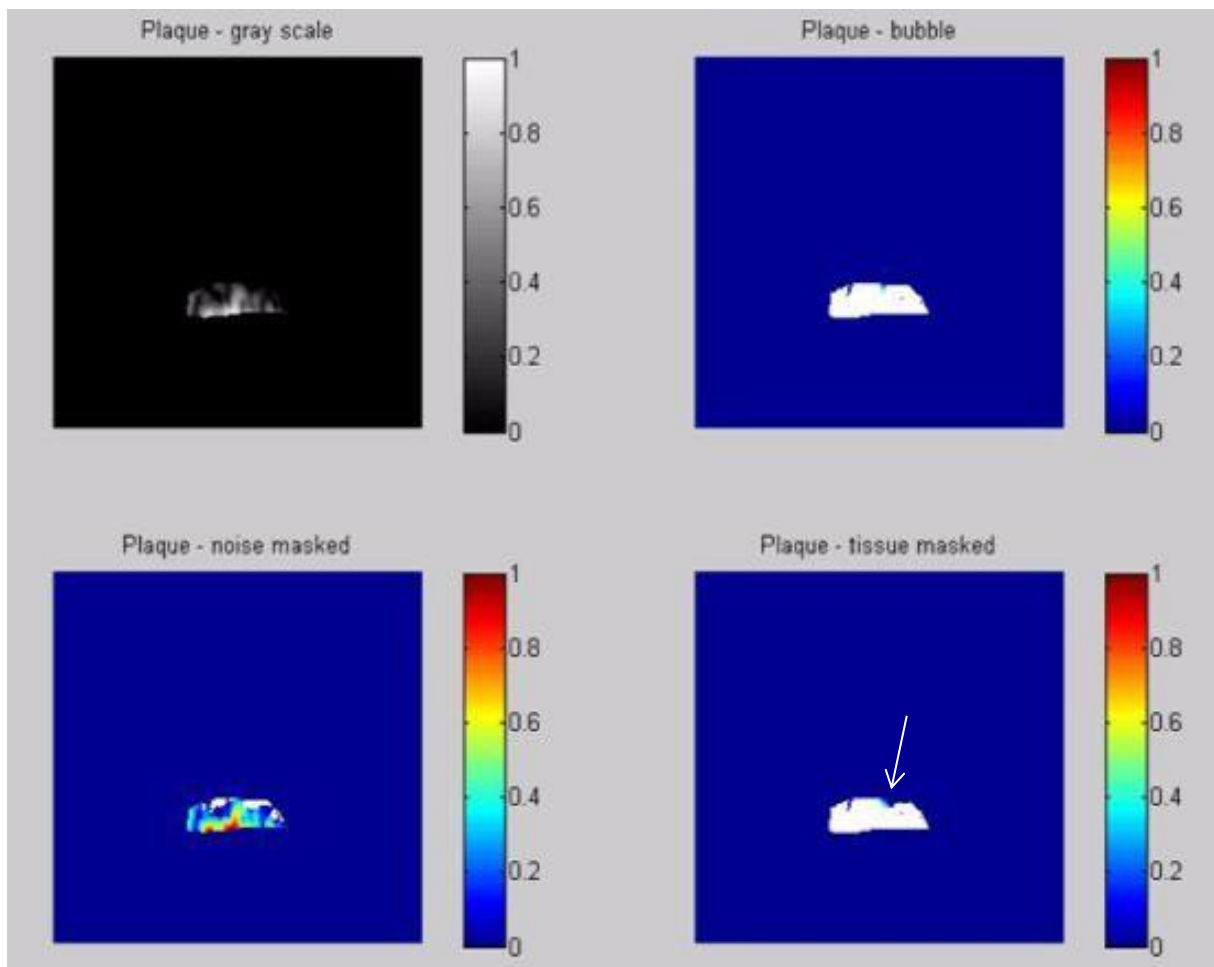


Figure 9.1: Scatter plots showing distribution of CVOT values (above) and % RAA (below) by visual IPN grade, illustrating significant overlap between each category.



*Figure 9.2: Quantification algorithm output in which a grade 0 plaque is **correctly** identified as containing no IPN. [Top left: the region of interest as it appears during CEUS; top right: non-bubble pixels (tissue + noise) are masked with white, coloured pixels (if present) represent bubble; bottom left: noise pixels are masked with white (coloured pixel means a non-noise (i.e. bubble or tissue) pixel; bottom right: tissue is masked with white pixels (coloured pixel means non-tissue pixel – in this case, the bottom right panel is also white only, meaning the algorithm has not detected any IPN).*



*Figure 9.3: Snapshot from quantification algorithm in which a grade 0 plaque is **incorrectly** identified as containing IPN. [Top left: contrast image with selected region of interest; top right: identified bubble, non-bubble pixels (tissue + noise) masked with white, coloured pixels (if present) represent bubble; bottom left: noise masked with white (coloured pixel means non-noise (i.e. bubble or tissue) pixel; bottom right: tissue masked with white pixel (coloured pixel means non-tissue pixel – in this case, the bottom right panel is mostly white but there are coloured pixels (arrow), indicating that the algorithm has detected IPN, which did not match with the visual assessment).*

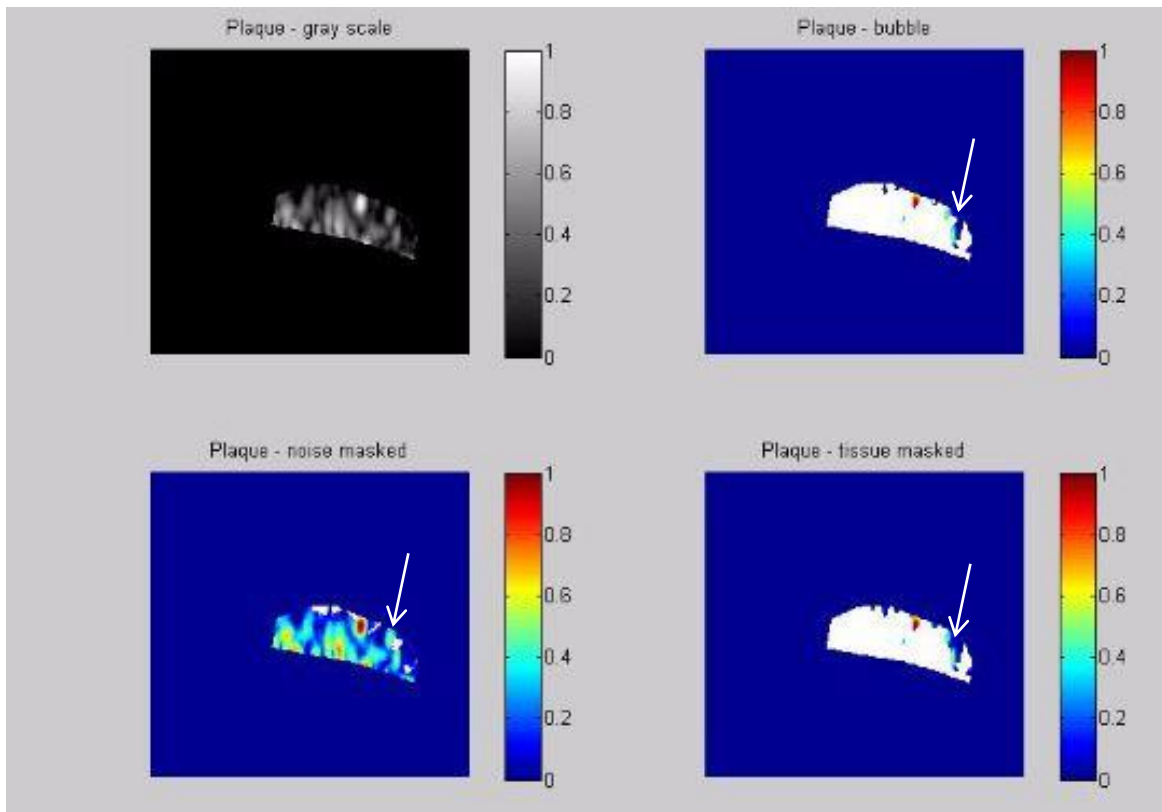


*Figure 9.4: Snapshot from quantification algorithm in which a grade 2 plaque is **correctly** identified as containing IPN (arrows). [Top left: contrast image with selected region of interest; top right: identified bubble, non-bubble pixels (tissue + noise) masked with white, coloured pixels (if present) represent bubble; bottom left: noise masked with white (coloured pixel means non-noise (i.e. bubble or tissue) pixel; bottom right: tissue masked with white pixel (coloured pixel means non-tissue pixel – in this case, the bottom right panel is mostly white but there are coloured pixels (arrow), indicating that the algorithm has detected IPN, which did match with the visual assessment).*

9.5 DISCUSSION

This study comparing the performance of the novel quantification software with visual assessment of IPN has found a moderate ability of the algorithm to identify presence or absence of IPN correctly. However, there was considerable overlap between values across the three groups, such that no clear cut-off values could be suggested, from which the algorithm could accurately distinguish between presence and absence of IPN.

There are several factors that may account for this. As already stated in the previous Chapter, the lack of simultaneous B-mode data for use in motion correction was a significant disadvantage in our study, in comparison with other groups also working on CEUS quantification techniques. Plaque motion within each cardiac cycle is inevitable and must be accounted (corrected) for. This is most easily achieved by having simultaneous B-mode data, which can be used to inform plaque motion directly. In the absence of this data, a separate and more complicated motion correction algorithm needed to be written. However, this has not performed as well as initially hoped, given that a number of plaques without IPN present visually had high CVOT / RAA values, suggesting inadequate motion compensation as one possible causative factor. Patients were not asked to suspend respiration for image acquisition and this could also help reduce motion of the vessel wall (and thus plaque) through the cycle.

There are also technical modifications required within the algorithm to improve the ability to distinguish between tissue, artefact (noise) and contrast bubble signal. This will require adjustments that can improve both the attenuation correction and motion compensation algorithms. Furthermore, adjustments to the bubble detection and quantification algorithms are required – in this study, signals from within the plaque were all summed, on the assumption

that non-bubble signals had been excluded. However, our results demonstrated that this was not the case. Improvements to the method by which contrast signal is initially detected and then tracked through the plaque will help to improve the accuracy of the algorithm. Work on these issues has already commenced and the biophysicists hope to have an improved algorithm for repeat testing imminently. Finally, it is acknowledged that this quantification algorithm, as with most previously reported algorithms, has only been tested on selected plaques of a certain size and is thus not applicable to all plaques – further studies are required – an no doubt improvements to the quantification algorithms – to allow quantitative analysis on carotid plaques of all shapes and sizes.

Conclusion

The novel quantification software has moderate ability to detect IPN on comparison with visual analysis of carotid plaques. Further work is required to improve the accuracy of the software. Changes in image acquisition – specifically the use of dual-mode imaging (permitting simultaneous side-by-side CEUS and B-mode images) is likely to be a crucial factor in the improvement of the quantification algorithm.

PART III

CONCLUSIONS

CHAPTER 10

Future Directions

Over the past decade, a large amount of basic and clinical research data has been accumulated with respect to plaque vulnerability. The data suggests that plaque composition plays a major role in plaque stability and that intra-plaque haemorrhage, thought to be secondary to rupture of leaky neovessels, is a pre-cursor to the unstable/vulnerable plaque. Contrast-enhanced ultrasound (CEUS) has emerged as a safe, painless and non-ionizing method of visualizing plaque neovascularisation. In this Thesis, several studies have been undertaken using CEUS to assess plaque neovessels.

The study of asymptomatic individuals from the LOLIPOP study found an overall incidence of IPN of approximately 50%, generating the further question of why some plaques develop IPN whilst others do not. The answer to this question is currently unknown. Furthermore, this study has identified, for the first time, a potential mechanism for the increased CVD risk amongst South Asian individuals, namely a greater incidence of IPN when compared to a European White population. This intriguing finding merits larger studies to confirm them but also throws up new questions, including the possible reasons for ethnic differences in neoangiogenesis within arterial plaques. A greater understanding of these mechanisms may help elucidate the reasons for greater CVD burden amongst South Asian individuals.

The collaborative cardio-oncological study with researchers from the Institute for Cancer Research at The Royal Marsden Hospital has, for the first time, explored differences in plaque composition between irradiated and un-irradiated carotid arteries amongst survivors of head &

neck malignancies. The results revealed a significantly increased incidence of neovessels within irradiated plaques, even though conventional thinking suggests radiation inhibits neoangiogenesis. These results suggest that radiotherapy may not simply increase IMT and plaque formation but also impact plaque composition and, thus, plaque vulnerability.

The ambition to design and validate a novel algorithm for quantitative analysis of CEUS images did not reach its desired conclusion. A secondary project comparing the algorithm against visual accuracy of IPN detection showed some promise but only moderate agreement overall and requires fine-tuning before use in larger studies. However, the attenuation and motion correction algorithms show promise and further refinements to the bubble detection algorithm should provide more robust software, which will require further validation.

Finally, analysis of the CEUS images from the LOLIPOP data-set also allowed study of the effect of contrast upon IMT visualization and plaque detection. CEUS was found to improve significantly the IMT visualization in the near wall and also all segments in the CCA and ICA. Furthermore, this did lead to a significant increase in plaque detection by CEUS. The clinical significance of this finding is yet to be determined but may have implications for primary prevention strategies, as greater interest in sub-clinical atherosclerosis yields new research studies.

The ‘hypothesis’ generated by considering IPN as a key component of the unstable (or potentially unstable) plaque is that plaque composition should be taken into account during clinical decision-making. Thus, an intriguing question that is raised by the plaque neovascularisation hypothesis is whether plaque composition rather than stenosis severity should dictate treatment strategy (e.g. surgical endarterectomy versus no surgery). There are

no randomised trials that have compared such management options, but there is growing awareness of the importance of plaque content with regards to likelihood of plaque erosion +/- rupture and thus likelihood of major CV events such as myocardial infarction and stroke. The results of these studies have demonstrated that not all plaques contain IPN and follow-up of such patient cohorts will hopefully allow further light to be shed on plaque neovascularisation as a potential novel imaging risk marker, not just in research studies but also in clinical practice.

CHAPTER 11

REFERENCES

1. World Health Organization (WHO). Global status report on noncommunicable diseases 2010. 2011;2014
2. World Health Organization (WHO). Global atlas on cardiovascular disease prevention and control. 2011;2014
3. Mathers CD, Loncar D. Projections of global mortality and burden of disease from 2002 to 2030. *PLoS Medicine*. 2006;3:e442
4. Nichols M TN, Luengo-Fernandez R, Leal J, Gray A, Scarborough P, Rayner M. European cardiovascular disease statistics 2012. *European Heart Network, Brussels, European Society of Cardiology, Sophia Antipolis*. 2012
5. Myerburg RJ, Interian A, Jr., Mitrani RM, Kessler KM, Castellanos A. Frequency of sudden cardiac death and profiles of risk. *Am J Cardiol* 1997;80:10F-19F
6. Wilson PW, D'Agostino RB, Levy D, Belanger AM, Silbershatz H, Kannel WB. Prediction of coronary heart disease using risk factor categories. *Circulation*. 1998;97:1837-1847
7. Third report of the National Cholesterol Education Program (NCEP) expert panel on detection, evaluation, and treatment of high blood cholesterol in adults final report. *Circulation*. 2002;106:3143-3421
8. Hippisley-Cox J, Coupland C, Vinogradova Y, Robson J, May M, Brindle P. Derivation and validation of qrisk, a new cardiovascular disease risk score for the United Kingdom: Prospective open cohort study. *BMJ*. 2007;335:136
9. Collins GS, Altman DG. An independent external validation and evaluation of qrisk cardiovascular risk prediction: A prospective open cohort study. *BMJ*. 2009;339:b2584

10. Hippisley-Cox J, Coupland C, Vinogradova Y, Robson J, Minhas R, Sheikh A, Brindle P. Predicting cardiovascular risk in England and Wales: Prospective derivation and validation of QRISK-2. *BMJ*. 2008;336:1475-1482
11. Collins GS, Altman DG. An independent and external validation of QRISK-2 cardiovascular disease risk score: A prospective open cohort study. *BMJ*. 2010;340:c2442
12. Collins GS, Altman DG. Predicting the 10 year risk of cardiovascular disease in the United Kingdom: Independent and external validation of an updated version of QRISK-2. *BMJ*. 2012;344:e4181
13. Conroy RM, Pyorala K, Fitzgerald AP, Sans S, Menotti A, De Backer G, De Bacquer D, Ducimetiere P, Jousilahti P, Keil U, Njolstad I, Oganov RG, Thomsen T, Tunstall-Pedoe H, Tverdal A, Wedel H, Whincup P, Wilhelmsen L, Graham IM. Estimation of ten-year risk of fatal cardiovascular disease in Europe: The SCORE project. *Eur Heart J* 2003;24:987-1003
14. Pignoli P, Tremoli E, Poli A, Oreste P, Paoletti R. Intimal plus medial thickness of the arterial wall: A direct measurement with ultrasound imaging. *Circulation*. 1986;74:1399-1406
15. Lorenz MW, Markus HS, Bots ML, Rosvall M, Sitzer M. Prediction of clinical cardiovascular events with carotid intima-media thickness: A systematic review and meta-analysis. *Circulation*. 2007;115:459-467
16. Eleid MF, Lester SJ, Wiedenbeck TL, Patel SD, Appleton CP, Nelson MR, Humphries J, Hurst RT. Carotid ultrasound identifies high risk subclinical atherosclerosis in adults with low Framingham risk scores. *J Am Soc Echocardiogr* 2010;23:802-808
17. Naqvi TZ, Mendoza F, Rafii F, Gransar H, Guerra M, Lepor N, Berman DS, Shah PK. High prevalence of ultrasound detected carotid atherosclerosis in subjects with low Framingham risk score: Potential implications for screening for subclinical atherosclerosis *J Am Soc Echocardiogr* 2010;23:809-815
18. Folsom AR, Kronmal RA, Detrano RC, O'Leary DH, Bild DE, Bluemke DA, Budoff MJ, Liu K, Shea S, Szklo M, Tracy RP, Watson KE, Burke GL. Coronary artery calcification compared with carotid

- intima-media thickness in the prediction of cardiovascular disease incidence: The multi-ethnic study of atherosclerosis (MESA). *Archives of internal medicine*. 2008;168:1333-1339
19. Polak JF, Pencina MJ, Pencina KM, O'Donnell CJ, Wolf PA, D'Agostino RB, Sr. Carotid-wall intima-media thickness and cardiovascular events. *New Engl J Med* 2011;365:213-221
 20. Using nontraditional risk factors in coronary heart disease risk assessment: U.S. Preventive services task force recommendation statement. *Ann Intern Med*. 2009;151:474-482
 21. Helfand M, Buckley DI, Freeman M, Fu R, Rogers K, Fleming C, Humphrey LL. Emerging risk factors for coronary heart disease: A summary of systematic reviews conducted for the u.S. Preventive services task force. *Ann Intern Med*. 2009;151:496-507
 22. O'Leary DH, Bots ML. Imaging of atherosclerosis: Carotid intima-media thickness. *Eur Heart J* 2010;31:1682-1689
 23. Stork S, van den Beld AW, von Schacky C, Angermann CE, Lamberts SW, Grobbee DE, Bots ML. Carotid artery plaque burden, stiffness, and mortality risk in elderly men: A prospective, population-based cohort study. *Circulation*. 2004;110:344-348
 24. Handa N, Matsumoto M, Maeda H, Hougaku H, Ogawa S, Fukunaga R, Yoneda S, Kimura K, Kamada T. Ultrasonic evaluation of early carotid atherosclerosis. *Stroke*. 1990;21:1567-1572
 25. Touboul PJ, Hennerici MG, Meairs S, Adams H, Amarenco P, Desvarieux M, Ebrahim S, Fatar M, Hernandez Hernandez R, Kownator S, Prati P, Rundek T, Taylor A, Bornstein N, Csiba L, Vicaut E, Woo KS, Zannad F. Mannheim intima-media thickness consensus. *Cerebrovasc Dis*. 2004;18:346-349
 26. Touboul PJ, Hennerici MG, Meairs S, Adams H, Amarenco P, Bornstein N, Csiba L, Desvarieux M, Ebrahim S, Fatar M, Hernandez Hernandez R, Jaff M, Kownator S, Prati P, Rundek T, Sitzer M, Schminke U, Tardif JC, Taylor A, Vicaut E, Woo KS, Zannad F, Zureik M. Mannheim carotid intima-media thickness consensus (2004-2006). *Cerebrovasc Dis*. 2007;23:75-80

27. Crouse JR, Harpold GH, Kahl FR, Toole JF, McKinney WM. Evaluation of a scoring system for extracranial carotid atherosclerosis extent with b-mode ultrasound. *Stroke*. 1986;17:270-275
28. Mathiesen EB, Johnsen SH, Wilsgaard T, Bonna KH, Lochen ML, Njolstad I. Carotid plaque area and intima-media thickness in prediction of first-ever ischemic stroke: A 10-year follow-up of 6584 men and women: The Tromso study. *Stroke*. 2011;42:972-978
29. Johnsen SH, Mathiesen EB, Joakimsen O, Stensland E, Wilsgaard T, Lochen ML, Njolstad I, Arnesen E. Carotid atherosclerosis is a stronger predictor of myocardial infarction in women than in men: A 6-year follow-up study of 6226 persons: The Tromso study. *Stroke*. 2007;38:2873-2880
30. Ebrahim S, Papacosta O, Whincup P, Wannamethee G, Walker M, Nicolaides AN, Dhanjil S, Griffin M, Belcaro G, Rumley A, Lowe GD. Carotid plaque, intima media thickness, cardiovascular risk factors, and prevalent cardiovascular disease in men and women: The British Regional Heart Study. *Stroke*. 1999;30:841-850
31. Spence JD, Eliasziw M, DiCicco M, Hackam DG, Galil R, Lohmann T. Carotid plaque area: A tool for targeting and evaluating vascular preventive therapy. *Stroke*. 2002;33:2916-2922
32. Inaba Y, Chen JA, Bergmann SR. Carotid plaque, compared with carotid intima-media thickness, more accurately predicts coronary artery disease events: A meta-analysis. *Atherosclerosis*. 2012;220:128-133
33. Nambi V, Chambless L, Folsom AR, He M, Hu Y, Mosley T, Volcik K, Boerwinkle E, Ballantyne CM. Carotid intima-media thickness and presence or absence of plaque improves prediction of coronary heart disease risk: The ARIC (Atherosclerosis Risk In Communities) study. *J Am Coll Cardiol* 2010;55:1600-1607
34. Cook NR, Ridker PM. Advances in measuring the effect of individual predictors of cardiovascular risk: The role of reclassification measures. *Ann Intern Med*. 2009;150:795-802
35. Stein JH, Johnson HM. Carotid intima-media thickness, plaques, and cardiovascular disease risk: Implications for preventive cardiology guidelines. *J Am Coll Cardiol* 2010;55:1608-1610

36. Greenland P, Alpert JS, Beller GA, Benjamin EJ, Budoff MJ, Fayad ZA, Foster E, Hlatky MA, Hodgson JM, Kushner FG, Lauer MS, Shaw LJ, Smith SC, Jr., Taylor AJ, Weintraub WS, Wenger NK, Jacobs AK. 2010 ACCF/AHA guideline for assessment of cardiovascular risk in asymptomatic adults: A report of the ACC/AHA task force on practice guidelines. *Circulation*. 2010;122:e584-636
37. Montalescot G, Sechtem U, Achenbach S, Andreotti F, Arden C, Budaj A, Bugiardini R, Crea F, Cuisset T, Di Mario C, Ferreira JR, Gersh BJ, Gitt AK, Hulot JS, Marx N, Opie LH, Pfisterer M, Prescott E, Ruschitzka F, Sabate M, Senior R, Taggart DP, van der Wall EE, Vrints CJ, Zamorano JL, Baumgartner H, Bax JJ, Bueno H, Dean V, Deaton C, Erol C, Fagard R, Ferrari R, Hasdai D, Hoes AW, Kirchhof P, Knuuti J, Kolh P, Lancellotti P, Linhart A, Nihoyannopoulos P, Piepoli MF, Ponikowski P, Sirnes PA, Tamargo JL, Tendera M, Torbicki A, Wijns W, Windecker S, Valgimigli M, Claeys MJ, Donner-Banzhoff N, Frank H, Funck-Brentano C, Gaemperli O, Gonzalez-Juanatey JR, Hamilos M, Husted S, James SK, Kervinen K, Kristensen SD, Maggioni AP, Pries AR, Romeo F, Ryden L, Simoons ML, Steg PG, Timmis A, Yildirim A. 2013 ESC guidelines on the management of stable coronary artery disease: The task force on the management of stable coronary artery disease of the European Society of Cardiology. *Eur Heart J* 2013;34:2949-3003
38. Mancia G, Fagard R, Narkiewicz K, Redon J, Zanchetti A, Bohm M, Christiaens T, Cifkova R, De Backer G, Dominiczak A, Galderisi M, Grobbee DE, Jaarsma T, Kirchhof P, Kjeldsen SE, Laurent S, Manolis AJ, Nilsson PM, Ruilope LM, Schmieder RE, Sirnes PA, Sleight P, Viigimaa M, Waeber B, Zannad F, Burnier M, Ambrosioni E, Caulfield M, Coca A, Olsen MH, Tsoufis C, van de Borne P, Zamorano JL, Achenbach S, Baumgartner H, Bax JJ, Bueno H, Dean V, Deaton C, Erol C, Ferrari R, Hasdai D, Hoes AW, Knuuti J, Kolh P, Lancellotti P, Linhart A, Nihoyannopoulos P, Piepoli MF, Ponikowski P, Tamargo JL, Tendera M, Torbicki A, Wijns W, Windecker S, Clement DL, Gillebert TC, Rosei EA, Anker SD, Bauersachs J, Hitij JB, Caulfield M, De Buyzere M, De Geest S, Derumeaux GA, Erdine S, Farsang C, Funck-Brentano C, Gerc V, Germano G, Gielen S, Haller H, Jordan J, Kahan T, Komajda M, Lovic D, Mahrholdt H, Ostergren J, Parati G, Perk J, Polonia J, Popescu BA, Reiner Z, Ryden L, Sirenko Y, Stanton A, Struijker-Boudier H, Vlachopoulos C, Volpe M, Wood DA. 2013 ESH/ESC guidelines for the management of arterial hypertension: The task force for the management of arterial hypertension of the European Society of Hypertension (ESH) and of the European Society of Cardiology (ESC). *Eur Heart J* 2013; 34:2159-2219

39. Barger AC, Beeuwkes R, 3rd, Lainey LL, Silverman KJ. Hypothesis: Vasa vasorum and neovascularization of human coronary arteries. A possible role in the pathophysiology of atherosclerosis. *New Engl J Med* 1984;310:175-177
40. Moreno PR, Sanz J, Fuster V. Promoting mechanisms of vascular health: Circulating progenitor cells, angiogenesis, and reverse cholesterol transport. *J Am Coll Cardiol* 2009;53:2315-2323
41. Ritman EL, Lerman A. The dynamic vasa vasorum. *Cardiovasc Res.* 2007;75:649-658
42. Moreno PR, Purushothaman M, Purushothaman KR. Plaque neovascularization: Defense mechanisms, betrayal, or a war in progress. *Ann N Y Acad Sci.* 2012;1254:7-17
43. Parry CH. An inquiry into the symptoms and causes of the syncope anginosa commonly called angina pectoris . *Bath, England.* 1799
44. Fenger CE. Beretning af obductionen over albert thorvaldsen (autopsy report of albert thorvaldsen). . *Ugeskr Laeger.* 1844;X:215-218
45. Virchow R. Die cellularpathologie in ihrer begründung auf physiologische und pathologische gewebelehre. *Verlag von August Hirschwald.* 1858;Berlin
46. Koster W. Endarteritis and arteritis. *Berl Klin Wochenschr.* 1876;13:454-455
47. Paterson JC. Vascularization and hemorrhage of the intima of the atherosclerotic coronary arteries. *Arch Pathol.* 1936;22:313-324
48. Winternitz MC. The relation of vascularity to disease of the vessel wall. *The biology of arteriosclerosis.* Baltimore, Maryland: Charles C. Thomas; 1936:58-79.
49. Imparato AM, Riles TS, Mintzer R, Baumann FG. The importance of hemorrhage in the relationship between gross morphologic characteristics and cerebral symptoms in 376 carotid artery plaques. *Ann Surg.* 1983;197:195-203

50. Davies MJ, Thomas A. Thrombosis and acute coronary-artery lesions in sudden cardiac ischemic death. *New Engl J Med* 1984;310:1137-1140
51. Glagov S, Weisenberg E, Zarins CK, Stankunavicius R, Kolettis GJ. Compensatory enlargement of human atherosclerotic coronary arteries. *The New England journal of medicine*. 1987;316:1371-1375
52. Muller JE, Tofler GH, Stone PH. Circadian variation and triggers of onset of acute cardiovascular disease. *Circulation*. 1989;79:733-743
53. Mann JM, Davies MJ. Vulnerable plaque. Relation of characteristics to degree of stenosis in human coronary arteries. *Circulation*. 1996;94:928-931
54. Virmani R, Kolodgie FD, Burke AP, Farb A, Schwartz SM. Lessons from sudden coronary death: A comprehensive morphological classification scheme for atherosclerotic lesions. *Arterioscler Thromb Vasc Biol*. 2000;20:1262-1275
55. Sluimer JC, Kolodgie FD, Bijnens AP, Maxfield K, Pacheco E, Kutys B, Duimel H, Frederik PM, van Hinsbergh VW, Virmani R, Daemen MJ. Thin-walled microvessels in human coronary atherosclerotic plaques show incomplete endothelial junctions relevance of compromised structural integrity for intraplaque microvascular leakage. *J Am Coll Cardiol* 2009;53:1517-1527
56. Xu J, Lu X, Shi GP. Vasa vasorum in atherosclerosis and clinical significance. *Int J Mol Sci* 2015;16:11574-11608
57. Fleiner M, Kummer M, Mirlacher M, Sauter G, Cathomas G, Krapf R, Biedermann BC. Arterial neovascularization and inflammation in vulnerable patients: Early and late signs of symptomatic atherosclerosis. *Circulation* 2004;110:2843-2850
58. Dunmore BJ, McCarthy MJ, Naylor AR, Brindle NP. Carotid plaque instability and ischemic symptoms are linked to immaturity of microvessels within plaques. *J Vasc Surg*. 2007;45:155-159

59. Hellings WE, Peeters W, Moll FL, Piers SR, van Setten J, Van der Spek PJ, de Vries JP, Seldenrijk KA, De Bruin PC, Vink A, Velema E, de Kleijn DP, Pasterkamp G. Composition of carotid atherosclerotic plaque is associated with cardiovascular outcome: A prognostic study. *Circulation*. 2010;121:1941-1950
60. Gronholdt ML, Wiebe BM, Laursen H, Nielsen TG, Schroeder TV, Sillesen H. Lipid-rich carotid artery plaques appear echolucent on ultrasound b-mode images and may be associated with intraplaque haemorrhage. *Eur J Vasc Endovasc Surg*. 1997;14:439-445
61. Carotid artery plaque composition--relationship to clinical presentation and ultrasound b-mode imaging. European carotid plaque study group. *Eur J Vasc Endovasc Surg*. 1995;10:23-30
62. Gronholdt ML, Nordestgaard BG, Bentzon J, Wiebe BM, Zhou J, Falk E, Sillesen H. Macrophages are associated with lipid-rich carotid artery plaques, echolucency on b-mode imaging, and elevated plasma lipid levels. *J Vasc Surg*. 2002;35:137-145
63. ten Kate GL, Sijbrands EJ, Staub D, Coll B, ten Cate FJ, Feinstein SB, Schinkel AF. Noninvasive imaging of the vulnerable atherosclerotic plaque. *Curr Probl Cardiol* 2010;35:556-591
64. AbuRahma AF, Kyer PD, 3rd, Robinson PA, Hannay RS. The correlation of ultrasonic carotid plaque morphology and carotid plaque hemorrhage: Clinical implications. *Surgery*. 1998;124:721-726; discussion 726-728
65. Sztajzel R, Momjian S, Momjian-Mayor I, Murith N, Djebaili K, Boissard G, Comelli M, Pizolatto G. Stratified gray-scale median analysis and color mapping of the carotid plaque: Correlation with endarterectomy specimen histology of 28 patients. *Stroke*. 2005;36:741-745
66. Stewart MJ. Contrast echocardiography. *Heart*. 2003;89:342-348
67. Janardhanan R, Dwivedi G, Hayat S, Senior R. Myocardial contrast echocardiography: A new tool for assessment of myocardial perfusion. *Indian Heart J*. 2005;57:210-216

68. Macioch JE, Katsamakidis CD, Robin J, Liebson PR, Meyer PM, Geohas C, Raichlen JS, Davidson MH, Feinstein SB. Effect of contrast enhancement on measurement of carotid artery intimal medial thickness. *Vasc Med*. 2004;9:7-12
69. Sirlin CB, Lee YZ, Girard MS, Peterson TM, Steinbach GC, Baker KG, Mattrey RF. Contrast-enhanced b-mode us angiography in the assessment of experimental in vivo and in vitro atherosclerotic disease. *Academic radiology*. 2001;8:162-172
70. Shah F, Balan P, Weinberg M, Reddy V, Neems R, Feinstein M, Dainauskas J, Meyer P, Goldin M, Feinstein SB. Contrast-enhanced ultrasound imaging of atherosclerotic carotid plaque neovascularization: A new surrogate marker of atherosclerosis? *Vasc Med*. 2007;12:291-297
71. Vicenzini E, Giannoni MF, Puccinelli F, Ricciardi MC, Altieri M, Di Piero V, Gossetti B, Valentini FB, Lenzi GL. Detection of carotid adventitial vasa vasorum and plaque vascularization with ultrasound cadence contrast pulse sequencing technique and echo-contrast agent. *Stroke*. 2007;38:2841-2843
72. Coli S, Magnoni M, Sangiorgi G, Marrocco-Trischitta MM, Melisurgo G, Mauriello A, Spagnoli L, Chiesa R, Cianflone D, Maseri A. Contrast-enhanced ultrasound imaging of intraplaque neovascularization in carotid arteries: Correlation with histology and plaque echogenicity. *J Am Coll Cardiol* 2008;52:223-230
73. Giannoni MF, Vicenzini E, Citone M, Ricciardi MC, Irace L, Laurito A, Scucchi LF, Di Piero V, Gossetti B, Mauriello A, Spagnoli LG, Lenzi GL, Valentini FB. Contrast carotid ultrasound for the detection of unstable plaques with neoangiogenesis: A pilot study. *Eur J Vasc Endovasc Surg*. 2009;37:722-727
74. Xiong L, Deng YB, Zhu Y, Liu YN, Bi XJ. Correlation of carotid plaque neovascularization detected by using contrast-enhanced us with clinical symptoms. *Radiology*. 2009;251:583-589
75. Huang PT, Chen CC, Aronow WS, Wang XT, Nair CK, Xue NY, Shen X, Li SY, Huang FG, Cosgrove D. Assessment of neovascularization within carotid plaques in patients with ischemic stroke. *World J Cardiol* 2010;2:89-97

76. Staub D, Patel MB, Tibrewala A, Ludden D, Johnson M, Espinosa P, Coll B, Jaeger KA, Feinstein SB. Vasa vasorum and plaque neovascularization on contrast-enhanced carotid ultrasound imaging correlates with cardiovascular disease and past cardiovascular events. *Stroke*. 2010;41:41-47
77. Staub D, Partovi S, Schinkel AF, Coll B, Uthoff H, Aschwanden M, Jaeger KA, Feinstein SB. Correlation of carotid artery atherosclerotic lesion echogenicity and severity at standard us with intraplaque neovascularization detected at contrast-enhanced us. *Radiology*. 2011;258:618-626
78. Shalhoub J, Monaco C, Owen DR, Gauthier T, Thapar A, Leen EL, Davies AH. Late-phase contrast-enhanced ultrasound reflects biological features of instability in human carotid atherosclerosis. *Stroke*. 2011;42:3634-3636
79. Zhou Y, Xing Y, Li Y, Bai Y, Chen Y, Sun X, Zhu Y, Wu J. An assessment of the vulnerability of carotid plaques: A comparative study between intraplaque neovascularization and plaque echogenicity. *BMC medical imaging*. 2013;13:13
80. van den Oord SC, Akkus Z, Roeters van Lennep JE, Bosch JG, van der Steen AF, Sijbrands EJ, Schinkel AF. Assessment of subclinical atherosclerosis and intraplaque neovascularization using quantitative contrast-enhanced ultrasound in patients with familial hypercholesterolemia. *Atherosclerosis*. 2013;231:107-113
81. Zhu Y, Deng YB, Liu YN, Bi XJ, Sun J, Tang QY, Deng Q. Use of carotid plaque neovascularization at contrast-enhanced us to predict coronary events in patients with coronary artery disease. *Radiology*. 2013;268:54-60
82. Saba L, Caddeo G, Sanfilippo R, Montisci R, Mallarini G. Efficacy and sensitivity of axial scans and different reconstruction methods in the study of the ulcerated carotid plaque using multidetector-row ct angiography: Comparison with surgical results. *AJNR. Am J Neuroradiol* 2007;28:716-723
83. de Weert TT, Ouhlous M, Meijering E, Zondervan PE, Hendriks JM, van Sambeek MR, Dippel DW, van der Lugt A. In vivo characterization and quantification of atherosclerotic carotid

- plaque components with multidetector computed tomography and histopathological correlation. *Arterioscler Thromb Vasc Biol.* 2006;26:2366-2372
84. Wintermark M, Jawadi SS, Rapp JH, Tihan T, Tong E, Glidden DV, Abedin S, Schaeffer S, Acevedo-Bolton G, Boudignon B, Orwoll B, Pan X, Saloner D. High-resolution ct imaging of carotid artery atherosclerotic plaques. *AJNR. Am J Neuroradiol* 2008;29:875-882
85. Pohle K, Achenbach S, Macneill B, Ropers D, Ferencik M, Moselewski F, Hoffmann U, Brady TJ, Jang IK, Daniel WG. Characterization of non-calcified coronary atherosclerotic plaque by multi-detector row ct: Comparison to ivus. *Atherosclerosis.* 2007;190:174-180
86. Iriart X, Brunot S, Coste P, Montaudon M, Dos-Santos P, Leroux L, Labeque JN, Jais C, Laurent F. Early characterization of atherosclerotic coronary plaques with multidetector computed tomography in patients with acute coronary syndrome: A comparative study with intravascular ultrasound. *European Radiology.* 2007;17:2581-2588
87. Mitsumori LM, Hatsukami TS, Ferguson MS, Kerwin WS, Cai J, Yuan C. In vivo accuracy of multisequence mr imaging for identifying unstable fibrous caps in advanced human carotid plaques. *Journal of magnetic resonance imaging : JMRI.* 2003;17:410-420
88. Cai J, Hatsukami TS, Ferguson MS, Kerwin WS, Saam T, Chu B, Takaya N, Polissar NL, Yuan C. In vivo quantitative measurement of intact fibrous cap and lipid-rich necrotic core size in atherosclerotic carotid plaque: Comparison of high-resolution, contrast-enhanced magnetic resonance imaging and histology. *Circulation.* 2005;112:3437-3444
89. Chu B, Kampschulte A, Ferguson MS, Kerwin WS, Yarnykh VL, O'Brien KD, Polissar NL, Hatsukami TS, Yuan C. Hemorrhage in the atherosclerotic carotid plaque: A high-resolution mri study. *Stroke.* 2004;35:1079-1084
90. Yuan C, Kerwin WS, Ferguson MS, Polissar N, Zhang S, Cai J, Hatsukami TS. Contrast-enhanced high resolution mri for atherosclerotic carotid artery tissue characterization. *Journal of magnetic resonance imaging : JMRI.* 2002;15:62-67

91. Ruehm SG, Corot C, Vogt P, Kolb S, Debatin JF. Magnetic resonance imaging of atherosclerotic plaque with ultrasmall superparamagnetic particles of iron oxide in hyperlipidemic rabbits. *Circulation*. 2001;103:415-422
92. Chan JM, Monaco C, Wylezinska-Arridge M, Tremoleda JL, Gibbs RG. Imaging of the vulnerable carotid plaque: Biological targeting of inflammation in atherosclerosis using iron oxide particles and mri. *Eur J Vasc Endovasc Surg*. 2014;47:462-469
93. Tawakol A, Migrino RQ, Hoffmann U, Abbara S, Houser S, Gewirtz H, Muller JE, Brady TJ, Fischman AJ. Noninvasive in vivo measurement of vascular inflammation with f-18 fluorodeoxyglucose positron emission tomography. *Journal of Nuclear Cardiology* 2005;12:294-301
94. Tawakol A, Migrino RQ, Bashian GG, Bedri S, Vermylen D, Cury RC, Yates D, LaMuraglia GM, Furie K, Houser S, Gewirtz H, Muller JE, Brady TJ, Fischman AJ. In vivo 18f-fluorodeoxyglucose positron emission tomography imaging provides a noninvasive measure of carotid plaque inflammation in patients. *J Am Coll Cardiol* 2006;48:1818-1824
95. Marnane M, Merwick A, Sheehan OC, Hannon N, Foran P, Grant T, Dolan E, Moroney J, Murphy S, O'Rourke K, O'Malley K, O'Donohoe M, McDonnell C, Noone I, Barry M, Crowe M, Kavanagh E, O'Connell M, Kelly PJ. Carotid plaque inflammation on 18f-fluorodeoxyglucose positron emission tomography predicts early stroke recurrence. *Annals of neurology*. 2012;71:709-718
96. Wagenknecht L, Wasserman B, Chambless L, Coresh J, Folsom A, Mosley T, Ballantyne C, Sharrett R, Boerwinkle E. Correlates of carotid plaque presence and composition as measured by mri: The atherosclerosis risk in communities study. *Circ Cardiovasc Imaging*. 2009;2:314-322
97. Danaraj TJ, Acker MS, Danaraj W, Wong HO, Tan BY. Ethnic group differences in coronary heart disease in singapore: An analysis of necropsy records. *Am Heart J*. 1959;58:516-526
98. Chen AJ. Recent trends in the mortality and morbidity of cardiovascular diseases. *Annals of the Academy of Medicine, Singapore*. 1980;9:411-415

99. Shaper AG, Jones KW. Serum-cholesterol, diet, and coronary heart-disease in africans and asians in uganda. *Lancet*. 1959;2:534-537
100. Wild S, McKeigue P. Cross sectional analysis of mortality by country of birth in England and Wales, 1970-92. *BMJ*. 1997;314:705-710
101. Balarajan R. Ethnicity and health: The challenges ahead. *Ethnicity & health*. 1996;1:3-5
102. Bhatnagar D, Anand IS, Durrington PN, Patel DJ, Wander GS, Mackness MI, Creed F, Tomenson B, Chandrashekhar Y, Winterbotham M, et al. Coronary risk factors in people from the indian subcontinent living in west London and their siblings in India. *Lancet*. 1995;345:405-409
103. McKeigue PM, Shah B, Marmot MG. Relation of central obesity and insulin resistance with high diabetes prevalence and cardiovascular risk in south asians. *Lancet*. 1991;337:382-386
104. Chambers JC, Eda S, Bassett P, Karim Y, Thompson SG, Gallimore JR, Pepys MB, Kooner JS. C-reactive protein, insulin resistance, central obesity, and coronary heart disease risk in Indian Asians from the United Kingdom compared with European Whites. *Circulation*. 2001;104:145-150
105. Zacho J, Tybjaerg-Hansen A, Jensen JS, Grande P, Sillesen H, Nordestgaard BG. Genetically elevated c-reactive protein and ischemic vascular disease. *New Engl J Med* 2008;359:1897-1908
106. Chambers JC, Obeid OA, Refsum H, Ueland P, Hackett D, Hooper J, Turner RM, Thompson SG, Kooner JS. Plasma homocysteine concentrations and risk of coronary heart disease in UK Indian Asian and European men. *Lancet*. 2000;355:523-527
107. Williams R, Bhopal R, Hunt K. Coronary risk in a british punjabi population: Comparative profile of non-biochemical factors. *Int J Epidemiol* 1994;23:28-37
108. Bansal M, Shrivastava S, Mehrotra R, Agarwal V, Kasliwal RR. Low Framingham risk score despite high prevalence of metabolic syndrome in asymptomatic North-Indian population. *The Journal of the Association of Physicians of India*. 2009;57:17-22

109. Tillin T, Forouhi NG, McKeigue PM, Chaturvedi N. Southall and Brent revisited: Cohort profile of SABRE, a UK population-based comparison of cardiovascular disease and diabetes in people of European, Indian Asian and African Caribbean origins. *Int J Epidemiol* 2012;41:33-42
110. Kanjilal S, Rao VS, Mukherjee M, Natesha BK, Renuka KS, Sibi K, Iyengar SS, Kakkar VV. Application of cardiovascular disease risk prediction models and the relevance of novel biomarkers to risk stratification in Asian Indians. *Vascular health and risk management*. 2008;4:199-211
111. Cappuccio FP, Cook DG, Atkinson RW, Strazzullo P. Prevalence, detection, and management of cardiovascular risk factors in different ethnic groups in South London. *Heart*. 1997;78:555-563
112. McKeigue PM, Ferrie JE, Pierpoint T, Marmot MG. Association of early-onset coronary heart disease in South Asian men with glucose intolerance and hyperinsulinemia. *Circulation*. 1993;87:152-161
113. Holman N, Forouhi NG, Goyder E, Wild SH. The association of public health observatories (PHOs) diabetes prevalence model: Estimates of total diabetes prevalence for England, 2010-2030. *Diabetic medicine : a Journal of the British Diabetic Association*. 2011;28:575-582
114. Chahal NS, Lim TK, Jain P, Chambers JC, Kooner JS, Senior R. Does subclinical atherosclerosis burden identify the increased risk of cardiovascular disease mortality among United Kingdom Indian Asians? A population study. *Am Heart J*. 2011;162:460-466
115. Sidhu PS, Allan PL, Cattin F, Cosgrove DO, Davies AH, Do DD, Karakagil S, Langholz J, Legemate DA, Martegani A, Llull JB, Pezzoli C, Spinazzi A. Diagnostic efficacy of SonoVue, a second generation contrast agent, in the assessment of extracranial carotid or peripheral arteries using colour and spectral Doppler ultrasound: A multicentre study. *Br J Radiol*. 2006;79:44-51
116. Lancellotti P, Nkomo VT, Badano LP, Bergler-Klein J, Bogaert J, Davin L, Cosyns B, Coucke P, Dulgheru R, Edvardsen T, Gaemperli O, Galderisi M, Griffin B, Heidenreich PA, Nieman K, Plana JC, Port SC, Scherrer-Crosbie M, Schwartz RG, Sebag IA, Voigt JU, Wann S, Yang PC. Expert consensus for multi-modality imaging evaluation of cardiovascular complications of

- radiotherapy in adults: A report from the european association of cardiovascular imaging and the american society of echocardiography. *Eur Heart J - Cardiovascular Imaging*. 2013;14:721-740
117. Jordan LC, Duffner PK. Early-onset stroke and cerebrovascular disease in adult survivors of childhood cancer. *Neurology*. 2009;73:1816-1817
118. Louis EL, McLoughlin MJ, Wortzman G. Chronic damage to medium and large arteries following irradiation. *Journal of the Canadian Association of Radiologists*. 1974;25:94-104
119. Plummer C, Henderson RD, O'Sullivan JD, Read SJ. Ischemic stroke and transient ischemic attack after head and neck radiotherapy: A review. *Stroke*. 2011;42:2410-2418
120. Haynes JC, Machtay M, Weber RS, Weinstein GS, Chalian AA, Rosenthal DI. Relative risk of stroke in head and neck carcinoma patients treated with external cervical irradiation. *The Laryngoscope*. 2002;112:1883-1887
121. Dorresteijn LD, Kappelle AC, Boogerd W, Klokman WJ, Balm AJ, Keus RB, van Leeuwen FE, Bartelink H. Increased risk of ischemic stroke after radiotherapy on the neck in patients younger than 60 years. *J Clin Oncol*. 2002;20:282-288
122. Smith GL, Smith BD, Buchholz TA, Giordano SH, Garden AS, Woodward WA, Krumholz HM, Weber RS, Ang KK, Rosenthal DI. Cerebrovascular disease risk in older head and neck cancer patients after radiotherapy. *J Clin Oncol*. 2008;26:5119-5125
123. Bowers DC, McNeil DE, Liu Y, Yasui Y, Stovall M, Gurney JG, Hudson MM, Donaldson SS, Packer RJ, Mitby PA, Kasper CE, Robison LL, Oeffinger KC. Stroke as a late treatment effect of hodgkin's disease: A report from the childhood cancer survivor study. *J Clin Oncol*. 2005;23:6508-6515
124. Sonveaux P, Brouet A, Havaux X, Gregoire V, Dessy C, Balligand JL, Feron O. Irradiation-induced angiogenesis through the up-regulation of the nitric oxide pathway: Implications for tumor radiotherapy. *Cancer research*. 2003;63:1012-1019

125. Kozin SV, Duda DG, Munn LL, Jain RK. Neovascularization after irradiation: What is the source of newly formed vessels in recurring tumors? *Journal of the National Cancer Institute*. 2012;104:899-905
126. Grabham P, Sharma P. The effects of radiation on angiogenesis. *Vascular cell*. 2013;5:19
127. Akkus Z, Hoogi A, Renaud G, van den Oord SC, Ten Kate GL, Schinkel AF, Adam D, de Jong N, van der Steen AF, Bosch JG. New quantification methods for carotid intra-plaque neovascularization using contrast-enhanced ultrasound. *Ultrasound Med Biol*. 2014;40:25-36
128. Moguillansky D, Leng X, Carson A, Lavery L, Schwartz A, Chen X, Villanueva FS. Quantification of plaque neovascularization using contrast ultrasound: A histologic validation. *Eur Heart J* 2011;32:646-653
129. Hoogi A, Adam D, Hoffman A, Kerner H, Reisner S, Gaitini D. Carotid plaque vulnerability: Quantification of neovascularization on contrast-enhanced ultrasound with histopathologic correlation. *AJR Am J Roentgenol*. 2011;196:431-436
130. Hoogi A, Akkus Z, van den Oord SC, ten Kate GL, Schinkel AF, Bosch JG, de Jong N, Adam D, van der Steen AF. Quantitative analysis of ultrasound contrast flow behavior in carotid plaque neovasculature. *Ultrasound Med Biol*. 2012;38:2072-2083
131. Hjelmgren O, Holdfeldt P, Johansson L, Fagerberg B, Prah U, Schmidt C, Bergstrom GM. Identification of vascularised carotid plaques using a standardised and reproducible technique to measure ultrasound contrast uptake. *Eur J Vasc Endovasc Surg*. 2013;46:21-28
132. van den Oord SC, ten Kate GL, Akkus Z, Renaud G, Sijbrands EJ, ten Cate FJ, van der Lugt A, Bosch JG, de Jong N, van der Steen AF, Schinkel AF. Assessment of subclinical atherosclerosis using contrast-enhanced ultrasound. *Eur Heart J - Cardiovascular Imaging*. 2013;14:56-61
133. Muller HF, Viacoz A, Kuzmanovic I, Bonvin C, Burkhardt K, Bochaton-Piallat ML, Sztajzel R. Contrast-enhanced ultrasound imaging of carotid plaque neo-vascularization: Accuracy of visual analysis. *Ultrasound Med Biol*. 2014;40:18-24

134. Zhang Q, Li C, Han H, Dai W, Shi J, Wang Y, Wang W. Spatio-temporal quantification of carotid plaque neovascularization on contrast enhanced ultrasound: Correlation with visual grading and histopathology. *Eur J Vasc Endovasc Surg.* 2015;50:289-296
135. Huang PT, Huang FG, Zou CP, Sun HY, Tian XQ, Yang Y, Tang JF, Yang PL, Wang XT. Contrast-enhanced sonographic characteristics of neovascularization in carotid atherosclerotic plaques. *J Clin Ultrasound.* 2008;36:346-351
136. van den Oord SC, Akkus Z, Bosch JG, Hoogi A, ten Kate GL, Renaud G, Sijbrands EJ, Verhagen HJ, van der Lugt A, Adam D, de Jong N, van der Steen AF, Schinkel AF. Quantitative contrast-enhanced ultrasound of intraplaque neovascularization in patients with carotid atherosclerosis. *Ultraschall Med.* 2015;36:154-161
137. van den Oord SC, Akkus Z, Renaud G, Bosch JG, van der Steen AF, Sijbrands EJ, Schinkel AF. Assessment of carotid atherosclerosis, intraplaque neovascularization, and plaque ulceration using quantitative contrast-enhanced ultrasound in asymptomatic patients with diabetes mellitus. *Eur Heart J - Cardiovascular Imaging* 2014;15:1213-1218
138. O'Leary DH, Polak JF, Kronmal RA, Savage PJ, Borhani NO, Kittner SJ, Tracy R, Gardin JM, Price TR, Furberg CD. Thickening of the carotid wall. A marker for atherosclerosis in the elderly? Cardiovascular health study collaborative research group. *Stroke.* 1996;27:224-231
139. O'Leary DH, Polak JF, Kronmal RA, Manolio TA, Burke GL, Wolfson SK, Jr. Carotid-artery intima and media thickness as a risk factor for myocardial infarction and stroke in older adults. Cardiovascular health study collaborative research group. *New Engl J Med* 1999;340:14-22
140. Chambless LE, Heiss G, Folsom AR, Rosamond W, Szklo M, Sharrett AR, Clegg LX. Association of coronary heart disease incidence with carotid arterial wall thickness and major risk factors: The Atherosclerosis Risk In Communities (ARIC) study, 1987-1993. *Am J Epidemiol.* 1997;146:483-494
141. Chambless LE, Folsom AR, Clegg LX, Sharrett AR, Shahar E, Nieto FJ, Rosamond WD, Evans G. Carotid wall thickness is predictive of incident clinical stroke: The Atherosclerosis Risk In Communities (ARIC) study. *Am J Epidemiol.* 2000;151:478-487

142. Bots ML, Hoes AW, Koudstaal PJ, Hofman A, Grobbee DE. Common carotid intima-media thickness and risk of stroke and myocardial infarction: The Rotterdam Study. *Circulation*. 1997;96:1432-1437
143. Newman AB, Naydeck BL, Ives DG, Boudreau RM, Sutton-Tyrrell K, O'Leary DH, Kuller LH. Coronary artery calcium, carotid artery wall thickness, and cardiovascular disease outcomes in adults 70 to 99 years old. *Am J Cardiol* 2008;101:186-192
144. Wong M, Edelstein J, Wollman J, Bond MG. Ultrasonic-pathological comparison of the human arterial wall. Verification of intima-media thickness. *Arteriosclerosis and thrombosis* 1993;13:482-486
145. Gray-Weale AC, Graham JC, Burnett JR, Byrne K, Lusby RJ. Carotid artery atheroma: Comparison of preoperative b-mode ultrasound appearance with carotid endarterectomy specimen pathology. *J Cardiovasc Surg* 1988;29:676-681
146. Arnold JA, Modaresi KB, Thomas N, Taylor PR, Padayachee TS. Carotid plaque characterization by duplex scanning: Observer error may undermine current clinical trials. *Stroke*. 1999;30:61-65
147. Stein JH, Korcarz CE, Hurst RT, Lonn E, Kendall CB, Mohler ER, Najjar SS, Rembold CM, Post WS. Use of carotid ultrasound to identify subclinical vascular disease and evaluate cardiovascular disease risk: A consensus statement from the american society of echocardiography carotid intima-media thickness task force. Endorsed by the society for vascular medicine. *J Am Soc Echocardiogr* 2008;21:93-111; quiz 189-190
148. Grundy SM. Coronary plaque as a replacement for age as a risk factor in global risk assessment. *Am J Cardiol* 2001;88:8E-11E
149. Greenland P, Smith SC, Jr., Grundy SM. Improving coronary heart disease risk assessment in asymptomatic people: Role of traditional risk factors and noninvasive cardiovascular tests. *Circulation*. 2001;104:1863-1867

150. Lorenz MW, von Kegler S, Steinmetz H, Markus HS, Sitzer M. Carotid intima-media thickening indicates a higher vascular risk across a wide age range: Prospective data from the carotid atherosclerosis progression study (caps). *Stroke*. 2006;37:87-92
151. Kitamura A, Iso H, Imano H, Ohira T, Okada T, Sato S, Kiyama M, Tanigawa T, Yamagishi K, Shimamoto T. Carotid intima-media thickness and plaque characteristics as a risk factor for stroke in Japanese elderly men. *Stroke*. 2004;35:2788-2794
152. Salonen JT, Salonen R. Ultrasound b-mode imaging in observational studies of atherosclerotic progression. *Circulation*. 1993;87:II56-65
153. Rosvall M, Janzon L, Berglund G, Engstrom G, Hedblad B. Incident coronary events and case fatality in relation to common carotid intima-media thickness. *Journal of Internal Medicine*. 2005;257:430-437
154. van der Meer IM, Bots ML, Hofman A, del Sol AI, van der Kuip DA, Witteman JC. Predictive value of noninvasive measures of atherosclerosis for incident myocardial infarction: The rotterdam study. *Circulation*. 2004;109:1089-1094
155. Polak JF, Szklo M, Kronmal RA, Burke GL, Shea S, Zavodni AE, O'Leary DH. The value of carotid artery plaque and intima-media thickness for incident cardiovascular disease: The multi-ethnic study of atherosclerosis. *Journal of the American Heart Association*. 2013;2:e000087
156. Ahmadvazir S, Zacharias K, Shah BN, Pabla JS, Senior R. Role of simultaneous carotid ultrasound in patients undergoing stress echocardiography for assessment of chest pain with no previous history of coronary artery disease. *Am Heart J* 2014;168:229-236
157. Finn AV, Nakano M, Narula J, Kolodgie FD, Virmani R. Concept of vulnerable/unstable plaque. *Arterioscler Thromb Vasc Biol*. 2010;30:1282-1292
158. Virmani R, Kolodgie FD, Burke AP, Finn AV, Gold HK, Tulenko TN, Wrenn SP, Narula J. Atherosclerotic plaque progression and vulnerability to rupture: Angiogenesis as a source of intraplaque hemorrhage. *Arterioscler Thromb Vasc Biol*. 2005;25:2054-2061

159. Feinstein SB. Contrast ultrasound imaging of the carotid artery vasa vasorum and atherosclerotic plaque neovascularization. *J Am Coll Cardiol* 2006;48:236-243
160. Harding S, Rosato M, Teyhan A. Trends for coronary heart disease and stroke mortality among migrants in England and Wales, 1979-2003: Slow declines notable for some groups. *Heart*. 2008;94:463-470
161. Chahal NS, Lim TK, Jain P, Chambers JC, Kooner JS, Senior R. The increased prevalence of left ventricular hypertrophy and concentric remodeling in U.K. Indian Asians compared with European Whites. *Journal of Human Hypertension*. 2013;27:288-293
162. Cappuccio FP, Oakeshott P, Strazzullo P, Kerry SM. Application of Framingham risk estimates to ethnic minorities in United Kingdom and implications for primary prevention of heart disease in general practice: Cross sectional population based study. *BMJ*. 2002;325:1271
163. Nissen SE, Nicholls SJ, Sipahi I, Libby P, Raichlen JS, Ballantyne CM, Davignon J, Erbel R, Fruchart JC, Tardif JC, Schoenhagen P, Crowe T, Cain V, Wolski K, Goormastic M, Tuzcu EM. Effect of very high-intensity statin therapy on regression of coronary atherosclerosis: The ASTEROID trial. *JAMA* 2006;295:1556-1565
164. Hattori K, Ozaki Y, Ismail TF, Okumura M, Naruse H, Kan S, Ishikawa M, Kawai T, Ohta M, Kawai H, Hashimoto T, Takagi Y, Ishii J, Serruys PW, Narula J. Impact of statin therapy on plaque characteristics as assessed by serial OCT, grayscale and integrated backscatter-IVUS. *JACC Cardiovasc Imaging*. 2012;5:169-177
165. Jain RK, Finn AV, Kolodgie FD, Gold HK, Virmani R. Antiangiogenic therapy for normalization of atherosclerotic plaque vasculature: A potential strategy for plaque stabilization. *Nature clinical practice. Cardiovascular medicine*. 2007;4:491-502
166. Michel JB, Virmani R, Arbustini E, Pasterkamp G. Intraplaque haemorrhages as the trigger of plaque vulnerability. *European heart journal*. 2011;32:1977-1985, 1985a, 1985b, 1985c

167. Koole D, Heyligers J, Moll FL, Pasterkamp G. Intraplaque neovascularization and hemorrhage: Markers for cardiovascular risk stratification and therapeutic monitoring. *J Cardiovasc Med* 2012;13:635-639
168. Gujral DM, Chahal N, Senior R, Harrington KJ, Nutting CM. Radiation-induced carotid artery atherosclerosis. *Radiotherapy and Oncology* 2014; 110(1): 31-38
169. Wilbers J, Dorresteijn LD, Haast R, Hoebbers FJ, Kaanders JH, Boogerd W, van Werkhoven ED, Nowee ME, Hansen HH, de Korte CL, Kappelle AC, van Dijk EJ. Progression of carotid intima media thickness after radiotherapy: A long-term prospective cohort study. *Radiotherapy and Oncology* 2014;113:359-363
170. Dubec JJ, Munk PL, Tsang V, Lee MJ, Janzen DL, Buckley J, Seal M, Taylor D. Carotid artery stenosis in patients who have undergone radiation therapy for head and neck malignancy. *Br J Radiol.* 1998;71:872-875
171. Moritz MW, Higgins RF, Jacobs JR. Duplex imaging and incidence of carotid radiation injury after high-dose radiotherapy for tumors of the head and neck. *Arch Surg.* 1990;125:1181-1183
172. Zidar N, Ferluga D, Hvala A, Popovic M, Soba E. Contribution to the pathogenesis of radiation-induced injury to large arteries. *The Journal of laryngology and otology.* 1997;111:988-990
173. Barnett HJ, Taylor DW, Eliasziw M, Fox AJ, Ferguson GG, Haynes RB, Rankin RN, Clagett GP, Hachinski VC, Sackett DL, Thorpe KE, Meldrum HE, Spence JD. Benefit of carotid endarterectomy in patients with symptomatic moderate or severe stenosis. North american symptomatic carotid endarterectomy trial collaborators. *New Engl J Med* 1998;339:1415-1425
174. Ambrose JA, Tannenbaum MA, Alexopoulos D, Hjemdahl-Monsen CE, Leavy J, Weiss M, Borrico S, Gorlin R, Fuster V. Angiographic progression of coronary artery disease and the development of myocardial infarction. *J Am Coll Cardiol* 1988;12:56-62
175. Little WC, Constantinescu M, Applegate RJ, Kutcher MA, Burrows MT, Kahl FR, Santamore WP. Can coronary angiography predict the site of a subsequent myocardial infarction in patients with mild-to-moderate coronary artery disease? *Circulation.* 1988;78:1157-1166

176. Randomised trial of endarterectomy for recently symptomatic carotid stenosis: Final results of the mrc european carotid surgery trial (ecst). *Lancet*. 1998;351:1379-1387
177. Senior R, Becher H, Monaghan M, Agati L, Zamorano J, Vanoverschelde JL, Nihoyannopoulos P. Contrast echocardiography: Evidence-based recommendations by european association of echocardiography. *Eur J Echocardiogr* 2009;10:194-212
178. Kaul S, Jayaweera AR. Coronary and myocardial blood volumes: Noninvasive tools to assess the coronary microcirculation? *Circulation*. 1997;96:719-724
179. Wei K, Jayaweera AR, Firoozan S, Linka A, Skyba DM, Kaul S. Quantification of myocardial blood flow with ultrasound-induced destruction of microbubbles administered as a constant venous infusion. *Circulation*. 1998;97:473-483
180. Kaul S, Senior R, Dittrich H, Raval U, Khattar R, Lahiri A. Detection of coronary artery disease with myocardial contrast echocardiography: Comparison with 99mTc-sestamibi single-photon emission computed tomography. *Circulation*. 1997;96:785-792
181. Janardhanan R, Moon JC, Pennell DJ, Senior R. Myocardial contrast echocardiography accurately reflects transmural extent of myocardial necrosis and predicts contractile reserve after acute myocardial infarction. *American heart journal*. 2005;149:355-362
182. Senior R, Janardhanan R, Jeetley P, Burden L. Myocardial contrast echocardiography for distinguishing ischemic from nonischemic first-onset acute heart failure: Insights into the mechanism of acute heart failure. *Circulation*. 2005;112:1587-1593
183. Cheung WK, Gujral DM, Shah BN, Chahal NS, Bhattacharyya S, Cosgrove DO, Eckersley RJ, Harrington KJ, Senior R, Nutting CM, Tang MX. Attenuation correction and normalisation for quantification of contrast enhancement in ultrasound images of carotid arteries. *Ultrasound Med Biol*. 2015;41:1876-1883
184. Wesisstein EW. Affine transformation. 2015

185. Kim RJ, Wu E, Rafael A, Chen EL, Parker MA, Simonetti O, Klocke FJ, Bonow RO, Judd RM. The use of contrast-enhanced magnetic resonance imaging to identify reversible myocardial dysfunction. *New Engl J Med* 2000;343:1445-1453

186. Shah BN, Chahal NS, Bhattacharyya S, Li W, Roussin I, Khattar RS, Senior R. The feasibility and clinical utility of myocardial contrast echocardiography in clinical practice: Results from the incorporation of myocardial perfusion assessment into clinical testing with stress echocardiography study. *J Am Soc Echocardiogr* 2014;27:520-530

APPENDIX 1 – LOLIPOP IPN STUDY

Inter-observer variability between a cardiologist familiar with the CEUS technique (observer 2) in comparison with myself (observer 1).

Study Number	IPN Present Observer 2	IPN Present Observer 1
1	Yes	Yes
2	No	No
3	Yes	No
4	No	No
5	Yes	Yes
6	Yes	Yes
7	Yes	No
8	No	No
9	Yes	Yes
10	No	No
11	Yes	Yes
12	No	No
13	Yes	Yes
14	No	No
15	Yes	Yes
16	No	No
17	No	No
18	Yes	Yes
19	Yes	Yes
20	No	Yes

Inter-observer agreement was $17/20 = 85\%$.

This yielded a kappa statistic (k) of 0.85.

Intra-observer variability performed by myself by re-analysing the 20 scans, in a random order, more than one month after initial analysis.

Study Number	First Analysis IPN present	Second Analysis IPN Present
1	Yes	Yes
2	No	No
3	No	No
4	No	No
5	Yes	Yes
6	Yes	Yes
7	No	No
8	No	No
9	Yes	Yes
10	No	No
11	Yes	Yes
12	No	No
13	Yes	Yes
14	No	No
15	Yes	Yes
16	No	Yes
17	No	No
18	Yes	Yes
19	Yes	Yes
20	Yes	Yes

Intra-observer agreement was $19/20 = 95\%$.

This yielded a kappa statistic (k) of 0.95

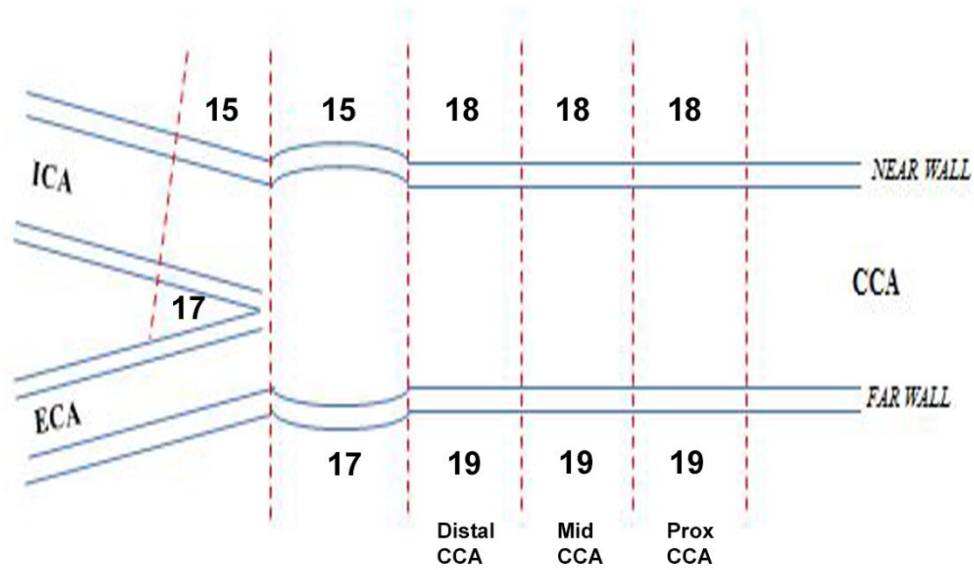
APPENDIX 2

The following eight diagrams all illustrate the carotid tree divided into the segments that were analysed as described in the main text. There are five segments in each near and each far wall, thus making 10 segments in each artery [each wall had the proximal, mid and distal sections of the CCA, the carotid bulb and the internal carotid artery]. As both the left and right arteries were scanned, this means there were 20 segments analysed in each patient.

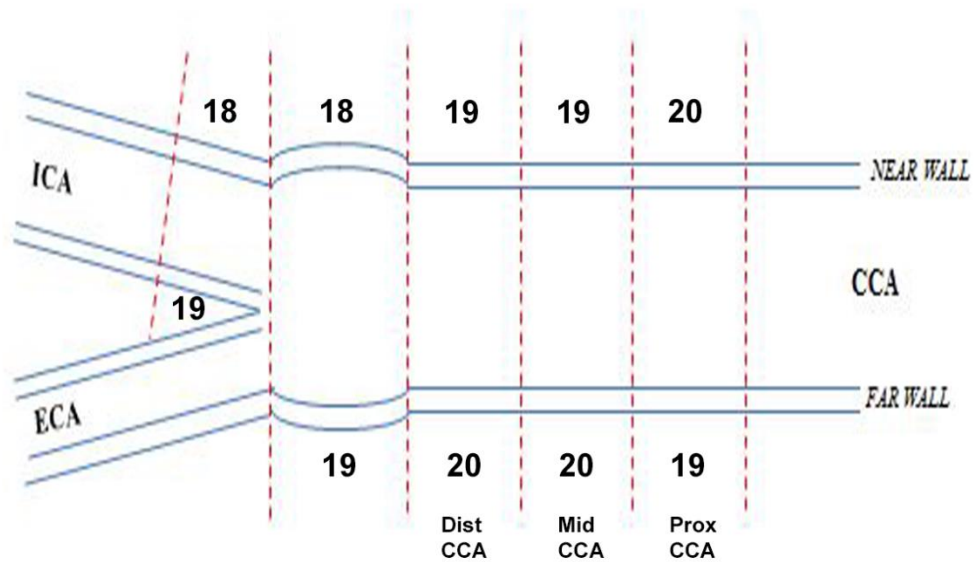
The numbers adjacent to each segment (with a maximum of 20) represent the instances of agreement (intra-observer and inter-observer) observed in the reproducibility analyses – for example, 18/20 means that in 18 of the 20 instances that that particular segment was assessed, there was agreement (i.e. 90% agreement).

Cohen's kappa statistic was calculated for each of these scores. In summary, moderate-excellent agreement was observed in all segments, with higher values obtained for CEUS images in comparison with B-mode images, particularly in the near wall segments.

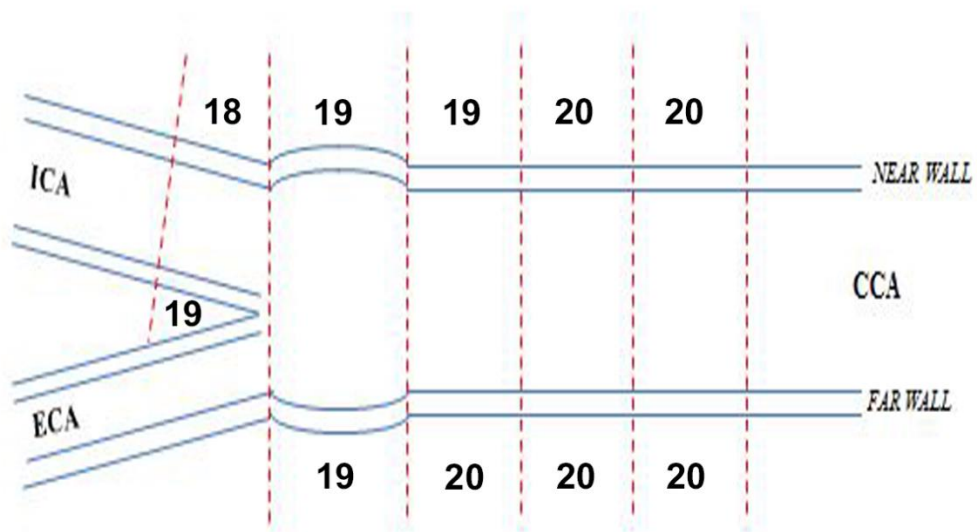
Intra-Observer Agreement on IMT Visualization Score – B-mode Imaging



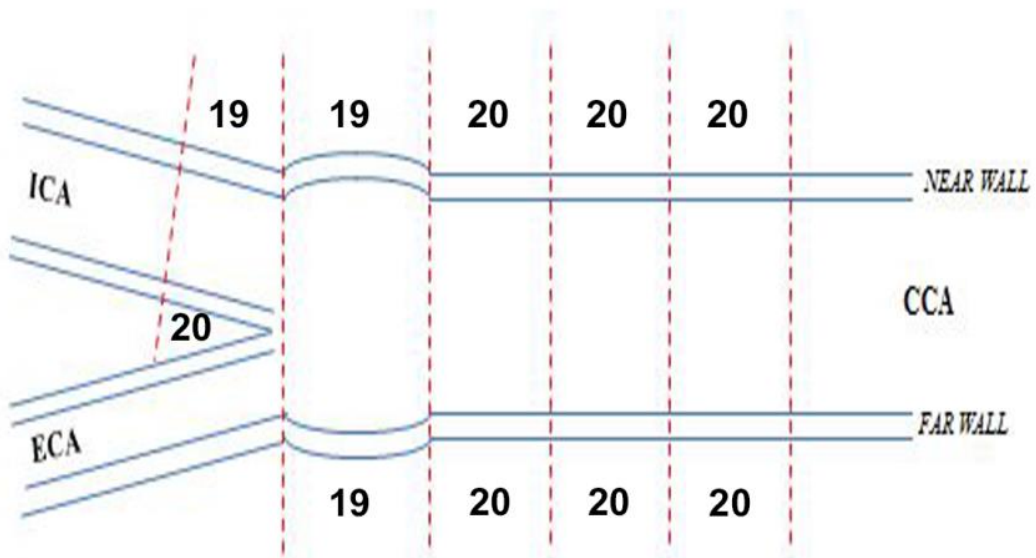
Intra-Observer Agreement on IMT Visualization Score – CEUS Imaging



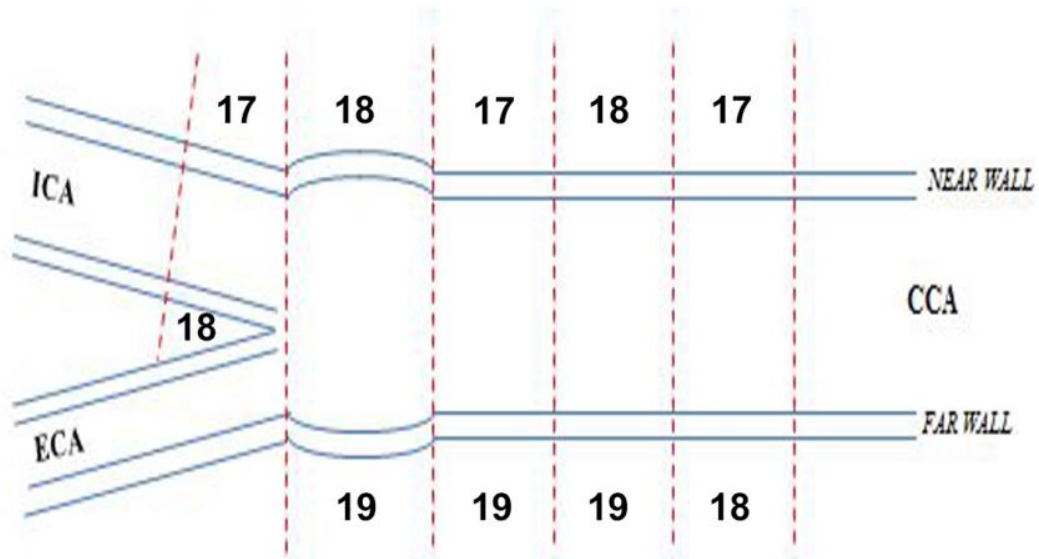
Intra-Observer Agreement on Plaque Presence / Absence – B-Mode Imaging



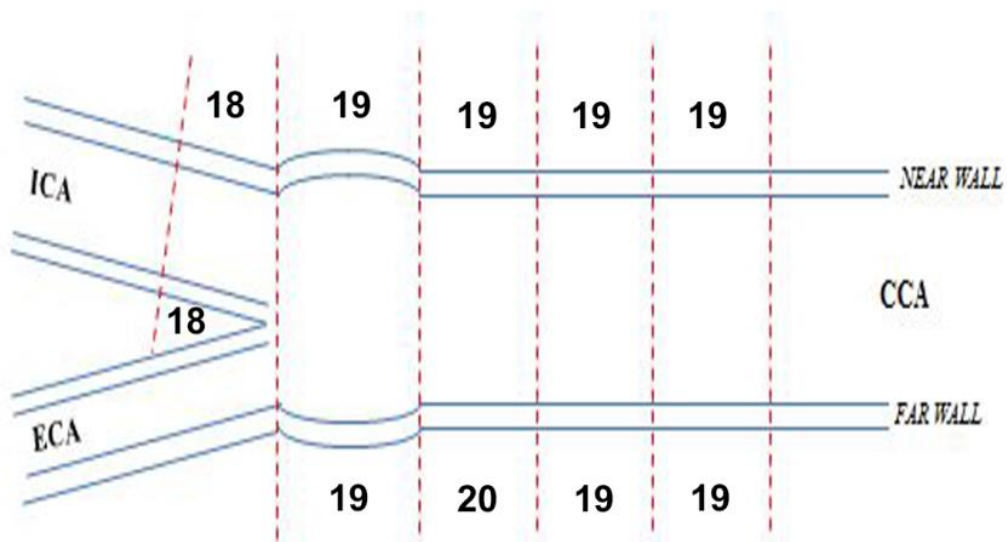
Intra-Observer Agreement on Plaque Presence / Absence – CEUS Imaging



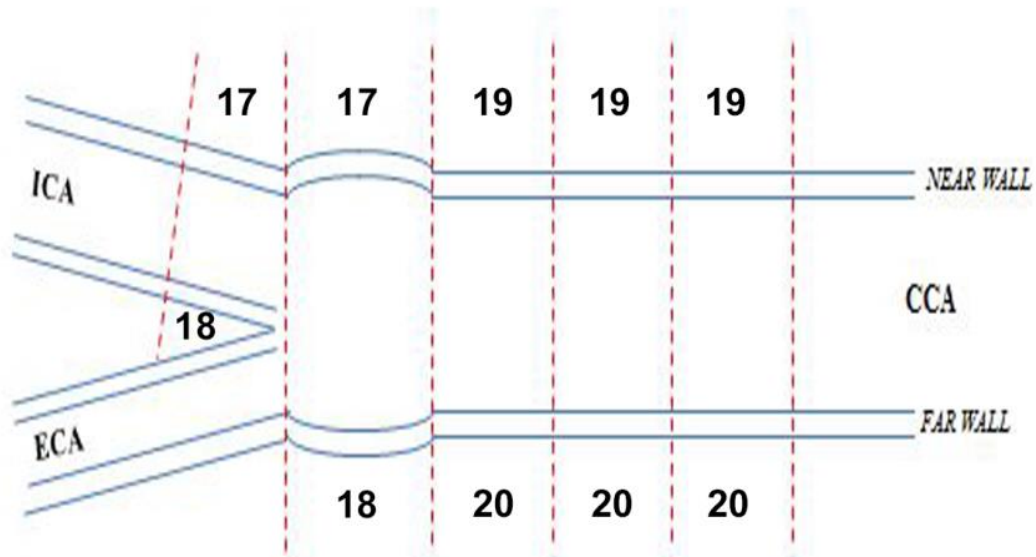
Inter-Observer Agreement on IMT Visualization Score – B-mode Imaging



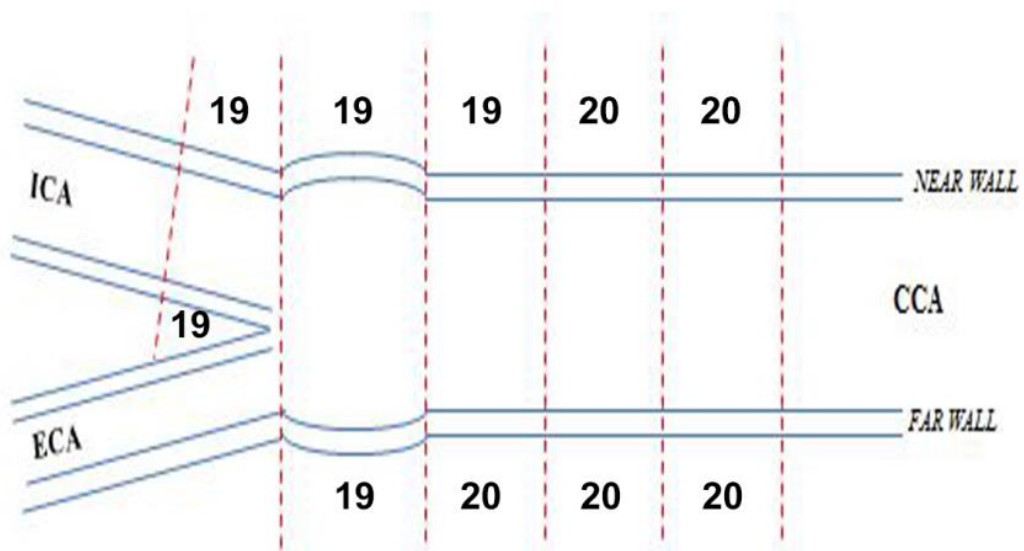
Inter-Observer Agreement on IMT Visualization Score – CEUS Imaging



Inter-Observer Agreement on Plaque Presence / Absence – B-Mode Imaging



Inter-Observer Agreement on Plaque Presence / Absence – CEUS Imaging



APPENDIX 3

Inter-observer variability between a second observer (observer 2), familiar with the CEUS technique, in comparison with myself (observer 1).

Study Number	IPN Present Observer 2	IPN Present Observer 1
1	Yes	Yes
2	No	No
3	No	No
4	Yes	Yes
5	Yes	Yes
6	No	No
7	No	No
8	No	No
9	No	No
10	No	No
11	Yes	Yes
12	No	No
13	No	No
14	Yes	Yes
15	Yes	Yes
16	No	No
17	Yes	Yes
18	Yes	Yes
19	Yes	Yes
20	Yes	Yes

Inter-observer agreement was $20/20 = 100\%$.

This yielded a kappa statistic (k) of 1.0

Inter-observer variability between an independent observer, new to the CEUS technique (observer 3), in comparison with myself (observer 1).

Study Number	IPN Present Observer 3	IPN Present Observer 1
1	Yes	Yes
2	No	No
3	Yes	No
4	Yes	Yes
5	Yes	Yes
6	No	No
7	No	No
8	No	No
9	Yes	No
10	No	No
11	Yes	Yes
12	No	No
13	No	No
14	Yes	Yes
15	No	Yes
16	No	No
17	Yes	Yes
18	Yes	Yes
19	Yes	Yes
20	No	Yes

Inter-observer agreement was $16/20 = 80\%$.

This yielded a kappa statistic (k) of 0.60.

Intra-observer variability performed by myself by re-analysing the 20 scans, in a random order, one month after initial analysis.

Study Number	First Analysis IPN present	Second Analysis IPN Present
1	Yes	Yes
2	No	No
3	No	No
4	Yes	Yes
5	Yes	Yes
6	No	No
7	No	No
8	No	No
9	No	No
10	No	No
11	Yes	Yes
12	No	No
13	No	No
14	Yes	Yes
15	Yes	Yes
16	No	No
17	Yes	Yes
18	Yes	Yes
19	Yes	Yes
20	Yes	Yes

Intra-observer agreement was $20/20 = 100\%$.

This yielded a kappa statistic (k) of 1.0.